Kobe University Repository : Kernel

PDF issue: 2025-02-01

Studies on blue metalloanthocyanin biosynthesis of Nemophila menziesii～aiming for generation of blue flower by genetic engineering

興津，奈央子

(Degree)
博士（理学）

(Date of Degree)
2019-03-06

(Date of Publication)
2020-03-01

(Resource Type)
doctoral thesis

(Report Number)
乙第3367号

(URL)
https://hdl.handle.net/20.500.14094/D2003367

※ 当コンテンツは神戸大学の学術成果です。無断複製・不正使用等を禁じます。著作権法で認められている範囲内で、適切にご利用ください。

博　士　論　文

Studies on blue metalloanthocyanin biosynthesis of *Nemophila menziesii* ~ aiming for generation of blue flower by genetic engineering

（ネモフィラの青いメタロアントシアニン生合成機構に関する研究
～遺伝子組換え技術による青い花の開発を目指して）

平成 31 年 1 月

興　津　奈　央　子

CONTENTS

Abbreviations

- A3AT: anthocyanidin 3-*O*-glucoside-6″-*O*-*p*-coumaroyltransferase
- A3G5GT: anthocyanidin 3-*O*-glucoside 5-*O*-glucosyltransferase
- A3GT: anthocyanidin 3-*O*-glucosyltransferase
- A3′MT: anthocyanin 3′-*O*-methyltransferase
- A3′5′MT: anthocyanin 3′,5′-*O*-methyltransferase
- A5MaT: anthocyanin 5-*O*-glucoside-6″-*O*-malonyltransferase
- AAT: anthocyanin acyltransferase
- ABC protein: ATP binding cassette protein
- AMT: *S*-adenosylmethionine-dependent anthocyanin *O*-methyltransferase
- ANS: anthocyanidin synthase
- anthocyanidin 3,5-diG: anthocyanidin 3,5-*O*-diglucoside
- anthocyanidin 3G: anthocyanidin 3-*O*-glucoside
- anthocyanidin 5,3GT: anthocyanidin 5,3-*O*-glucosyltransferase
- anthocyanin 3′,5′GT: anthocyanin 3′,5′-*O*-glucosyltransferase
- anthocyanin 5GT: anthocyanin 5-*O*-glucosyltransferase
- apigenin 4′G: apigenin 4′-*O*-glucoside
- apigenin 7G: apigenin 7-*O*-glucoside
- apigenin 7,4′-diG: apigenin 7,4′-*O*-diglucoside
- apigenin 7G4′MG: apigenin 7-*O*-β-glucoside-4′-*O*-(6-*O*-malonyl)-*O*-β-glucoside
- AT: acyltransferase
- BAHD: benzylalcohol acetyltransferase,
  anthocyanin-*O*-hydroxycinnamoyltransferase,

anthranilate-*N*-hydroxycinnamoyl/benzoyltransferase and deacetylvindoline acetyltransferase

- bHLH: basic helix-loop-helix
- BiFC: biomolecular fluorescence complementation
- CaMV35S: *Cauliflower mosaic virus* 35S
- CHI: chalcone isomerase
- CHS: chalcone synthase
- cyanidin 3G: cyanidin 3-*O*-glucoside
- cyanidin 3,5-diG: cyanidin 3,5-*O*-diglucoside
- delphinidin 3G: delphinidin 3-*O*-glucoside
- delphinidin 3,5-diG: delphinidin 3,5-*O*-diglucoside
- DFR: dihydroflavonol 4-reductase
- DHK: dihydrokaempferol
- DHM: dihydromyricetin
- DHQ: dihydroquercetin
- DTT: dithiothreitol
- EFP: enhancer of flavonoid production
- F3′5′H: flavonoid 3′,5′-hydroxylase
- F3′H: flavonoid 3′-hydroxylase
- F3H: flavanone 3-hydroxylase
- F4′G7GT: flavone 4′-*O*-glucoside 7-*O*-glucosyltransferase
- F4′GT: flavone 4′-*O*-glucosyltransferase
- flavone 7,4′-diG: flavone 7,4′-*O*-diglucoside
- flavonoid 3′/7GT: flavonoid 3′/7-*O*-glucosyltransferase

- Flavonol 3GT: flavonol 3-*O*-glucosyltransferase
- flavonol/anthocyanidin 3GT: flavonol/anthocyanidin 3-*O*-glucosyltransferase
- FLS: flavonol synthase
- FNS: flavone synthase
- FNSI: flavone synthase I
- FNSII: flavone synthase II
- GGT: flavonoid glucoside glucosyltransferase
- GH: glycoside hydrolase
- GST: glutathione *S*-transferase
- GT: glucosyltranferase
- GT family 1: glycosyltransferase family 1
- GyT: glycosyltransferase
- IF7GT: isoflavone 7-*O*-glucosyltransferases
- kaempferol 3G: kaempferol 3-*O*-glucoside
- kaempferol 7G: kaempferol 7-*O*-glucoside
- KPB: potassium phosphate buffer
- luteolin 4′G: luteolin 4′-*O*-glucoside
- luteolin 7G: luteolin 7-*O*-glucoside
- malvidin 3G: malvidin 3-*O*-glucoside
- malvidin 3,5-diG: malvidin 3,5-*O*-diglucoside
- MATE: multidrug and toxic compound extrusion
- MBW complex: MYB-bHLH-WDR protein complex
- MRP: multidrug resistance-associated protein
- pelargonidin 3G: pelargonidin 3-*O*-glucoside

- pelargonidin 3,5-diG: pelargonidin 3,5-*O*-diglucoside
- petunidin 3G: petunidin 3-*O*-glucoside
- petunidin 3,5-diG: petunidin 3,5-*O*-diglucoside
- petunidin 3*p*CG5MG: petunidin 3-*O*-[6-*O*-(*trans*-*p*-coumaroyl)-β-glucoside]-5-*O*-[6-*O*-(malonyl)-β-glucoside]
- quercetin 3G: quercetin 3-*O*-glucoside
- quercetin 4′G: quercetin 4′-*O*-glucoside
- RPKM: reads per kilobase of exon per million mapped reads
- SCPL: serine carboxypeptidase-like
- SU: split-ubiquitin
- UFGT: UDP-glycose-dependent flavonoid glycosyltransferase
- UGT: UDP-glycose-dependent glycosyltransferase
- UV: ultraviolet
- TFA: trifluoroacetic acid
- THC: 2′,4,4′,6′-tetrahydroxychalcone
- tobacco BY-2: *Nicotiana tabacum* Bright Yellow 2
- Tris: tris (hydroxymethyl) aminomethane
- WDR: WD40 Repeat

Abbreviations (Scientific name of plant species)

- *A. majus: Antirrhinum majus*
- *A. thaliana: Arabidopsis thaliana*
- *B. vulgaris: Beta vulgaris*
- *C. communis: Commelina communis*
- *C. cyanus: Centaurea cyanus*
- *C. medium: Campanula medium*
- *C. moriflolium: Chrysanthemum moriflolium*
- *C. persicum: Cyclamen persicum*
- *C. ternatea: Clitoria ternatea*
- *D. bellidiformis: Dorotheanthus bellidiformis*
- *D. caryophyllus: Dianthus caryophyllus*
- *D. grandiflorum: Delphinium grandiflorum*
- *F. hybrida: Freesia hybrida*
- *G. max: Glycine max*
- *G. triflora: Gentiana triflora*
- *H. lupulus: Humulus lupulus*
- *I. ensata: Iris ensata*
- *I. hollandica: Iris hollandica*
- *I. nil: Ipomoea nil*
- *N. menziesii: Nemophila menziesii*
- *N. tabacum: Nicotiana tabacum*
- *O. sativa: Oryza sativa*

- *P. communis: Pyrus communis*
- *P. crispum: Petroselinum crispum*
- *P. frutescens: Perilla frutescens*
- *P. hybrida: Petunia hybrida*
- *P. patens: Physcomitrella patens*
- *P. suffruticosa: Paeonia suffruticosa*
- *R. hybrida: Rosa hybrida*
- *S. baicalensis: Scutellaria baicalensis*
- *S. lycopersicum: Solanum lycopersicum*
- *S. patens: Salvia patens*
- *S. splendens: Salvia splendens*
- *S. uliginosa: Salvia uliginosa*
- *T. hybrida: Torenia hybrida*
- *V. vinifera: Vitis vinifera*
- *V. wittrockiana: Viola wittrockiana*

Summary

Flower color plays an important role to attract pollinators. The color is mainly derived from floral pigments, typically flavonoids, betalains, carotenoids and chlorophylls. Among them, anthocyanins, a colored class of flavonoids, are the most colorful compounds and confer orange, red, magenta, purple and blue colors.

Flower color also attracts human beings and is one of the most important characters of ornamental flowers. Plant breeders have been aiming to generate a novel flower color which native plants do not have. In flower markets, top-selling cut flowers such as roses and carnations lack violet or blue flower color due to genetic constraints of the species. Owing to recent advances in plant biotechnology, novel roses and carnations wearing blue hues were generated by engineering of flavonoid biosynthetic pathway and accompanying accumulation of delphinidin-based anthocyanins which most blue flowers accumulate. However, their colors are still bluish purple. Further improvement is necessary to achieve pure blue flowers. ‘Pure blue’ is defined as the blue color group of the Royal Horticultural Society Colour Charts (5th edition) in this study.

The pure blue color of *Nemophila menziesii* flower is derived from metalloanthocyanin, nemophilin, which consists of anthocyanin (petunidin 3-*O*-[6-*O*-(*trans*-*p*-coumaroyl)-β-glucoside]-5-*O*-[6-*O*-(malonyl)-β-glucoside]), flavone (apigenin 7-*O*-β-glucoside-4′-*O*-(6-*O*-malonyl)-*O*-β-glucoside) and metal ions (Mg^{2+} and Fe^{3+}). In spite of the pure blue of *N. menziesii* flowers, the flavonoid biosynthetic pathway of *N. menziesii* has not yet been studied. In the present study, the flavonoid biosynthetic pathway of *N. menziesii* flower has become understood comprehensively.

RNA-Seq analysis of the petals yielded 61,491 contigs and 21 genes encoding 15

proteins belonging to the flavonoid biosynthetic pathway in *N. menziesii* petals were identified. The spatio-temporal transcriptome analysis indicated that the genes involved in the early part of the pathway are strongly expressed during early stages of petal development and that those in the late part at late stages, but they are rarely expressed in leaves. The *flavanone 3-hydroxylase* cDNA and the *flavonoid 3′,5′-hydroxylase* cDNA were successfully expressed in yeast to confirm their activities.

Among the enzymes encoded by the isolated genes, the enzymes involved in modification of the flavonoids of nemophilin were further elucidated. The recombinant enzymes of cDNAs encoding anthocyanin modification enzymes [anthocyanidin 3-*O*-glucosyltransferase, anthocyanidin 3-*O*-glucoside 5-*O*-glucosyltransferase and *S*-adenosylmethionine-dependent anthocyanin *O*-methyltransferases (AMT)] were biochemically characterized by their expression in *Escherichia coli*. *Nm*AMT almost exclusively yielded petunidin 3-*O*-glucoside rather than malvidin 3-*O*-glucoside when delphinidin 3-*O*-glucoside was used as a substrate. This specificity is consistent with the anthocyanin composition of *N. menziesii* petals. The cDNA encoding AMT promoting petunidin-based anthocyanins accumulation was isolated for the first time among flowering plants accumulating mainly petunidin-based anthocyanins.

The two glucosyl moieties at the 7- and 4′-*O* positions of flavone, one of the components of nemophilin, have been shown to be essential for its formation. After revealing that apigenin is glucosylated first at the 4′-*O* position and then at the 7-*O* position by using the crude protein extract prepared from *N. menziesii* petals, the cDNA encoding flavone 4′-*O*-glucosyltransferase (F4′GT) and the cDNA encoding flavone 4′-*O*-glucoside 7-*O*-glucosyltransferase (F4′G7GT) were isolated for the first time and extensively characterized in this study. The transgenic *Nicotiana tabacum* Bright Yellow

2 cells expressing *NmF4′GT* and *NmF4′G7GT* converted efficiently apigenin into apigenin 7,4′-*O*-diglucoside, confirming their activities *in vivo* successfully identified.

In this study, a set of the flavonoid biosynthetic genes was isolated from *N. menziesii* and the biochemical properties of their enzymes were characterized. That will contribute to our better understanding of nemophilin biosynthesis. These genes are also expected to be useful molecular tools to engineer novel pure blue flowers by metalloanthocyanin formation.

Chapter 1 General Introduction

1. 1. Flower colors and pigments

Flower color plays an important role in plant hybridization by attracting pollinators, such as insects and birds (Tanaka et al. 2010). The major pigments responsible for flower color are flavonoids, betalains, carotenoids and chlorophylls (Davies 2000). Flavonoids, a group of secondary metabolites belonging to the class of phenylpropanoids, have a wide range of colors: pale yellow, orange, red, magenta, purple and blue. They are water-soluble and stored in the vacuoles. Betalains, nitrogen-containing compounds derived from tyrosine, result in yellow, orange, red and purple color. They are also water-soluble and stored in the vacuoles. Betalains, however, are found only in families of *Caryophyllales* (expect for *Caryophyllaceae* and *Molluginaceae*). To date, no plants producing both anthocyanins and betalains have been discovered (Brockington et al. 2015). Carotenoids, which are isoprenoids and are essential components of photosynthetic apparatus, produce yellow, orange and red colors in flowers. In many species, both flavonoids and carotenoids, in combination, contribute to the wider range of available colors, producing brown in addition to yellow, orange and red (Davies 2000). Chlorophylls, which have an important and well-understood role in photosynthesis, produce a green color, which is visible in flowers in a few cases, such as *Helleborus* (Davies 2000), *Dianthus caryophyllus* (Ohmiya et al. 2014) and *Chrysanthemum moriflolium* (Ohmiya et al. 2017).

1. 2. Flavonoid and its biosynthetic pathway relevant to flower colors

Flavonoids are the most common pigments in flowers and are responsible for the widest

range of flower colors among four main pigments, producing color ranging from pale yellow, orange, red, magenta, purple and blue. Flavonoids play various important roles for a plant's survival in nature in addition to the attraction of pollinators. By absorbing ultraviolet (UV) -B, they can protect plant organs from UV damage (Ryan et al. 2001). Flavonoids also serve as antioxidants, scavenging radicals that are formed during various biotic and abiotic processes. This antioxidant activity is assumed to have a role in supporting human health and well-being. Some flavonoids have an inhibitory effect on insect feeding and they protect plant's interactions with microorganisms (Harborne and Williams 2000).

'Flavonoid' is a general term for a group of phenylpropanoid compounds having C6-C3-C6 structures. The flavonoids are classified into about a dozen of groups depending on their structures (Forkmann and Heller 1999). Among these groups, anthocyanins, flavones, flavonols, chalcones and aurones mainly contribute to flower color (**Fig. 1**).

Anthocyanins, a colored class of flavonoids, show orange, red, magenta, purple and blue flower colors. Anthocyanidins are aglycones of anthocyanins and are the precursors of anthocyanins. They are unstable under normal physiological conditions and do not accumulate *in vivo*. They are stabilized to form the corresponding anthocyanins by glycosylation, methylation and/or acylation. Flower color largely depends on anthocyanin structures and especially the number of hydroxyl groups on the B-ring. Orange/intense red flowers, red/magenta flowers and violet/blue flowers tend to accumulate pelargonidin, cyanidin and delphinidin-based anthocyanins, respectively. Flavones and flavonols are very pale yellow and are mostly invisible to the human eye, but since they absorb UV, they are visible to some insects. When flavones and flavonols

accumulate with anthocyanins in flower petals, they form complexes with anthocyanins. This complex formation causes a bluer and deeper color shift (baothochromic shift) among the anthocyanin molecules in the complex. For this reason, flavones and flavonols are described as co-pigments (Goto et al. 1987). Chalcones and aurones confer a pale and intense yellow color in flowers, such as in *D. caryophyllus* and *Antirrhinum majus*, respectively.

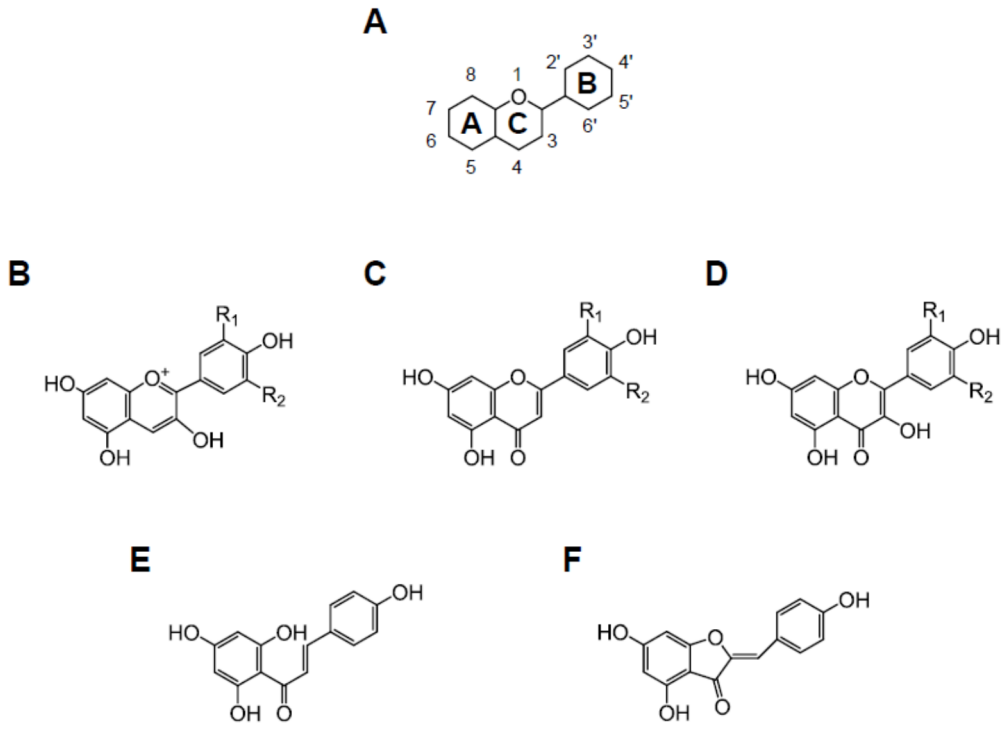

Fig. 1 Structures of the major flavonoids contibuting to flower color. (A) The basic flavonoid structure. The numbers of the carbons of flavonoids and the letterings of the carbon rings are shown. (B) Anthocyanidin. R1 and R2 = H, pelarginidin; R1 = OH and R2 = H, cyanidin; R1 and R2 = OH, delphinidin. (C) Flavone. R1 and R2 = H, apigenin; R1 = OH and R2 = H, luteolin; R1 and R2 = OH, tricetin. (D) Flavonol. R1 and R2 = H, kaempferol; R1 = OH and R2 = H, quercetin; R1 and R2 = OH, myricetin. (E) Chalcone. (F) Aurone.

The flavonoid biosynthetic pathway has been well characterized in terms of molecular biology, biochemistry, evolution and interaction with pollinators (Grotewold 2006; Rausher 2006; Tanaka et al. 2008). The pathways leading to the biosynthesis of anthocyanidins and flavone/flavonol aglycones are well conserved among flowering plant species. The flavonoid biosynthetic pathway leading to anthocyanins, flavones and flavonols is provided in **Figure 2**.

1. 2. 1. The general pathway

The first enzyme committed in flavonoid biosynthesis is chalcone synthase (CHS), which catalyzes the condensation of one molecule of *p*-coumaroyl-CoA and three molecules of malonyl-CoA to yield 2′,4,4′,6′-tetrahydroxychalcone (THC). THC, an unstable compound, can be spontaneously isomerized to naringenin, but *in vivo* it is stereospecifically isomerized to (2*S*)-naringenin by chalcone isomerase (CHI). (2*S*)-naringenin, a flavanone, is converted to dihydrokaempferol (DHK), a dihydroflavonol, by the catalysis of flavanone 3-hydroxylase (F3H). Flavonoid 3′-hydroxylase (F3′H) and flavonoid 3′,5′-hydroxylase (F3′5′H) catalyze the hydroxylation of DHK to form dihydroquercetin (DHQ) and dihydromyricetin (DHM), respectively. F3′H and F3′5′H also catalyze hydroxylation of flavanones, flavones and flavonols. Dihydroflavonols (DHK, DHQ and DHM) are reduced to leucoanthocyanidins by the actions of dihydroflavonol 4-reductase (DFR). The DFRs of some species have strict substrate specificities as shown in DFRs of *Petunia hybrida* and *Cymbidium hybrida*, which do not recognize DHK (Meyer et al. 1987; Johnson et al. 1999). This is the reason that these species lack pelargonidin-based anthocyanins and thus lack flowers of an orange/brick red color. Leucoanthocyanidins are converted to the

corresponding anthocyanidins by the catalysis of anthocyanidin synthase (ANS).

The typical co-pigments, apigenin (flavone) and kaempferol (flavonol), are converted from flavanone and DHK by flavone synthase (FNS) and flavonol synthase (FLS), respectively. Interestingly, there are two types of FNS. FNSI, which belongs to the 2-oxoglutarate-dependent dioxygenase family, has been found in *Petroselinum crispum* and evolved from F3H (Martens et al. 2003). FNSII is more common and belongs to the cytochrome P450 family.

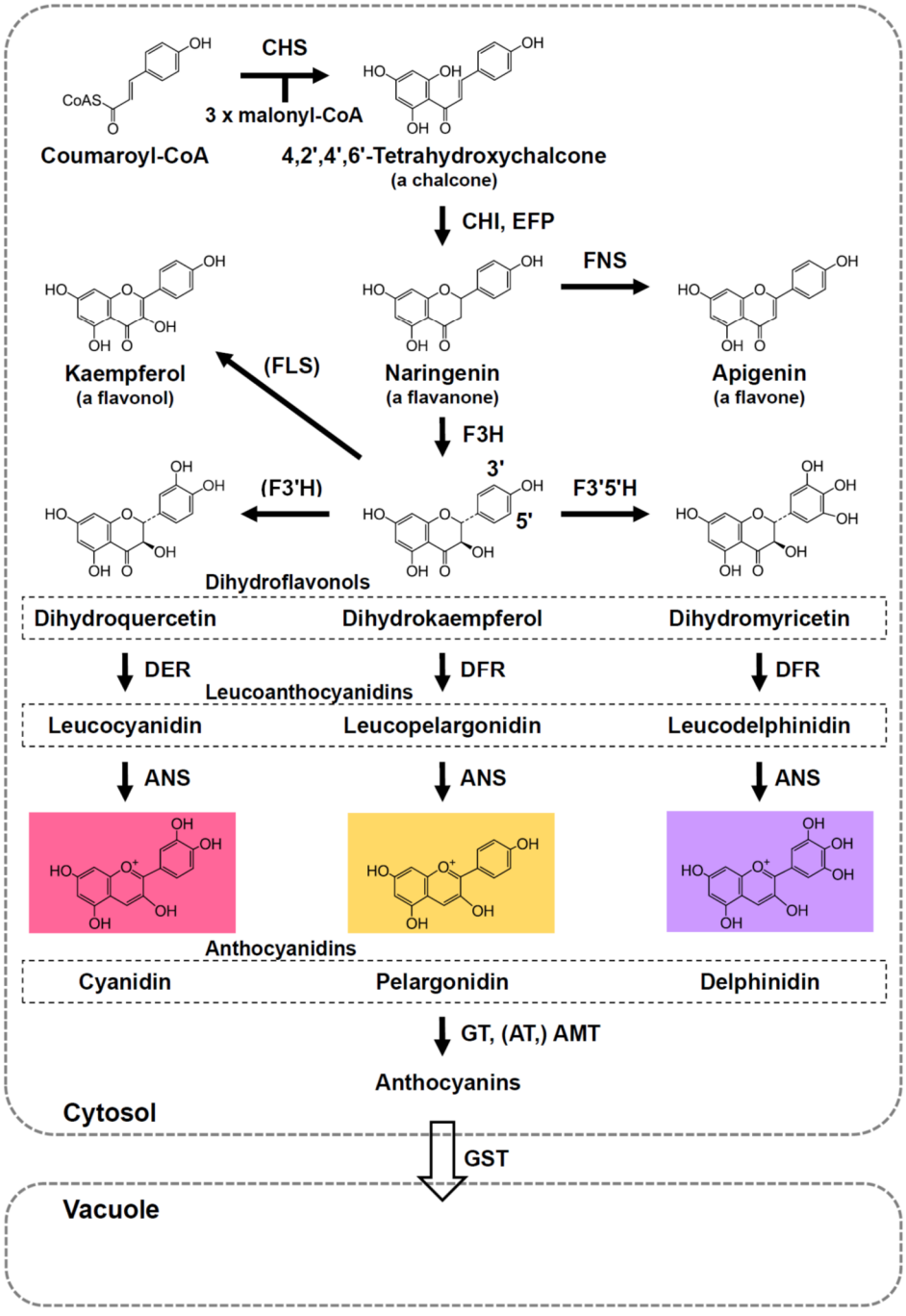
CHS
3 x malonyl-CoA
Coumaroyl-CoA
4,2',4',6'-Tetrahydroxychalcone
(a chalcone)
CHI, EFP
FNS
Kaempferol
(a flavonol)
(FLS)
Naringenin
(a flavanone)
Apigenin
(a flavone)
F3H
(F3'H)
3'
5'
F3'5'H
Dihydroflavonols
Dihydroquercetin
Dihydrokaempferol
Dihydromyricetin
DER
DFR
DFR
Leucoanthocyanidins
Leucocyanidin
Leucopelargonidin
Leucodelphinidin
ANS
ANS
ANS
Anthocyanidins
Cyanidin
Pelargonidin
Delphinidin
GT, (AT,) AMT
Anthocyanins
Cytosol
GST
Vacuole

Fig. 2 A schematic of a general flavonoid biosynthetic pathway relevant to flower color. Genes represented in parenthesis, including flavonol synthase (FLS), flavonoid 3′-hydroxylase (F3′H) and acyltransferases (AT), are not studied here. CHS, chalcone synthase; CHI, chalcone isomerase; EFP, enhancer of flavonoid production; FLS, flavonol synthase; FNSII, flavone synthase II; F3H, flavanone 3-hydroxylase; F3′H, flavonoid 3′-hydroxylase; F3′5′H, flavonoid 3′,5′-hydroxylase; DFR, dihydroflavonol 4-reductase; ANS, anthocyanidin synthase; GT, glucosyltransferase; AMT, *S*-adenosylmethionin-dependent anthocyanin *O*-methyltransferase; GST, glutathione *S*-transferase.

1. 2. 2. Flavonoid modification

Anthocyanins are unstable at neutral pH and must be stabilized by glycosylation, methylation and/or acylation. In contrast to the well-conserved general flavonoid biosynthetic pathway shown in **Fig. 2** (Heller and Forkmann 1994; Tanaka et al. 1998), these modifications of flavonoids are plant species-dependent and are responsible for structural diversities of flavonoids.

UDP-glycose-dependent flavonoid glycosyltransferases (UFGTs) catalyze the glycosylation of flavonoids. UFGTs belong to glycosyltransferase family 1 (GT family 1) of the glycosyltransferase (GyT) superfamily. UFGTs generally form distinctive clusters on the basis of their region-specificity for sugar acceptors such as flavonol/anthocyanidin 3-*O*-glucosyltransferase (flavonol/anthocyanidin 3GT) cluster, anthocyanin 5-*O*-glucosyltransferase (anthocyanin 5GT) cluster, flavonoid 3′/7-*O*-glucosyltransferase (flavonoid 3′/7GT) cluster and cluster of flavonoid glucoside

glucosyltransferase (GGT), which catalyzes glycosylation at the sugar moiety attached to flavonoids (Fukuchi-Mizutani et al. 2003; Nakatsuka et al. 2008; Yonekura-Sakakibara et al. 2014; Yin et al. 2017). It indicated that genes encoding UFGT had diverted before specification of flowering plants (Yonekura-Sakakibara et al. 2014). 3-*O*-Glucosylation of anthocyanidins almost exclusively precedes other glucosylations, methylation and acylation (Heller and Forkmann 1994; Tanaka et al. 1998). The methylation of anthocyanins is catalyzed by *S*-adenosylmethionine-dependent anthocyanin *O*-methyltransferase (AMT). Peonidin-based anthocyanins are synthesized from cyanidin-based anthocyanins, and petunidin- and malvidin-based anthocyanins are from delphinidin-based anthocyanins (Tanaka et al. 1998). The biosynthesis of acylated anthocyanins required the activity of acyl-CoA-dependent anthocyanin acyltransferases (AATs). AATs belong to the benzylalcohol acetyltransferase, anthocyanin-*O*-hydroxycinnamoyltransferase, anthranilate-*N*-hydroxycinnamoyl/benzoyltransferase and deacetylvindoline acetyltransferase (BAHD) family. AATs are classified on the basis of their acyl-donor specificity into two categories; aliphatic (e.g., acetyl, malonyl and malyl) and aromatic (e.g., *p*-coumaroyl, caffeoyl and *p*-hydroxybenzoyl) acyltransferases (Nakayama et al. 2003). These modifications proceed in the cytosols. Anthocyanins are modified by these enzymes in a specific order, as shown in *Clitoria ternatea* (Kogawa et al. 2007) and *Lobelia erinus* (Hsu et al. 2017).

More recently some glucosylation and acylation reactions have been found most likely to proceed in the vacuole, catalyzed by acyl-glucose (i.e., 1-*O*-β-D-glucose esters of organic acids)-dependent anthocyanin glucosyltransferases (GTs) and acyltransferases (ATs). This type of GT was studied for the first time in *D. caryophyllus*

(5-*O*-glucosylation of anthocyanidin 3-*O*-glucosides, Matsuba et al. 2010) and *Delphinium grandiflorum* (7-*O*-glucosylation of anthocyanidin 3-*O*-glucosides, Matsuba et al. 2010), followed by *Agapanthus africanus* (7-*O*-glucosylation of anthocyanidin 3-*O*-glucosides, Miyahara et al. 2012), *Arabidopsis thaliana* (glucosylation of 4-coumarate moiety of the anthocyanin molecule, Miyahara et al. 2013), *D. grandiflorum* (7-poly-*O*-glucosylation, Nishizaki et al. 2013) and *Campanula medium* (7-*O*-glucosylation of anthocyanidin 3-*O*-rutinoside, Miyahara et al. 2014). These GTs belong to members of glycoside hydrolase (GH) family 1. *Acyl-glucose-dependent AAT* genes have been isolated from *C. ternatea* (transferring a *p*-coumaroyl group from *p*-coumaroyl-glucose to the glucose moiety on the 3′-*O* position of anthocyanin, Noda et al. 2006), *D. caryophyllus* (1-*O*-malyl-β-D-glucose-dependent 1-*O*-malylglucose: pelargonidin 3-glucoside-6″-*O*-malyltransferase, Umemoto et al. 2014), *A. thaliana* and *D. grandiflorum* (*p*-hydroxybenzoylation of anthocyanin, Nishizaki et al. 2013). These AATs are serine carboxypeptidase-like (SCPL). It is particularly interesting that *p*-hydroxybenzoyl-glucose is a ‘zwitter donor’ for both GH1-GT and SCPL-AAT (Nishizaki et al. 2013). UDP-glucose-dependent GT catalyzing acyl-glucose synthesis has been identified in *A. thaliana* (Miyahara et al. 2013) and *D. grandiflorum* (Nishizaki et al. 2014).

Flavone *C*-glucoside is a strong co-pigment inducing of anthocyanins, as observed in *Iris ensata* (Yabuya et al. 1997). However, its biosynthesis had been a mystery. The biosynthetic pathway of flavone *C*-glucoside was revealed in *Oryza sativa*. An open chain form of a 2-hydroxyflavanone synthesized from a flavanone by a catalysis P450 enzyme (flavanone 2-hydroxylase) is glucosylated by the catalysis of a GT and then

dehydrated to flavone *C*-glucoside by a dehydratase (Brazier-Hicks et al. 2009) while flavone *O*-glucosides are synthesized by direct *O*-glucosylation of the flavone skeletons mediated by GT as reported in *Torenia hybrida, A. majus and Garbera hybrida* (Akashi et al. 1999; Martens and Forkmann 1999). The *O. sativa* type GT has also been isolated from *Fagopyrum esculentum* (Nagatomo et al. 2014). More recently, Sasaki et al. (2015) isolated the gene of the GT catalyzing the direct transfer of a glucose moiety to the C-6 position of a flavone from *Gentiana triflora*. Isoorientin (luteolin 6-*C*-glucoside) is accumulated in its flowers and leaves.

1. 2. 3. Flavonoid transport to the vacuole

Most flavonoids are synthesized in the cytosol and are transported to the vacuole. Plant cells utilize various mechanisms such as (i) glutathione *S*-transferase (GST)/multidrug resistance-associated protein (MRP)/ATP binding cassette protein (ABC protein)-mediated transport, (ii) membrane transport by multidrug and toxic compound extrusion (MATE) transporter and (iii) vesicle trafficking to achieve this transfer, as reviewed by Zhao (2015). These mechanisms are not exclusive and can co-exist in a single plant cell.

The involvement of GST in the transport of flavonoids is well established, as shown in the *Zea mays* mutant Bz2, *P. hybrida* AN9, *A. thaliana* TT19, *Vitis vinifera* and other examples (Zhao 2015). However, it is not clear how GST participates biochemically in anthocyanin transport to the vacuoles. GST itself neither transports flavonoids and glutathione nor forms a conjugate with flavonoids (Zhao 2015). MRP is a C-type of ABC protein and has been shown to be a glutathione-dependent malvidin 3-*O*-glucoside (malvidin 3G) transporter in *V. vinifera* (Francisco et al. 2013).

MATE transporters have been shown to transport epicatechin 3′-*O*-glucoside in *Medicago truncatura* and proanthocyanidin precursors in *A. thaliana* (Zhao and Dixon 2009). Anthocyanins and proanthocyanidins are transported to the vacuoles by vesicle trafficking in the Golgi. *A. thaliana* GFS9 (TT9) is a peripheral membrane protein localized in the Golgi apparatus that is required for vacuolar development though membrane fusion at the vacuoles. GFS9 is an essential component of the vesicle-mediated transport of proteins and phytochemicals such as proanthocyanidins and flavonols (Ichino et al. 2014).

In case that these transport systems have specificities to flavonoid structures, genetic engineering of the transport system for a target species may be one strategy for accumulating desirable flavonoids.

1. 2. 4. Regulation of enzymes in the flavonoid biosynthetic pathway

It has been reported in various plants that the spatial and temporal expression of structural genes in flavonoid biosynthesis is determined by a combination of R2R3-MYB, basic helix-loop-helix (bHLH) and WD40 Repeat (WDR) proteins. They interact to form a MYB-bHLH-WDR protein complex (MBW complex) that activates flavonoid biosynthesis. R2R3-MYB and bHLH bind specific sequence motifs in regulatory regions of the transcription of flavonoid biosynthetic genes. WDR protein facilitates protein–protein interaction for the formation of MBW complexes. In *P. hybrida* petals, AN2 (R2R3-MYB), AN1 (bHLH) and AN11 (WDR) activate *DFR* expression (de Vetten et al. 1997; Spelt et al. 2000). In *A. thaliana*, TT2 (R2R3-MYB), TT8 (bHLH) and TTG1 (WDR) are involved in proanthocyanin accumulation by the regulation of expression of *BANYULS*, a negative regulator of flavonoid biosynthesis

that prevents accumulation of proanthocyanins in the seed coats (Baudry et al. 2004). In *G. triflora* petals, GtMYB3 interacts with GtbHLH1, and the complex of these two proteins activates the expression of *F3′5′H* and *anthocyanin 5,3′-aromatic acyltransferase*, which belong to the late flavonoid biosynthetic pathway (Nakatsuka et al. 2008).

Some transcriptional factors controlling early flavonoid biosynthesis specially flavonol accumulation, have been reported in several plant species, including *A. thaliana* (Mehrtens et al. 2005; Stracke et al. 2007), *V. vinifera* (Czemmel et al. 2009) and *Solanum lycopersicum* (Ballester et al. 2010). In the case of *G. triflora*, the expression profiles of *GtMYBP3* and *GtMYBP4* genes correlated with flavone accumulation in petals and activated the expression of *CHS*, *FNSII* and *F3′H*, belonging to the early flavonoid biosynthetic pathway (Nakatsuka et al. 2012).

The ectopic expression of an *A. thaliana R2R3-MYB* gene (*PAP1* (*AtMYB75*)) activates anthocyanin biosynthesis, and thus results in the darker pink flower color in *Nicotiana tabacum* (He et al. 2017). Expression of an *A. majus R2R3-MYB* gene (*Rosea1*) and an *A. majus bHLH* gene (*Delila*) under a fruit-specific promoter in *S. lycopersicum* yielded purple fruits accumulating anthocyanins at a concentration comparable to the anthocyanin levels found in blackberries and blueberries (Butelli et al. 2008). Because the expression of the *R2R3-MYB* and/or *bHLH* genes of the MBW complex activates transcription of a set of flavonoid biosynthetic genes and results in ectopic accumulations of anthocyanins often accompanying darker flower color, these genes are considered powerful tools for the engineering of the flavonoid biosynthetic pathway in most flowering plants.

1. 2. 5. Multi-enzyme complexes (Metabolons)

Metabolic enzymes of a biosynthetic pathway are proposed to form a protein complex called a ‘metabolon’ (Winkel 2004). Direct evidence of a protein–protein interaction in flavonoid biosynthetic enzymes was presented in *A. thaliana* (Burbulis and Winkel-Shirley 1999), where yeast two-hybrid experiments showed interactions of CHS, CHI and DFR and affinity chromatography and immunoprecipitation assays revealed the interaction of CHS, CHI and F3H. Further convincing results supporting metabolon formation have been obtained recently. Interactions between *Glycine max* 2-hydroxyisoflavone synthase (a P450) and CHS or CHI were shown by a split-ubiquitin (SU) membrane yeast two-hybrid system and biomolecular fluorescence complementation (BiFC) using *N. tabacum* leaf cells. More interestingly, fluorescence signals derived from the interaction exhibited network-like intracellular patterns similar to the endoplasmic reticulum-localized fluorescence patterns of *G. max* isoflavone synthase labelled with a fluorescent protein (Waki et al. 2016). Chalcone synthase, CHI and DFR have been shown to interact with FNSII in *A. majus* by a SU membrane yeast two-hybrid system and *T. hybrida* by BiFC with *N. tabacum* leaf cells (Fujino et al. 2018). These observed interaction partnerships in *A. thaliana, G. max* and two *Lamiales* plants (*A. majus* and *T. hybrida*) were different, suggesting that the organization of flavonoid metabolons may differ among plant species.

A series of enzymes and proteins involved in flavonoid biosynthesis have been isolated from *Ipomoea nil* using mutants and transposon tagging. An *enhancer of flavonoid production (EFP)* gene has been identified from a pale color mutant. EFP belongs to a group of CHI-related type IV enzymes. Mutation of the *EFP* gene resulted in a dramatic decrease of anthocyanins and flavonols (about one fourth) in *I. nil*. Its

counterpart genes were isolated from *P. hybrid* and *T. hybrid*. Downregulation of these genes in transgenic plants resulted in a decrease of anthocyanin's and flavonols (*P. hybrida*) or flavones (*T. hybrida*) by about 70–80% and a more pale flower color (Morita et al. 2014). Recently, the other EFPs were isolated from *A. majus*, *D. caryophyllus* and *C. moriflolium* (Morita et al. 2015). The EFP homologs of noncatalytic CHI-like proteins, which function to promote flavonoid production, were reported from *Physcomitrella patens* (Wolf et al. 2010), *A. thaliana* (Jiang et al. 2015) and *Humulus lupulus* (Ban et al. 2018).

The role of EFP in flavonoid biosynthesis is not clear. However, it is suggested that EFP is unlikely to be a CHI, a transcriptional factor or an anthocyanin transporter. It is also reported that EFP may activate at least the early steps of flavonoid biosynthesis (Morita et al. 2014). EFP may enhance CHS activity and/or EFP may be one component of the flavonoid biosynthesis enzyme complex (Morita and Hoshino 2018). More recently, Ban et al. (2018) showed *H. lupulus* EFP physically interacts with CHS to increase its activity and then enhance flavonoid production in the trichomes. EFP are found in land plants including moss *P. patens*. Interestingly, *P. patens* contain EFP but not CHI, which may indicate that EFP appeared earlier then CHI (Morita et al. 2014).

In case there is specificity in the protein–protein interaction of flavonoid biosynthetic proteins, the compatibility of endogenous proteins and exogenous proteins should be considered as a tool for color modification.

1. 3. Blue flower coloration

Flower colors are also attractive and of considerable interest to people, in addition to pollinators. Particularly for ornamental plants, flower color is one of the most important

characters that attract consumers. Therefore, diversification of flower color has been an important goal for plant breeders. Since roses, carnations, chrysanthemums, lilies and gerberas, all of which are top-selling cut flowers, do not naturally have blue color flowers, blue varieties of these species have long been desired, especially for roses as ‘queen of flowers’. A term ‘blue rose’ has been a synonym for the impossible due to the absence in nature.

1. 3. 1. Blue flowers in nature

The mechanism of blue coloration in petals is one of the most intriguing questions for chemists because delphinidin-based anthocyanin, which most blue flowers contain, itself shows a purple color (Yoshida et al. 2009). Thus, the chemical mechanisms of blue coloration have been studied well (Yoshida et al. 2009). It has been shown that blue color in petals is exhibited through a combination of several factors, such as anthocyanin modification, co-existence of co-pigment and/or metal ions and higher vacuolar pH in addition to accumulation of delphinidin-based anthocyanin (Yoshida et al. 2009).

The aromatic acylation of anthocyanins shifts their absorption maxima toward a longer wavelength (a bluer color). Intermolecular stacking of anthocyanins modified with multiple aromatic acyl groups such as in *G. triflora* (Goto et al. 1982), *Senecio cruentus* (Goto et al. 1984), *D. grandiflorum* (Kondo et al. 1991) and *C. ternatea* (Kazuma et al. 2003) results in a stable blue color. The presence of co-pigments, typically glucosides of flavones and flavonols, causes a bathochromic shift in the anthocyanins by intramolecular stacking to yield darker and bluer hues, as in the case of *Veronica persica* (Mori et al. 2009) and *Ceanothus papillosus* (Bloor 1997), respectively.

Flavone *C*-glucosides are especially strong co-pigments, as shown for isovitexin (apigenin 6-*C*-glucoside) in *I. ensata* Thunb. (Yabuya et al. 1997). Complexation with metal ions such as Al^{3+} and Fe^{3+} results in blue color in *Hydrangea macrophylla* (Yoshida et al. 2003) and *Tulipa gesneriana* cv. Murasakizuisho (Shoji et al. 2007), respectively. Since anthocyanin color depends on pH to great extent, the pH of vacuoles where anthocyanins localize affects the color. In the case of *Ipomoea tricolor* cv. Heavenly Blue, transient elevation of vacuolar pH from pH 6.6 at the bud stage to pH7.7 at the fully-opened stage by expression of K^+/H^+ antiporter results in flower color change from magenta to blue (Yoshida et al. 2005).

The formation of a complex of six molecules each of aromatically acylated anthocyanin and flavone glucoside with two metal ions (Fe^{3+} and/or Mg^{2+}), which is called a ‘metalloanthocyanin’, is another tactic to generate some blue flowers. A pure blue color arises from the metalloanthocyanin in *Commelina communis* (Tamura et al. 1986), *Salvia patens* (Takeda et al. 1994), *Centaurea cyanus* (Kondo et al. 1998), *Salvia uliginosa* (Mori et al. 2008) and *Nemophila menziesii* (Yoshida et al. 2009). *In vivo*, *C. cyanus* and *C. communis* metalloanthocyanins contain additional Ca^{2+} and Mg^{2+}, respectively (Shiono et al. 2005; Shiono et al. 2008).

1. 3. 2. Blue flowers generated by genetic engineering

Most currently cultivated floricultural crops have been developed through a combination of extensive hybridization breeding techniques. However, this approach suffers from genetic constraints within a species. Genetic engineering liberates plant breeders from such constraints. Genetic engineering has led to the generation of novel blue colors in the major cut flower species of roses, carnations and chrysanthemums, all

of which lack the ability to produce violet/blue flowers in nature, primary due to a genetic deficiency in F3′5′H and thus a deficiency in delphinidin-based anthocyanin. The expression of a *F3′5′H* gene in these species has successfully resulted in delphinidin accumulation in their petals, resulting in flowers wearing novel blue hues (Katsumoto et al. 2007; Brugliera et al. 2013; Tanaka and Brugliera 2013); the transgenic roses expressing the *Viola wittrockiana F3′5′H* gene and carnations expressing the *P. hybrida* or *V. wittrockiana F3′5′H* gene have been commercialized (**Figs. 3A, B**). The transgenic chrysanthemums expressing *C. medium F3′5′H* and *C. ternatea anthocyanin 3′,5′-O-glucosyltransferase (anthocyanin 3′,5′GT)* exhibited a pure blue color (Noda et al. 2017; **Fig. 3C**). Their blue color is derived from intermolecular interactions between delphinidin 3-*O*-(6-*O*-malonylglucoside) 3′,5′-*O*-diglucoside and endogenous flavone 7-*O*-(6-*O*-malonylglucoside) (Noda et al. 2017).

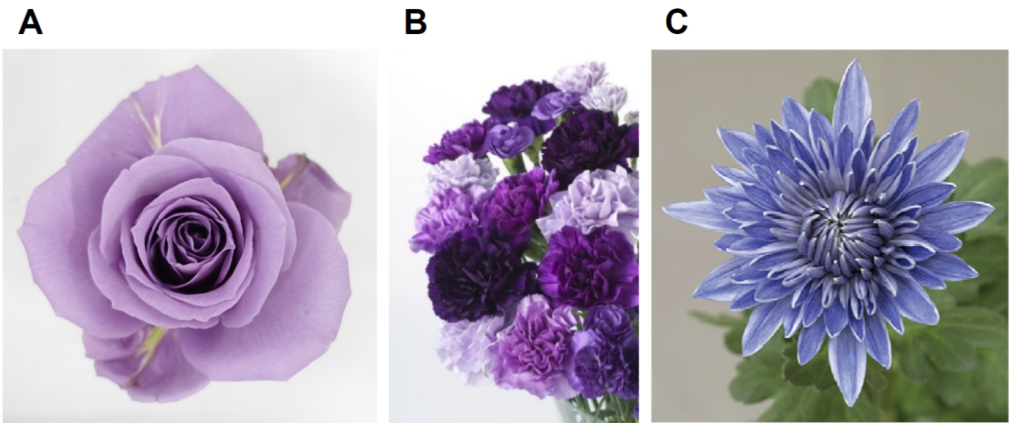

Fig. 3 Photos of transgenic blue flowers accumulating delphinidin-based anthocyanidin by expression of a *F3′5′H* gene. (A) Roses, Suntory Blue Rose APPLAUSE. (B) Carnations, Florigene Moon series. (C) Chrysanthemums with pure blue flower color. This photo was taken by Dr. Noda of National Agriculture and Food Research Organization, used with permission from him.

Blue phalaenopsis and blue dahlias have also been produced by expressing the *C. communis F3′5′H* (Mii 2012) but the details of the results have not been published yet. Qi et al. (2013) reported the transient co-expression of *Phalaenopsis hybrida F3′5′H* and *Hyacinthus orientalis DFR* in the pink lily ‘Sorbonne’ perianth. The transgenes expressing cell turned a purple color from the pink (Qi et al. 2013). Various novel blue flowers have been generated by genetic engineering, but these flowers do not exhibit a pure blue flower color except for the transgenic chrysanthemums. Thus, further improvements are required to achieve pure blue flowers.

As mentioned previously, currently available transgenic rose (Suntory Blue Rose Applause™) by the expression of the *V. wittrockiana F3′5′H* gene (**Fig. 3A**) has been marketed in Japan since 2009. It has a bluish purple flower. This is because it does not

satisfy any blue flower coloration conditions apart from delphinidin-based anthocyanin accumulation. Rose petals are generally deficient in aromatic acyltransferase activity and strong co-pigments such as flavones. The vacuolar pH is also very low (from pH 3.69 to 5.78) (Biolley and Jay 1993; Katsumoto et al. 2007). In order to develop pure blue roses, a combination of multilateral strategies is necessary. So far, many genes involved in the aromatic acylation of anthocyanins, co-pigmentation, the transport of metal ions and the control of vacuolar pH have already been cloned (Tanaka and Brugliera 2006; Shoji et al. 2007). However, crucial genes for metalloanthocyanin formation have not yet been identified.

1. 3. 3. *Nemophila menziesii* and its mechanism of blue flower coloration

Nemophila menziesii Hook. and Arn., commonly known as ‘baby blue eyes’, is a *Boraginaceae* plant native to western North America. *N. menziesii* cultivar ‘Insignis Blue’ is used as a garden and pot plant to exhibit pure blue flowers (**Fig. 4A**). The color results from a metalloanthocyanin, nemophilin, which comprises six petunidin 3-*O*-[6-*O*-(*trans*-*p*-coumaroyl)-β-glucoside]-5-*O*-[6-*O*-(malonyl)-β-glucoside] (petunidin 3*p*CG5MG) molecules, six apigenin 7-*O*-β-glucoside-4′-*O*-(6-*O*-malonyl)-*O*-β-glucoside (apigenin 7G4′MG) molecules, one Mg^{2+} ion and one Fe^{3+} ion (Yoshida et al. 2009; Yoshida et al. 2015; **Figs. 4B–D**). *N. menziesii* living petals have two types of metalloanthocyanin, the blue-colored Fe^{3+}-Mg^{2+}-nemophilin and the purplish-blue-colored Mg^{2+}-Mg^{2+}-nemophilin. They may coexist in petals to develop a blue flower color variation (Yoshida et al. 2015). Its purple variant does not contain flavones (Tatsuzawa et al. 2014).

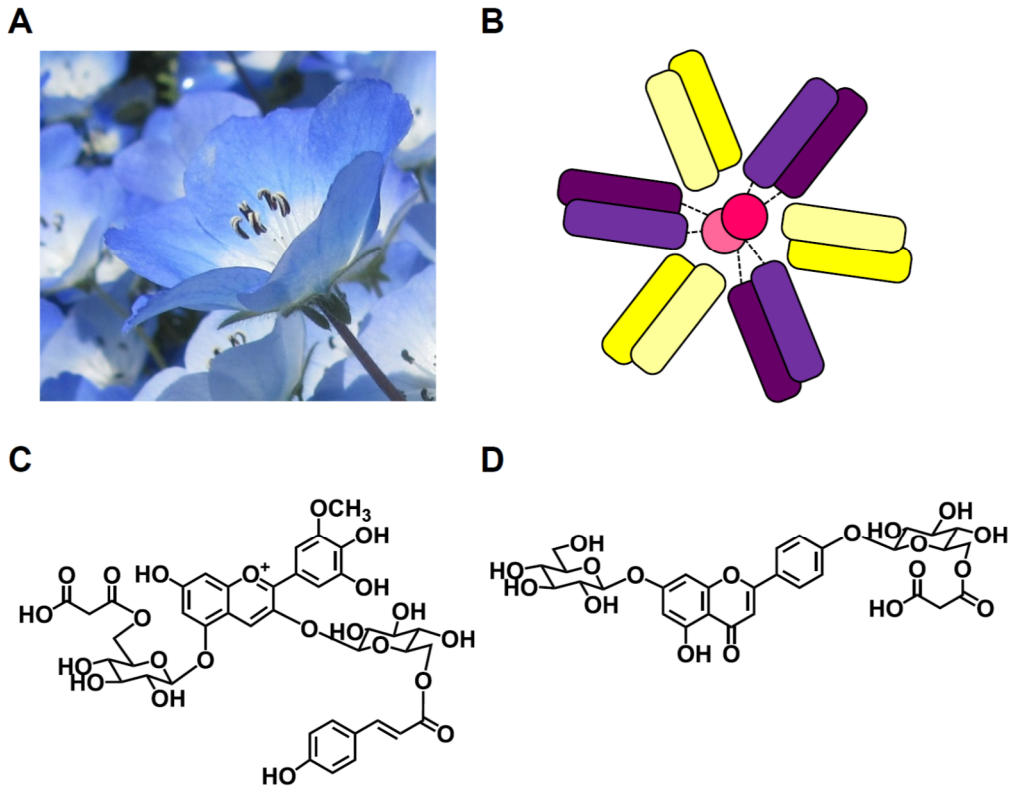

Fig. 4 *N. menziesii* flowers, schematic model of nemophilin and flavonoid components of nemophilin. (A) *N. menziesii* flowers. (B) A schematic model of nemophilin. Violet colored components, anthocyanins; yellow colored components, flavones; pink colored components, metal ions (Fe^{3+} and Mg^{2+}). (C) Petunidin 3-*O*-[6-*O*-(*trans*-*p*-coumaroyl)-β-glucoside]-5-*O*-[6-*O*-(malonyl) -β-glucoside]. (D) Apigenin 7-*O*-β-glucoside-4′-*O*-(6-*O*-malonyl)-*O*-β-glucoside.

In spite of the pure blue of *N. menziesii* flowers, the molecular and biochemical aspects of its flavonoid biosynthetic pathway have not yet been investigated. In the present study, a set of flavonoid biosynthetic genes from *N. menziesii* was isolated to understand nemophilin biosynthesis in terms of molecular biology and biochemistry.

Chapter 2 focuses on the general flavonoid biosynthetic genes. In Chapter 3, the anthocyanin modification enzymes were analyzed. In Chapter 4, the study on the flavone glucosyltransferase genes that are essential for blue metalloanthocyanin formation was described. These genes will be useful tools for engineering pure blue flowers by promoting metalloanthocyanin accumulation. The isolation and characterization of these genes will open the possibility to realize the dream of developing a ‘blue rose’.

Chapter 2 Analysis of flower pigments and molecular cloning of flavonoid biosynthetic pathway genes in *N. menziesii*

2. 1. Introduction

The pathway leading to the biosynthesis of anthocyanidins and flavone/flavonol aglycones is well conserved among flowering plant species (Grotewold 2006; Rausher 2006; Tanaka et al. 2008). *P. hybrida* is a model species for studying flower color and flavonoid biosynthesis (Koes et al. 2005). *T hybrida*, an ornamental plant, has also been used as a model species in the study of flower color and flower shape though genetic modifications (Aida 2009).

Notably, the development of DNA-sequencing technologies and transcriptome analysis has enabled the isolation of flavonoid biosynthetic genes from many species. Recently, the studies on genetics and molecular biology in ornamental plants, such as water lilies (Wu et al. 2016) and *Dendrobium hybrida* (Li et al. 2017), were reported. Most flavonoid genes appeared before the divergence of flowering plants (Rausher 2006). Thus, the function of isolated genes can usually be predicted on the basis of gene sequencing and phylogenetic analyses. However, convergent evolution has been reported in the case of two genes in this pathway, including flavone synthase I (FNSI), which evolved from that *F3H* gene in *Petroselinum crispum* (Martens et al. 2003), and the *F3'5'H* gene, which independently evolved from the *F3'H* gene (Seitz et al. 2015). Therefore, functional analyses of F3H/FNSI and F3'H/F3'5'H homologs are necessary to identify own functions of product from each gene.

N. menziesii petals contain anthocyanins (petunidin 3*p*CG5MG and petunidin 3-*O*-[6-*O*-(*cis-p*-coumaroyl)-β-glucoside]-5-*O*-[6-*O*-(malonyl)-β-glucoside]), flavones

(apigenin 7G4′MG and apigenin 7,4′-*O*-diglucoside (apigenin 7,4′-diG)) and flavonols (kaempferol 3-*O*-(6-rhamnosyl)-*O*-glucoside-7-*O*-glucoside and kaempferol 3-(2,6-*O*-dirhamnosyl)-*O*-glucoside) (Tatuszawa et al. 2014). In this chapter, to elucidate the biosynthesis of color constituents of *N. menziesii* flowers and to isolate possible useful molecular tools for engineering blue flower color, 16 genes encoding 11flavonoid biosynthetic proteins (CHS, CHI, F3H, FNSII, F3′5′H, DFR, ANS, GST, R2R3-MYB, bHLH and EFP) were isolated using petal transcriptome data. Among these, the functions of F3H and F3′5′H were confirmed by functional expression in yeast.

2. 2. Materials and Methods

2. 2. 1. Plant materials

N. menziesii cultivar, ‘Insignis Blue’, was purchased from a florist and cultivated. Its petals were classified into four developmental stages [stage 1, unpigmented/half pigmented buds tightly closed (2–5 mm in length); stage 2, pigmenting buds (5–10 mm in length); stage 3, fully pigmented buds before opening (10–15 mm in length); stage 4, fully opened flowers] (**Fig. 5**). The collected petals were immediately stored at −80 °C until the extraction of crude protein and total RNA.

2. 2. 2. Chemicals

β–Glucosidase and naringinase were purchased from Sigma-Aldrich (St. Louis, USA). DHK, eriodictyol, pentahydroxyflavanone and naringenin were obtained from Extrasynthese (Genay, France). All of them were of analytical grade.

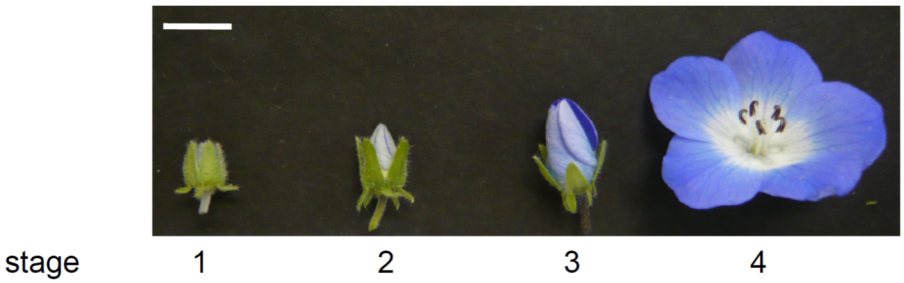

Fig. 5 Developmental stages of *N. menziesii* flowers. Stage 1, unpigmented/half pigmented buds tightly closed (2–5 mm in length); stage 2, pigmenting buds (5–10 mm in length); stage 3, fully pigmented buds before opening (10–15 mm in length); stage 4, fully opened flowers. The numbers indicate petal developmental stages. Bar = 1 cm.

2. 2. 3. Flavonoid analysis

The collected petals of the four stages of flowers and leaves were lyophilized and their flavonoids were extracted using eight times (v/w) of 50% acetonitrile (v/v) containing 0.1% trifluoroacetic acid (TFA).

For anthocyanidin analysis, petal and leaf extracts (0.2 ml) were dried, dissolved in 0.2 ml of 6N HCl, and acid hydrolyzed at 100 °C for 20 min to yield anthocyanidins. Anthocyanidins were extracted with 0.2 ml 1-pentanol and then subjected to HPLC on an ODS-A312 column (15 cm×6 mm; YMC, Kyoto, Japan) at a flow rate of 1 ml min^{-1} using an isocratic solvent (acetic acid:methanol:H_2O, 6:7:27, v/v/v). Anthocyanidins were detected at an absorbance of 400–600 nm using a photodiode array detector (SPD-M20A, Shimadzu, Kyoto, Japan). For flavone and flavonol aglycone analyses, the dried petal and leaf extracts (0.2 ml) were enzymatically hydrolyzed in 0.2 ml of 0.1 M potassium phosphate buffer (KPB) (pH 4.5) containing 6 units of β–glucosidase and 1

unit of naringinase for 16 h at 30 °C. The reaction was terminated by adding 0.2 ml of 90% (v/v) acetonitrile in water containing 0.1% TFA and then subjected to HPLC analysis using a Shim-pack FC-ODS column (15 cm×4.6 mm; Shimadzu) with solvents A (H_2O:TFA, 99.9:0.1, v/v) and B (H_2O:acetonitrile:TFA, 9.9:90:0.1, v/v). The elution consisted of 20% solvent B to 100% solvent B for 10 min, followed by isocratic elution using 100% solvent B for 6 min at a flow rate of 0.6 ml min^{-1}. Flavonoids were monitored by absorbance at 250–450 nm using an SPD-M20A photodiode array detector (SPD-M20A, Shimadzu). Peak identification was based on retention time, absorbance spectrum and co-chromatography with the standard.

2. 2. 4. Transcriptome analysis

Total RNA was isolated from the petals at all four stages and from leaves using RNeasy Plant Mini Kit (Qiagen, Hilden, Germany). Total RNA from petals was used for transcriptome analysis (Eurofingenomics, Erlangen, Germany). Briefly, a normalized cDNA library was constructed from total RNA and sequenced using the GS-FLX system (Roche, Basel, Switzerland). This generated approximately half a million reads with an average length of 400 bases, which were aligned to generate contigs with the use of a Burrows-Wheeler Alignment tool (BWA) (Li and Durbin 2009).

Total RNAs isolated from leaves and petals at four stages of were subjected to RNA-Seq analysis to obtain transcript profiles (Eurofingenomics). A total of 120 million reads were obtained using HiSeq 2000. The number of reads was mapped on the alignments with using the Sequence Alignment/Map Tool software package (Li et al. 2009)

2. 2. 5. Isolation of flavonoid biosynthetic genes

Generated sequences were searched with tBlastX using amino acid sequences of *P. hybrida* or *T. hybrida* flavonoid biosynthetic proteins [CHS, CHI, FNSII, F3H, F3′H, F3′5′H, FLS, DFR, ANS, GST, R2R3-MYB, bHLH and EFP] to obtain homologous contigs. The resulting sequences were aligned with their homologs from various plant species using CLUSTALW (DDBJ version; http://clustalw.ddbj.nig.ac.jp/, version 2.1, amino acid sequence alignment, default parameters). Those amino acid sequences isolated from *N. menziesii* were used for phylogenetic analysis. A Neighbour-Joining tree was constructed using 1,000 bootstrap replicates with CLUSTALW version 2.1 (http://clustalw.ddbj.nig.ac.jp/). A phylogenetic tree was constructed using Dendroscope version 3.5.9 (http://dendroscope.org/). Sequence reads for leaves and petals were mapped to contigs and used to calculate reads per kilobase of exon per million mapped reads (RPKM) values for each contig.

Full-length cDNAs were obtained by RT-PCR using oligonucleotides containing a putative initiation codon and oligo dT primer or oligonucleotides containing a 3′-sequence of a stop codon of each contig (**Table 1**). RT-PCR was conducted using total petal RNA as the template and PrimeSTAR Max DNA Polymerase (Takara Bio, Otsu, Japan). The PCR parameters were as follows: denaturation at 98 °C for 10 s, followed by 30 cycles of denaturation at 98 °C for 10 s, annealing at 55 °C for 5 s, and extension at 72 °C for 30 s, followed by a final extension at 72 °C for 30 s and subsequent cooling to 4 °C. The amplified DNA fragments were cloned into pCR-TOPO vector (Life Technologies, Carlsbad, CA) and sequenced.

Table 1 Flavonoid-related genes isolated in the present study

Clone name	Contig number	Forward primer/ Reverse primer	Accession number
NmCHS1	*c6935*	TCTACGATCATGGAAGAATA/ Oligo dT	LC328814
NmCHS2	*c7811*	TCTACGATCATGGAAGAATT/ Oligo dT	LC328815
NmCHS3	*c4802*	CCGGCCCGAGAATGGTTAGC/ Oligo dT	LC328816
NmCHI1	*c20729*	TATTCACAACAATGTCTACC/ Oligo dT	LC328817
NmFNSII2	*c518*	TCACTAACATGGAGCTTTCG/ Oligo dT	LC328818
NmF3H11	*c1990*	AACCCCATGGCAACATTAAC/ Oligo dT	LC328819
NmF3'5'H10	*c373*	TTATACCCAATGGCCATGGC/ Oligo dT	LC328820
NmDFR1	*c1165*	ACCAAGTATGACCACAATTG/ Oligo dT	LC328821
NmANS1	*c959*	CAAACACCTCTAAATTCACC/ Oligo dT	LC328822
NmGST	*c5620*	AACATGGTGGTTAAAGTTTATGG/ AAGAGATTGGATGAGTTGTGACG	LC328826
NmEFP3	*c8627*	CAAGAAGATGTCTAGTGAAGTTG/ ATCATTTGGATAATTCAGCCAGAG	LC328824
NmEFP4			LC328825
NmMYB1	*c1971*	ATGGGACGTTCACCTTGTTG Oligo dT	
NmMYB2	*c769*	ATGGGAAGATCTCCATGTTG	
NmMYB3	*c6336*	TCATTTCATCTCCAAGCTTC	
NmbHLH	*c1052*	ATGGCGGACCCACCTAGC Oligo dT	

NmA3GT	*c103*	CATATGTCAAAACAACACCATGTAGC/ GGATCCTCATAACAACATAGATAAGAGTG	LC368276
NmA3G5GT	*c1526*	ATGGAATGCAAAAATCCAGATTC/ CTAGGTAATAAATCTGAAATTATTG	LC328828
NmAMT3	*c2127*	CTCGAGATGTCTCTAGGACAAAC/ GGATCCTTAATAAAGACNCCGACATAG	LC330945
NmAMT6			LC328823

2. 2. 6. Functional expression analyses of *F3H* and *F3′5′H in vitro* using yeast

A yeast expression vector, pYES2 (Life Technologies), was used to express *NmF3H* and *NmF3′5′H* cDNAs following the manufacturer's protocol. Crude extracts of yeast transformants were subjected to 2-oxoglutarate-dependent dioxygenase assay for F3H (Saito et al. 1999) and cytochrome P450 monooxygenase assay for F3′5′H (Ueyama et al. 2002) using naringenin as the substrate. As a control, yeast was transformed with an empty pYES2 vector and the crude extract was assayed under the same conditions. The reaction mixtures were extracted with ethyl acetate, dried and subjected to HPLC analysis using a Shim-pack FC-ODS column (150 mm×4.6 mm; Shimadzu) at 40 °C and a flow rate of 0.6 ml min^{-1}. The elution using solvents A and C (H_2O:acetonitrile:TFA, 49.9:50:0.1, v/v) consisted of a 10 min linear gradient from 80% solvent A and 20% solvent C to 70% solvent C, 6 min isocratic elution with 70% solvent C, 1 min linear gradient to 20% solvent C and 11 min of 20% solvent C. Flavonoids were detected at an absorbance of 280 nm using a photodiode array detector (SPD-M20A, Shimadzu). Peak identification was based on retention time, absorbance spectrum and co-chromatography with the standard.

2. 3. Results and Discussion

2. 3. 1. Flavonoid analysis of *N. menziesii* petals

The results of flavonoid analyses are summarized in **Figures 6A** and **6B**. Pelargonidin and cyanidin were not detected. Small amounts of peonidin and malvidin were detected. No anthocyanidins were detected in leaves. The petunidin concentration at stage 4 petals was 0.86 μmol g^{-1} fresh weight. Luteolin, tricetin and myricetin were not detected. The stage 4 petals contained 4.28 μmol g^{-1} apigenin, 9.45 μmol g^{-1} kaempferol and 1.54 μmol g^{-1} quercetin. Leaves contained 0.03 μmol g^{-1} kaempferol and 0.36 μmol g^{-1} quercetin. Concentrations of anthocyanins, flavones and flavonols in petals decreased as petals developed, whereas leaves rarely contained flavonoids. It is known that biosynthesis of flavones/flavonols precedes that of anthocyanins in the petals of most plants, such as *T. hybrida* (Ueyama et al. 2002), *P. hybrida* (Holton et al. 1993) and *Rosa hybrida* (Tanaka et al. 2003). However, earlier synthesis of flavones/flavonols than anthocyanins was unclear in *N. menziesii*.

Apigenin was the almost abundant flavone. Although nemophilin composes of petunidin and apigenin glucosides in equal molar ratios, the amount of apigenin was about 2–3 times higher than that of anthocyanins. The petals contained a greater amount of flavonols than flavones and anthocyanins. The functions of flavonols in *N. menziesii* petals have not yet been elucidated. It is possible that flavonols and an excess amount of flavones function to attract pollinators because they absorb UV light or may have other important biological functions.

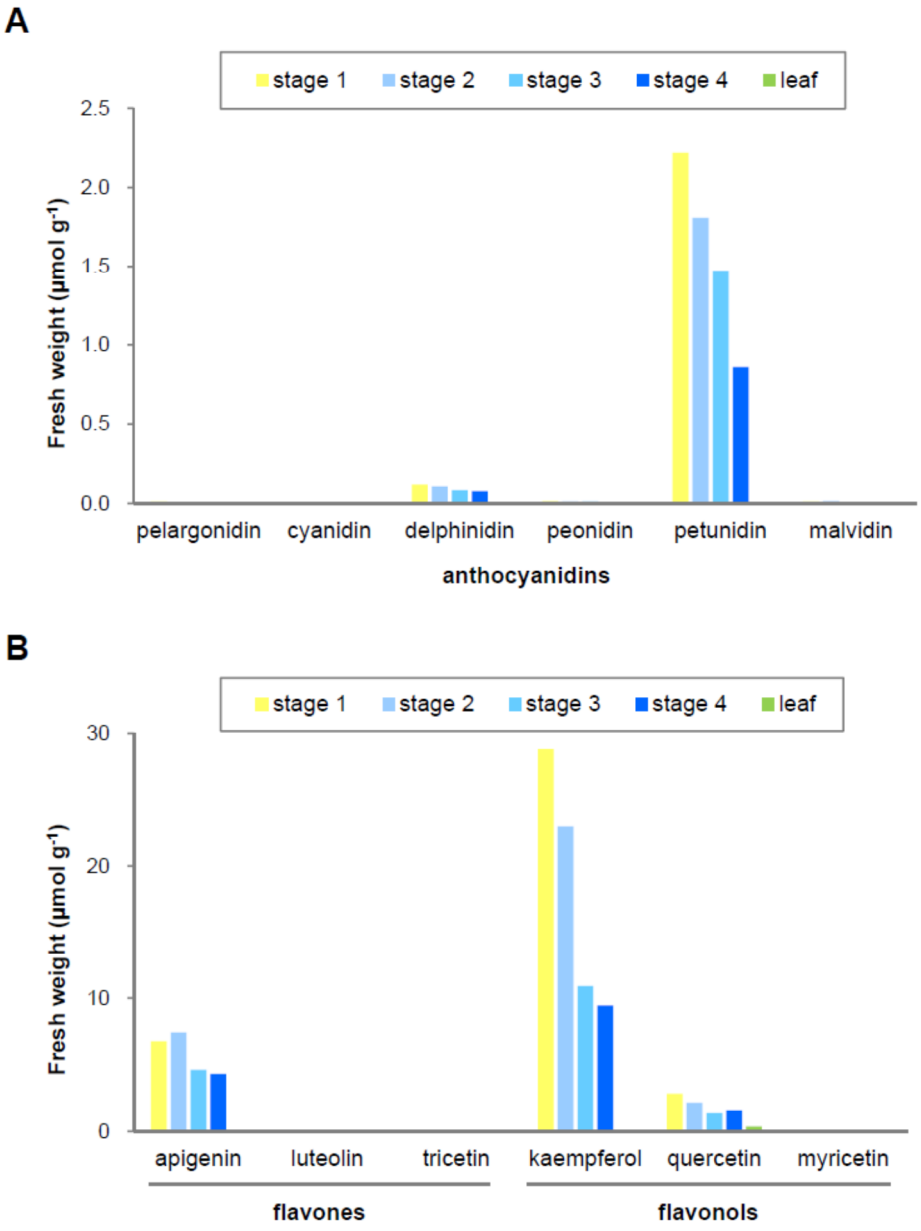

Fig. 6 Developmental flavonoid analysis of *N. menziesii* flowers.

(A) Anthocyanidins at the four developmental stages of the petals and leaves.

(B) Flavone and flavonol aglycones at the four developmental stages of the petals and leaves.

2. 3. 2. Expression and phylogenetic analysis of flavonoid-related genes

A total of 61,491 contigs was obtained and subjected to a search for flavonoid biosynthetic genes. The contig sequences of the flavonoid biosynthetic genes are summarized in **Table 1**. Three CHS homolog sequences were isolated, and two of them, *NmCHS1* (*c6935*) and *NmCHS2* (*c7811*), were very similar. These showed only five residue differences among 386 amino acid residues (98.4% and 98.4% identities in amino acid and nucleotide sequences, respectively). Another CHS homolog, *NmCHS3* (*c4802*), showed significant differences from NmCHS1 (89.1% and 83.3%, respectively) and NmCHS2 (90.4% and 83.4%, respectively). CHS homologs have been isolated from a number of plants. The genus *N. menziesii* belongs to the family *Boraginaceae*, which was previously a part of the order *Lamiales*; however, it is now classified under order *Boraginales* (APG IV 2016). The phylogenetic analysis of CHSs indicates that *N. menziesii* CHSs are related to CHSs of plants belonging to orders *Lamiales*, *Gentianales* and *Solanales*, but they are not included in the clades containing CHSs of these plant orders (**Fig. 7**).

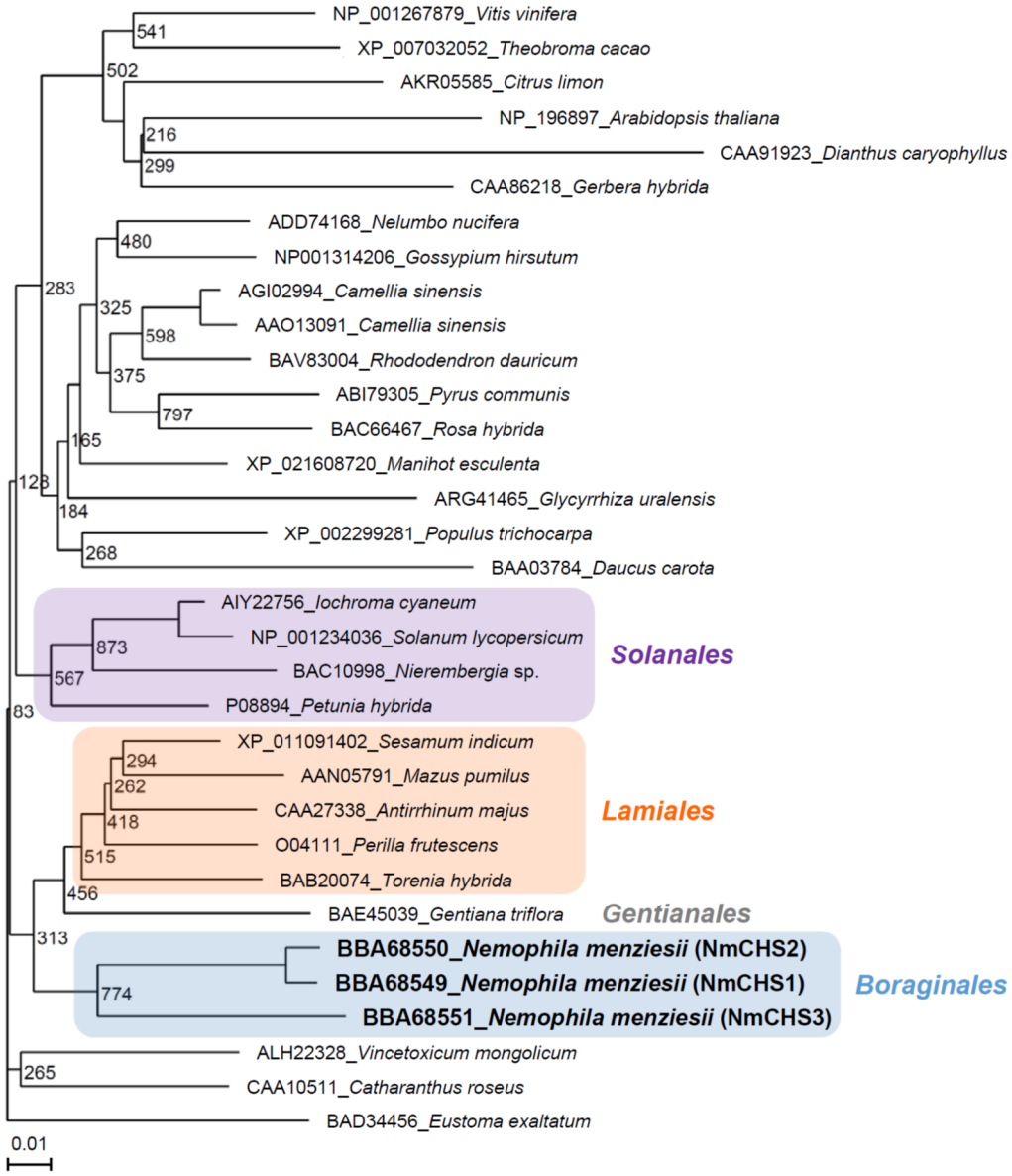

Fig. 7 A phylogenetic tree of CHSs. The amino acid sequences of three CHSs obtained from *N. menziesii* and 30 known CHSs from various plant species were aligned. Accession numbers for those CHSs in the database and species names are shown. Scale bar = 0.01 amino acid substitutions per site.

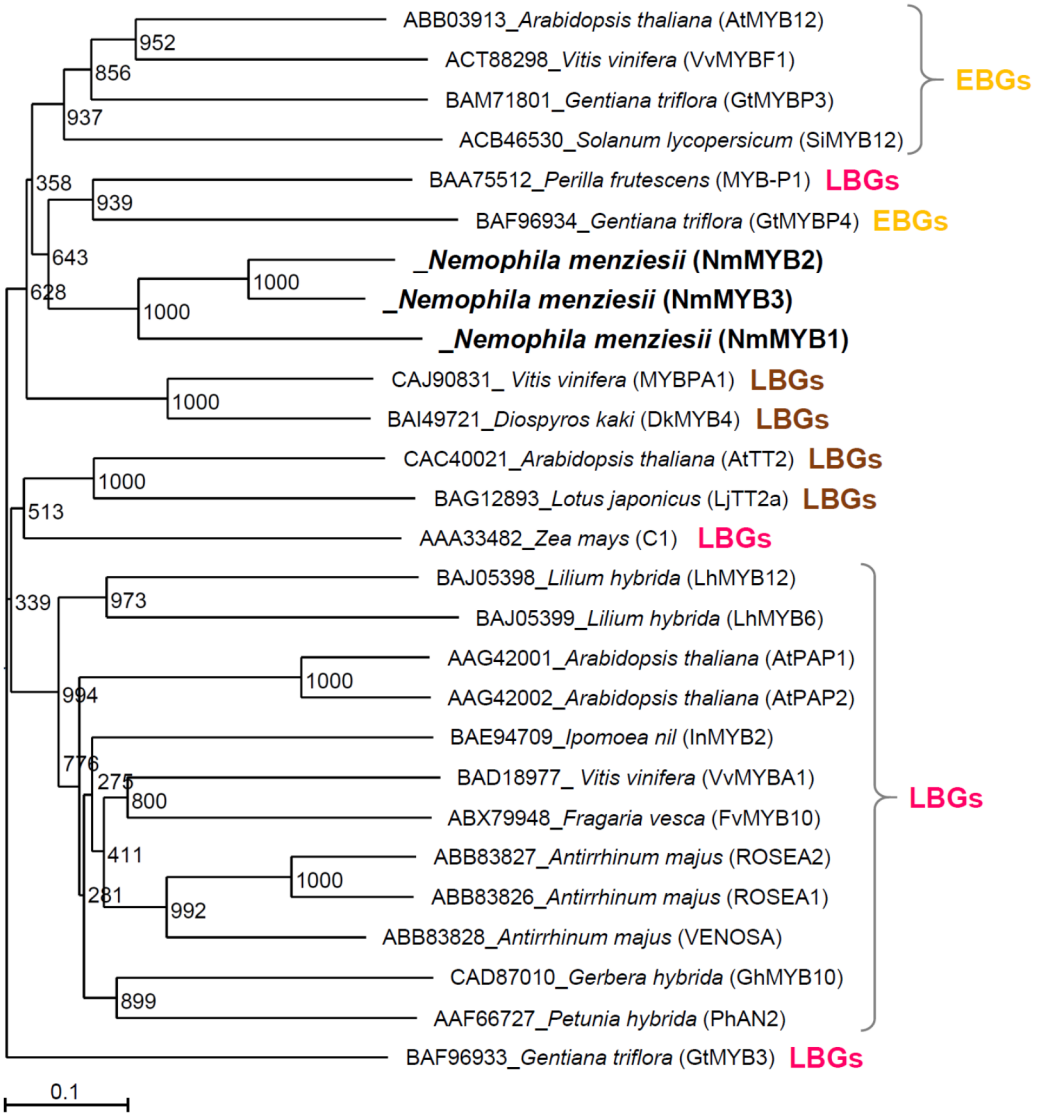

Fig. 8 A phylogenetic tree of R2R3-MYBs associated with the regulation of the flavonoid biosynthetic pathway. The amino acid sequences of three R2R3-MYBs obtained from *N. menziesii* and 24 known R2R3-MYBs from various plant species were aligned. EBGs, early biosynthetic genes (shown in yellow); LBGs, late biosynthetic genes, which are involved in anthocyanin biosynthesis (shown in red) and protoanthocyanin biosynthesis (shown in brown). Accession numbers for those R2R3-MYBs in the database and species names are shown. Scale bar = 0.1 amino acid substitutions per site.

Three types of R2R3-MYB homolog sequences were also isolated (*NmMYB1* (*c1971*), *NmMYB2* (*c769*) and *NmMYB3* (*c6336*)). *NmMYB2* and *NmMYB3* were 71% and 74% identities in amino acid and nucleotide sequences, respectively. Another R2R3-MYB homolog, *NmMYB1* showed more significant differences from NmMYB2 (49% and 51%, respectively) and NmMYB3 (48% and 49%, respectively). Their amino acid sequences were subjected to phylogenetic analysis with R2R3-MYB of proteins derived from other plant species. NmMYB1, NmMYB2 and NmMYB3 were categorized into a group regulating flavonoid biosynthesis (**Fig. 8**).

Two kinds of cDNAs per contig were isolated as the *EFP* genes (*NmEFP3* and *NmEFP4*, 98.1% and 97.0% identities in amino acid and nucleotide sequences, respectively). F3′H counterparts were not found in the *N. menziesii* transcriptome, although the presence of quercetin in petals (**Fig. 6B**) suggests the presence of the *F3′H* gene in the *N. menziesii* genome. Only partial sequences of *FLS* and candidate *WDR* were found. They were not further studied in the present study. In the case of WDR, because unlike R2R3-MYB and bHLH proteins, it is difficult to define a distinct family of proteins based solely on the presence of a WDR motif (Smith et al. 1999; van Nocker and Ludwig 2003).

Expression profiles of isolated genes on the basis of RPKM values are shown in **Figure 9**. *CHS3* expression was most abundant at stage 1 and *CHS3* was more abundant than the *CHS1* and *CHS2* expressions, suggesting that it may play a major role in flavonoid biosynthesis. *CHI* and *F3H* expressions were the highest at stage 2, whereas *F3′5′H* and *ANS* expressions were the highest at stage 3. Flavonoid biosynthetic genes have been divided into two groups, designated as ‘early’ and ‘late’ (Martin et al. 1991; Quattrocchio et al. 1993), which is also applicable for the *N. menziesii* flavonoid

pathway.

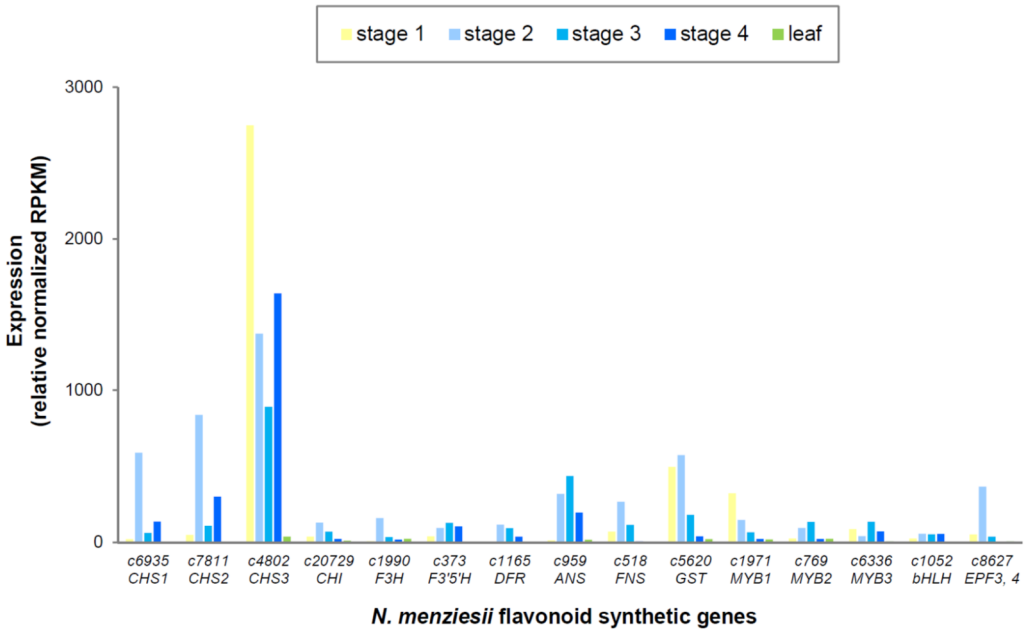

Fig. 9 Transcriptional profiles of flavonoid biosynthetic genes in *N. menziesii*. The genes analyzed and their respective contigs are indicated on the X-axis, while the RPKM values per contig are indicated along the Y-axis.

NmMYB1 is expressed strongly at stage 1 and stage 2 while *NmMYB2* and *NmMYB3* are expressed strongly at stage 3. The results indicated that NmMYB1 may regulate the early steps of the flavonoid biosynthetic pathway and NmMYB2 and NmMYB3 may regulate the late steps of the flavonoid biosynthetic pathway. *NmbHLH* was ubiquitously expressed during flower development as reported in most flowering plants (Koes et al. 2005).

Although the molecular mechanism of EFP function is unknown, the expression profile of *NmEFP* was consistent with those of *EFPs* already reported in *I. nil*, *P.*

hybrida and *T. hybrida* (Morita and Hoshino 2018), which are expressed strongly in the early steps of flavonoid biosynthetic pathway and are expressed co-ordinately with *CHS* (Morita and Hoshino 2018).

2. 3. 3. Functional analysis of NmF3H and NmF3′5′H

The flavonoid biosynthetic pathway involves several soluble 2-oxoglutarate dioxygenases (F3H, ANS, FLS and FNSI) and cytochrome P450 monooxygenases (F3′H, F3′5′H and FNSII), which are microsome membrane-bound enzymes. *NmF3H11* and *NmF3′5′H10* genes were expressed in yeast, and their activities were successfully measured in this study (**Fig. 10**). DHK was generated from naringenin when yeast extract containing recombinant NmF3H11 was subjected to the assay. Yeast expressing NmF3′5′H10 produced eriodictyol and pentahydroxyflavanone from naringenin. NmF3′5′H10 catalyzed the hydroxylation of naringenin more efficiently than *P. hybrida Hf1* F3′5′H expressed under the same conditions (data not shown). *NmF3′5′H10* can be a useful molecular tool for shifting the flavonoid biosynthetic pathway to delphinidin biosynthesis, by which flower colors can be modified to a blue hue (Tanaka and Brugliera 2013).

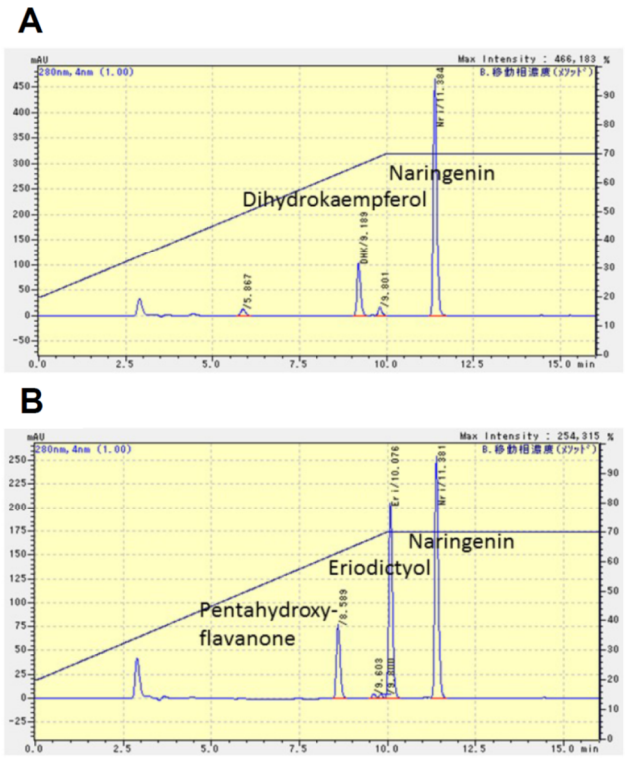

Fig. 10 Enzymatic activity of protein crude extracts of yeast expressing *NmF3H11* or *NmF3′5′H10*. HPLC chromatogram of (A) naringenin incubated with the extract of yeast expressing *NmF3H11*, and (B) naringenin incubated with the extract of yeast expressing *NmF3′5′H10*.

The study in this chapter showed the profiles of flavonoid composition during the developmental stages of *N. menziesii* petals and confirmed that flavonoid-related genes can be isolated comprehensively by the transcriptome analysis of petals. The genes isolated from *N. menziesii* were classified into early and late genes, and these genes were generally expressed in a well-coordinated manner, as reported in many other plants. The genes involved in anthocyanin modification are described in Chapter 3.

Chapter 3 Molecular and biochemical characterization of anthocyanin modification enzymes in *N. menziesii*

3. 1. Introduction

Anthocyanins are diverse in nature, comprising more than 500 molecular species (Andersen and Jordheim 2006). The diversity of anthocyanins enable plants to display various flower colors. Regardless of the structural diversity of anthocyanins, anthocyanidin aglycones usually consist of only three basic structures: pelargonidin, cyanidin and delphinidin (Strack and Wray 1992). The glycosylation, methylation and acylation of anthocyanidins are the primary sources of their structural diversities. Although the pathway leading to the biosynthesis of anthocyanidins is well conserved among plants, anthocyanidin modifications depend on species (Heller and Forkmann 1994; Tanaka et al. 1998).

Among anthocyanin modification enzymes, GyTs, which are ubiquitous in living organisms, catalyze the transfer of sugar moieties to specific acceptor molecules. The GyT superfamily consists of over 90 families, which are further classified into subfamilies on the basis of sequence identity. UDP-glycose-dependent glycosyltransferases (UGTs) which function in the glycosylation of plant secondary compounds, including flavonoids, belong to GT family 1, which are cytosolic enzymes and have been studied extensively (Tanaka et al. 2008; Yonekura-Sakakibara and Hanada 2011). Glycosylation is involved in various pathways, including the regulation of plant hormones, such as indole-3-acetic acid, abscisic acid, cytokinins and brassinosteroids (Gachon et al. 2005), and detoxification of fungal phytotoxins, such as destruxin B and homodestruxin B (MS Pedras et al. 2001). From a point of chemical

view, sugar conjugation results in both increased stability and water solubility. It has also been considered to be a biological flag controlling the compartmentalization of metabolites (Jones and Vogt 2001). The glycosylated forms of anthocyanins are considered to be easily transferrable from the cytoplasmic production site to the vacuole (Jones and Vogt 2001).

In most cases in plants, anthocyanins are first modified at the 3-*O*-glucosylation by anthocyanidin 3-*O*-glucosyltransferase (A3GT), except in a rare instance of *R. hybrida*, which accumulates anthocyanidin 3,5-*O*-diglucoside (anthocyanidin 3,5-diG), where 5-*O*-glucosylation precedes 3-*O*-glucosylation and both reactions are catalyzed by a single enzyme, anthocyanidin 5,3-*O*-glucosyltransferase (anthocyanidin 5,3GT) (Ogata et al. 2005). The genes encoding A3GTs have been isolated and well characterized in *A. majus* (Martin et al. 1991), *Perilla frutescens* (Gong et al. 1997) and *Iris hollandica* (Yoshihara et al. 2005). A3GTs isolated from *V. vinifera* (Sparvoli et al. 1994), *G. triflora* (Tanaka et al. 1996), *P. hybrida* (Yamazaki et al. 2002) and *Freesia hybrida* (Sui et al. 2011; Sun et al. 2016) catalyze 3-*O*-glucosylation of not only anthocyanidins but also flavonols.

The subsequent 5-*O*-glucosylation is catalyzed by anthocyanidin 3-*O*-glucoside 5-*O*-glucosyltransferase (A3G5GT). A3G5GT genes have been isolated from *P. frutescens* (Yamazaki et al. 1999), *Verbena hybrida* (Yamazaki et al. 2002), *P. hybrida* (Yamazaki et al., 2002), *I. hollandica* (Imayama et al., 2004), *G. triflora* (Nakatsuka et al. 2008) and *F. hybrida* (Ju et al. 2018). Recently, vacuolar acyl-glucose-dependent enzymes belonging to GH family 1 have also been shown to catalyze anthocyanin glucosylation (Sasaki and Nakayama 2015). *D. caryophyllus* acyl-glucose-dependent A3G5GT has been isolated as a vacuolar enzyme (Matsuba et al. 2010).

UFGTs catalyzing glycosylation of the 3- and 5-*O* position of flavonoids from different species usually belong to the flavonol/anthocyanidin 3GT cluster and the anthocyanin 5GT cluster, respectively (Fukuchi-Mizutani et al. 2003; Nakatsuka et al. 2008; Yonekura-Sakakibara et al. 2014; Yin et al. 2017).

Anthocyanins are methylated after their glucosylation. The methylation of anthocyanins is catalyzed by AMT. Peonidin-based anthocyanins are biosynthesized from cyanidin-based anthocyanins, and petunidin- and malvidin-based anthocyanins are biosynthesized from delphinidin-based anthocyanins. Further modifications of methylation of anthocyanin glucosides produce a wide variety of anthocyanin compounds that diversify the flower colors.

The *anthocyanin 3′,5′-O-methyltransferase (A3′5′MT)* gene encoding the enzyme that catalyze methylation of the 3′- and 5′-*O* positions to yield malvidin-based anthocyanin, has been isolated from many plants, including *V. vinifera* (Hugueney et al. 2009; Lucker et al. 2010), *Cyclamen persicum* (Akita et al. 2011), *P. hybrida* (Provenzano et al. 2014), *T. hybrida* (Nakamura et al. 2015) and *Paeonia suffruticosa* (Du et al. 2015). On the other hand, there is no report on the isolation of *anthocyanin 3′-O-methyltransferase* (*A3′MT*) from flowering plants that accumulate only petunidin-based anthocyanin. The only *A3′MT* gene was isolated from *P. hybrida* (*MT2*), which also weakly catalyzed 3′,5′-*O*-methylation of anthocyanins (Provenzano et al. 2014).

N. menziesii accumulates petunidin 3*p*CG5MG, which composes nemophilin. In this chapter, A3GT, A3G5GT and AMT were isolated and characterized biochemically *in vitro*. These enzymes are important to modify and stabilize anthocyanins. It is interesting that petunidin, rather than malvidin, is accumulated in the *N. menziesii* petals.

AMT expressed in *E. coli* was shown to selectively catalyze the biosynthesis of petunidin glucosides, rather than malvidin glucosides. This result was consistent with the anthocyanin composition of *N. menziesii* petals.

3. 2. Materials and Methods

3. 2. 1. Plant materials

The plant materials are described in **Chapter 2. 2. 1.**.

3. 2. 2. Chemicals

Pelargonidin, pelargonidin 3-*O*-glucoside (pelargonidin 3G), cyanidin, cyanidin 3-*O*-glucoside (cyanidin 3G), delphinidin, delphinidin 3-*O*-glucoside (delphinidin 3G), malvidin and malvidin 3,5-*O*-diglucoside (malvidin 3,5-diG) were purchased from Extrasynthese. Delphinidin 3,5-*O*-diglucoside (delphinidin 3,5-diG), peonidin, petunidin and malvidin 3G were obtained from Tokiwa Phytochemical (Tokyo, Japan). Pelargonidin 3,5-*O*-diglucoside (pelargonidin 3,5-diG), cyanidin 3,5-*O*-diglucoside (cyanidin 3,5-diG) and peonidin 3,5-*O*-diglucoside (peonidin 3,5-diG) were obtained from Polyphenols (Sandnes, Norway). Peonidin 3-*O*-glucoside (peonidin 3G) and petunidin 3-*O*-glucoside (petunidin 3G) were obtained from AppliChem (Darmstadt, Germany). UDP-glucose and UDP-galactose were obtained from Nacalai Tesque (Kyoto, Japan). *S*-adenosylmethionine was purchased from Sigma-Aldrich. All of them were of analytical grade.

3. 2. 3. Preparation of crude protein extract from *N. menziesii* petals

A 250-mg aqliquot of stage 1 and 2 petals was ground in liquid nitrogen with a mortar and pestle and then thawed in 2 ml of 0.1 M KPB (pH 7.5) containing 100 mM dithiothreitol (DTT), 1 mM polyvinylpyrrolidone 40, and 50 mg ml^{-1} sucrose. After centrifugation at 14,400×g for 10 min, ammonium sulfate was added to the supernatant to 30% saturation. The mixture was stirred for 1 h and centrifuged. Ammonium sulfate was added to the supernatant to 70% saturation, and the mixture was stirred for 1 h before the mixture was centrifuged. The precipitate was dissolved in 500 μl of 0.1 M tris (hydroxymethyl) aminomethane (Tris) –HCl buffer (pH 7.5) containing 2.5 mM DTT and 10 μM (*p*-amidinophenyl) methanesulfonyl fluoride and then desalted using a Sephadex G-25 NAP-5 Column (GE Healthcare, California, USA) equilibrated with the same buffer to obtain crude protein extract. All procedures were carried out at 4 °C. The protein concentration in the extract was quantified by Bio-Rad protein assay (Bio-Rad, Hercules, CA) using bovine serum albumin as standard.

3. 2. 4. Detection of *N. menziesii* A3G5GT activities

GT activities were measured in a 100 μl reaction mixture consisting of the crude protein extract (5μg), 1 mM UDP-glucose or UDP-galactose as a sugar donor and 20 μM delphinidin, delphinidin 3G, petunidin and petunidin 3G as an acceptor and 0.1 M KPB (pH 7.5). After a 10-min pre-incubation at 30 °C, the reaction was initiated by addition of the crude protein extract and acceptor. After incubation at 30 °C for 15 min, the reaction was terminated by the addition of 100 μl of 90% acetonitrile (v/v) containing 0.1% TFA and 0.24 N HCl. The mixture was centrifuged at 12,400×g for 5 min. The supernatant was subjected to HPLC analysis. HPLC was performed using a Shodex

RSpak DE-413L column (250 mm×4.6 mm, Showa Denko, Tokyo, Japan), operated at 40 °C, with a linear gradient using solvent D (H_2O:TFA, 99.5:0.5, v/v)) and E (H_2O:acetonitrile:TFA, 49.5:50:0.5, v/v); from 20% solvent E to 100% solvent B for 15 min, followed by isocratic elution using 100% solvent E for 10 min at a flow rate of 0.6 ml min^{-1}. Anthocyanins were detected at an absorbance of 520 nm using a photodiode array detector (SPD-M20A, Shimadzu). Peak identification was based on retention time, absorbance spectrum and co-chromatography with the standard.

3. 2. 5. Isolation of *NmA3GT, NmA3G5GT and AMT* gene

A BLAST homology search was performed with the amino acid sequences of *P. hybrida*, *T. hybrida* or *P. frutescens* proteins against a petal transcriptome database consisting of 61,491 contigs derived from the normalized cDNA sequence library of *N. menziesii* petals (**Chapter 2. 2. 4.**) to obtain homologous contigs. The resulting sequences were aligned with their homologs from various plant species using CLUSTALW (DDBJ version; http://clustalw.ddbj.nig.ac.jp/, version 2.1, amino acid sequence alignment, default parameters). Those amino acid sequences isolated from *N. menziesii* were used for phylogenetic analysis. A Neighbour-Joining tree was constructed using 1,000 bootstrap replicates with CLUSTALW version 2.1 (http://clustalw.ddbj.nig.ac.jp/). A phylogenetic tree was constructed using Dendroscope version 3.5.9 (http://dendroscope.org/).

The full-length cDNAs were amplified by RT-PCR using total petal RNA and a pair of primers (**Table 1**) designed based on the 5′ and 3′ parts of the genes with Super ScriptII Reverse Transcriptase (Invitrogen, Carlsbad, CA) and KOD-plus polymerase (TOYOBO, Osaka, Japan). The PCR conditions were: 2 min at 94 °C, followed by 30

cycles of 15 s at 94 °C, 30 s at 55 °C, and 30 s at 68 °C for 1 min, then cooling to 4 °C. The amplified DNA fragment (**Table 1**) was subcloned into pCR-TOPO vectors and sequenced. A GeneRacer kit (Invitrogen) was used to obtain full-length cDNA sequences when the contigs contained only partial sequences.

3. 2. 6. Characterization of NmA3GT and NmA3G5GT *in vitro*

cDNAs of *NmA3GT* and *NmA3G5GT* were isolated from *N. menziesii* and subcloned into a pET15b vector (Novagen, Darmstadt, Germany) and expressed in *E. coli* BL2 cells using the Overnight Express Auto Induction System 1 (Novagen) at 25 °C overnight.

The activities of NmA3GT toward anthocyanins were measured in 100 μl of a reaction mixture consenting of 100 ng of purified recombinant protein, 20 μM anthocyanins, 0.5 mM UDP-glucose and 0.1 M KPB (pH 7.5). The recombinant protein was purified to homogeneity by HisTag affinity chromatography with the Profinia protein purification system (Bio-Rad). The reaction mixture was incubated at 30 °C for 6 min. The activities of NmA3G5GT toward anthocyanins were measured in 100 μl of a reaction mixture consenting of 50 ng of purified recombinant protein, 20 μM anthocyanins, 0.5 mM UDP-glucose and 0.1 M KPB (pH 7.5). The reaction mixture was incubated at 30 °C for 12 min. The reaction was terminated by the addition of 100 μl of 90% acetonitrile (v/v) containing 0.1% TFA and 0.24 N HCl. The mixture was centrifuged at 12,400×g for 5 min. The supernatant was subjected to HPLC analysis. HPLC analysis was performed as described above (**Chapter 3. 2. 4.**).

A3GT activities toward flavonols, flavones and isoflavones were assessed in a 100 μl reaction mixture consisting of 50 ng of recombinant purified protein, 20 μM

flavonols, flavones or isoflavones, 1 mM UDP-glucose and 0.1 M Tris–HCl buffer (pH 7.5). The reaction mixture was incubated at 30 °C for 3 min, then the reaction was terminated by adding 100 μl of 90% acetonitrile (v/v) containing 0.1% TFA. The mixture was centrifuged at 12,400×g for 5 min. The supernatant was subjected to HPLC analysis. HPLC was performed using a Shim-pack FC-ODS column (15 cm×4.6 mm; Shimadzu), operated at 40 °C with a linear gradient using solvents A (H_2O:TFA, 99.9:0.1, v/v) and H (H_2O:methanol:TFA, 9.9:90:0.1, v/v), from 20% to 100% solvent H for 16 min, followed by isocratic elution using 100% solvent H for 6 min at a flow rate of 0.6 ml min^{-1}. Flavonoids were detected at a range of absorbances between 250 and 600 nm using a photodiode array detector (SPD-M20A, Shimadzu). Peak identification was based on retention time, spectra, and co-chromatography with the authentic compounds. Enzymatic reactions were performed in three replicates through this study.

3. 2. 7. Functional analysis of *AMT in vitro*

cDNAs of *NmAMT* and *P. hybrida* AMT encoded by the *MT2* locus (Provenzano et al., 2014) were sub-cloned into pET15b expression vector (Novagen) and expressed in *E. coli* using the Overnight Express Autoinduction System 1 (Novagen) at 18 °C for two nights. Recombinant proteins were purified using His-Tag affinity chromatography with the Profinia protein purification system (Bio-Rad). Purified proteins were quantified using the Bio-Rad protein assay (Bio-Rad). AMT assay mixture (0.1 ml) comprised 40 mM KPB (pH 7.5), 50 μM anthocyanin, 1 mM *S*-adenosylmethionine, 2 mM $MgCl_2$, and 3 μg recombinant protein. The mixture was incubated at 30ºC for 15 min, and the reaction was terminated by adding 90% acetonitrile containing 0.1% TFA and 0.24 N

HCl. The reacted mixture was then subjected to HPLC analysis. HPLC analysis was performed as described above (**Chapter 3. 2. 4.**).

The K_m value for delphinidin 3G was determined by 12 mins reaction with the substrate at concentrations ranging between 5 and 150 μM using the Lineweaver–Burk plot. This experiment was repeated three times.

3. 3. Results and Discussion

3. 3. 1. Analysis of A3GT and A3G5GT activities in crude petal protein extracts

When delphinidin was reacted with the crude protein extract from *N. menziesii* petals in the presence of UDP-glucose, it was converted into delphinidin 3,5-diG and a small amount of delphinidin 3G (**Fig. 11C**). Using delphinidin 3G and petunidin 3G as a substrate in the presence of UDP-glucose, they were converted into delphinidin 3,5-diG and petunidin 3,5-diG, respectively (**Figs. 11F, I**). These results indicate that the extract contains UDP-glucose-dependent A3GT and A3G5GT activities but not anthocyanidin 5-*O*-glucosyltransferase or anthocyanidin 5-*O*-glucoside 3-*O*-glucosyltransferase activities, suggesting that anthocyanidins are glucosylated at 3-*O* position and then at 5-*O* position in *N. menziesii* petals just as other plants. When UDP-galactose was used as a sugar donor, no products were detected (data not shown).

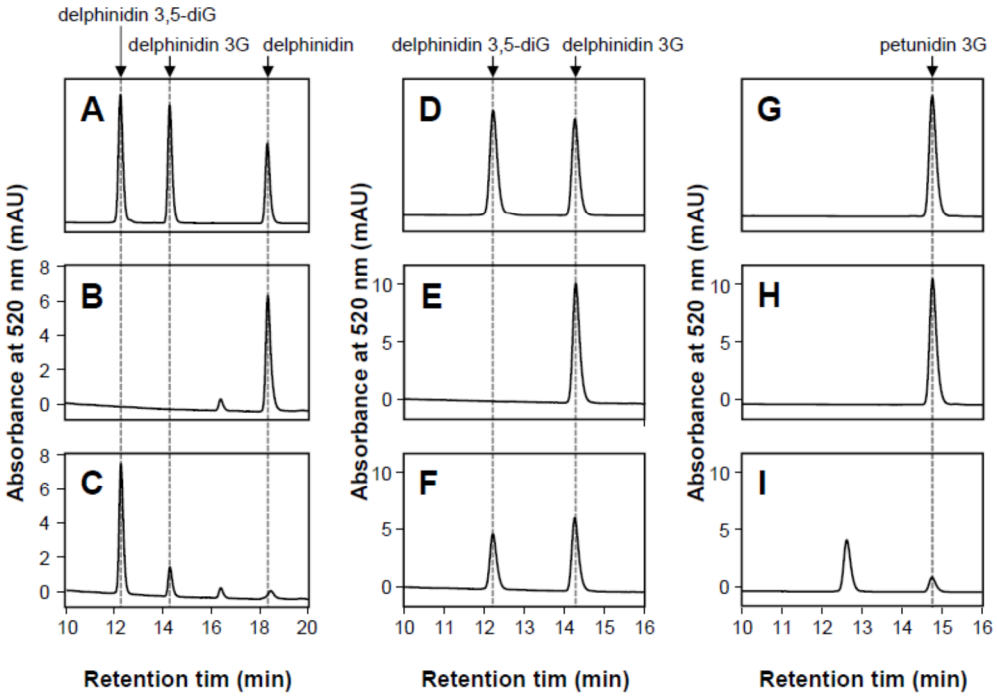

Fig. 11 Detection of A3G5GT activity in the crude protein extract from *N. menziesii* petal. HPLC chromatogram of (A) delphinidin, delphinidin 3-*O*-glucoside and delphinidin 3,5-*O*-diglucoside, (B) delphinidin incubated with the crude protein without UDP-glucose, (C) delphinidin incubated with the crude protein and UDP-glucose, (D) delphinidin 3-*O*-glucoside and delphinidin 3,5-*O*-diglucoside, (E) delphinidin 3-*O*-glucoside incubated with the crude protein without UDP-glucose, (F) delphinidin 3-*O*-glucoside incubated with the crude protein and UDP-glucose, (G) petunidin 3-*O*-glucoside, (H) petunidin 3-*O*-glucoside incubated with the crude protein without UDP-glucose, and (I) petunidin 3-*O*-glucoside incubated with the crude protein and UDP-glucose.

3. 3. 2. Expression and phylogenetic analysis of *NmA3GT, NmA3G5GT and NmAMT*

A total of 61,491 contigs were obtained from the *N. menziesii* transcriptome and subjected to searches for homolog sequences of A3GT, A3G5GT and AMT. *NmA3GT* (*c103*), *NmA3G5GT* (*c1526*) and *NmAMT* (*c2127*) were isolated. Phylogenetic analyses revealed that NmA3GT belongs to the flavonol/anthocyanidin 3GT cluster while NmA3G5GT does not belong to the anthocyanin 5GT cluster but is related to the anthocyanin 5GT cluster (**Fig. 12**). No contig belonging to the anthocyanin 5GT cluster was found in the *N. menziesii* transcriptome when *P. hybrida*, *T. hybrida* and *P. frutescens* A3G5GT homologs were used as queries.

Two kinds of cDNAs from the *c2127* were isolated as the *AMT* candidates (*NmAMT3* and *NmAMT6,* 97.8% and 97.9% identities in amino acid and nucleotide sequences, respectively) genes.

Interestingly, *NmA3GT*, *NmA3G5GT* and *NmAMT*, all of which function at later stages in the pathway than *ANS*, were expressed strongly at stages 1 and 2 (**Fig. 9; Fig. 13**).

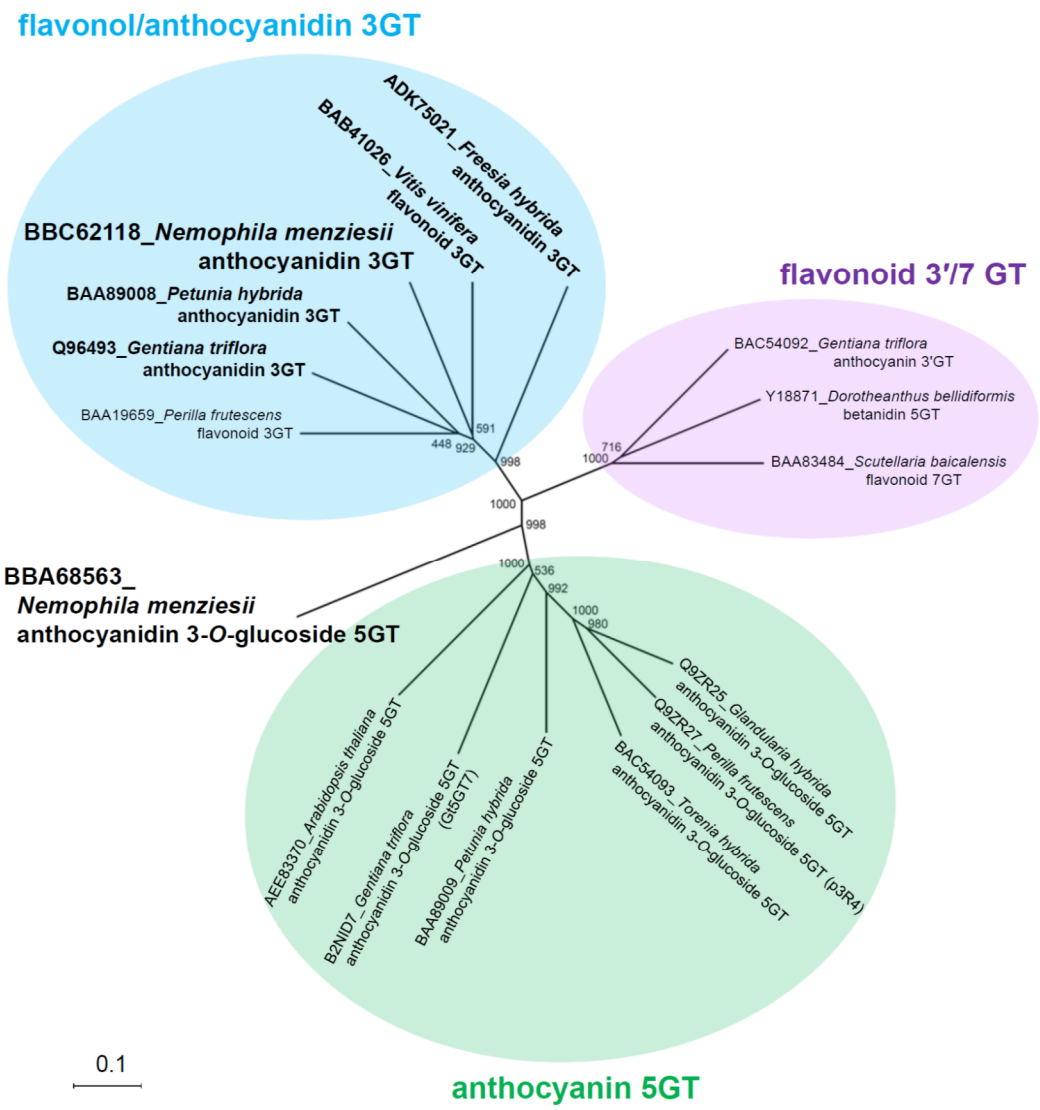

Fig. 12 A phylogenetic tree of flavonol/anthocyanidin 3GTs, anthocyanin 5GTs and flavonoid 3′/7GTs. The amino acid sequences of A3GT and A3G5GT obtained from *N. menziesii* and 14 known UFGTs from various plant species were aligned. Accession numbers for those GTs in the database and species names are shown. GTs catalyzing 3-*O*-glucosylation toward both anthocyanidins and flavonols are shown with bold letters. Scale bar = 0.1 amino acid substitutions per site.

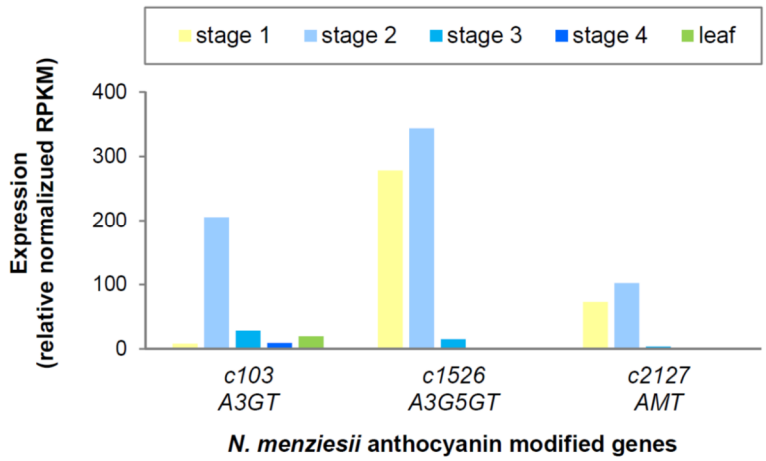

Fig. 13 Transcriptional profiles of anthocyanin-modified genes in *N. menziesii*. The genes analyzed and their respective contigs are indicated on the X-axis, while the RPKM values per contig are indicated along the Y-axis.

3. 3. 3. Characterization of recombinant NmA3GT and NmA3G5GT *in vitro*

The recombinant NmA3GT catalyzed the 3-*O*-glucosylation of delphinidin (**Fig. 14C**). It also catalyzed 3-*O*-glucosylation of pelargonidin more efficiently and of peonidin, petunidin and malvidin less efficiently. The activity toward cyanidin was low (**Table 2**). It did not catalyze glucosylation of anthocyanidin 3G. Since *N. menziesii* petals do not contain pelargonidin-based anthocyanins (Tatsuzawa et al. 2014; **Chapter 2**; **Fig. 6A**), A3GT activities of NmA3GT toward pelargonidin was not considered to be physiological. The recombinant A3GT protein also exhibited the 3GT activity toward flavonols (**Fig. 14 F**; **Table 3**) as reported in *V. vinifera* (Sparvoli et al. 1994), *G. triflora* (Tanaka et al. 1996), *P. hybrida* (Yamazaki et al. 2002) and *F. hybrida* (Sui et al. 2011; Sun et al, 2016). Kaempferol 7G could serve as the substrate while flavonol 3Gs, flavones and isoflavones could not (**Table 3**).

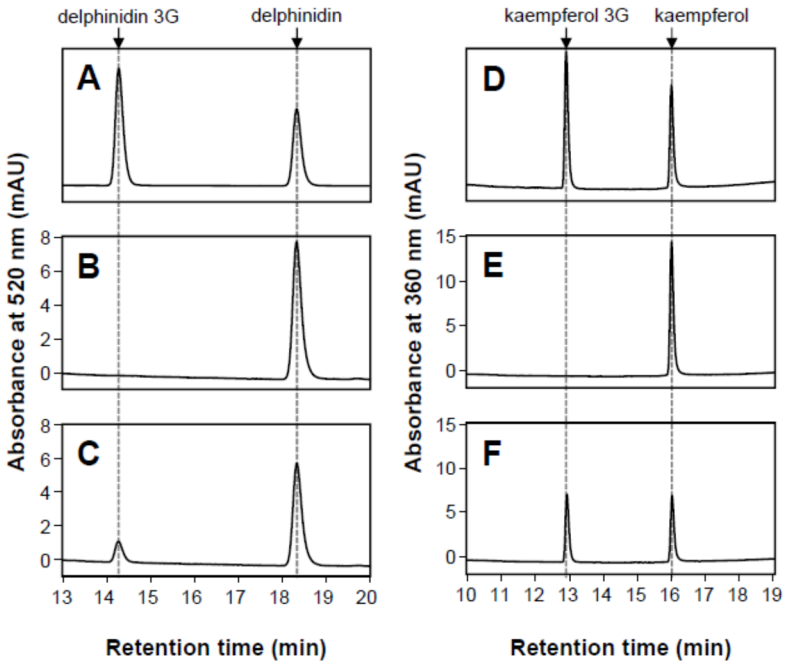

Fig. 14 Enzymatic activity of the purified recombinant NmA3GT expressed in *E. coli*. HPLC chromatogram of (A) delphinidin and delphinidin 3-*O*-glucoside, (B) delphinidin incubated without NmA3GT, (C) delphinidin incubated with NmA3GT, (D) kaempferol and kaempferol 3-*O*-glucoside, (E) kaempferol incubated without NmA3GT, and (F) kaempferol incubated with NmA3GT.

Table 2 Relative activity of the recombinant NmA3GT toward anthocyanins

Substrate	Product	Relative activity (%)
Pelargonidin	Pelargonidin 3G	200 ± 0.2
Cyanidin	Cyanidin 3G	8.1 ± 5.4
Delphinidin	Delphinidin 3G	100
Peonidin	Peonidin 3G	42.4 ± 2.2
Petunidin	Petunidin 3G	54.0 ± 4.4
Malvidin	Malvidin 3G	18.8 ± 3.0
Pelargonidin 3G	ND	ND
Cyanidin 3G	ND	ND
Delphinidin 3G	ND	ND
Peonidin 3G	ND	ND
Petunidin 3G	ND	ND
Malvidin 3G	ND	ND

Averages and SD of three reactions are shown. The relative activity of NmA3GT was calculated based on 100% activity toward delphinidin. ND, not detected.

Table 3 Relative activity of the recombinant NmA3GT toward flavones, flavonols and isoflavones

Substrate	Product	Relative activity (%)
Kaempferol	Kaempferol 3G	100
Kaempferol 3G	ND	ND
Kaempferol 7G	Kaempferol 3,7-diG	101 ± 5.9
Quercetin	Quercetin 3G	84.8 ± 7.6
Quercetin 3G	ND	ND
Apigenin	ND	ND
Apigenin 4'G	ND	ND
Apigenin 7G	ND	ND
Luteolin	ND	ND
Luteolin 4'G	ND	ND
Luteolin 7G	ND	ND
Genistein	ND	ND
Daidzein	ND	ND

Averages and SD of three reactions are shown. The relative activity of NmA3GT was calculated based on 100% activity toward kaempferol. The product derived from kaempferol 7G was tentatively determined as kaempferol 3,7-diG, because the product was different from kaempferol 3G and kaempferol 7G and the enzyme catalyzed 3-*O*-glucosylation of kaempferol and quercetin. See text for details. ND, not detected.

The recombinant NmA3G5GT catalyzed 5-*O*-glucosylation of delphinidin 3G and petunidin 3G to yield delphinidin 3,5-diG and petunidin 3,5-diG, respectively (**Figs. 15C, F**). The enzyme showed broad substrate specificities toward several anthocyanidin 3Gs to yield the corresponding anthocyanidin 3,5-*O*-diglucosides (**Table 4**). For the enzyme, the best substrates among anthocyanidin 3Gs examined were petunidin 3G and pelargonidin 3G. Since pelargonidin glucosides are not accumulated in *N. menziesii* petals (Tatsuzawa et al. 2014; **Chapter 2**; **Fig. 6A**), A3GT5GT activities of NmA3G5GT toward pelargonidin 3G was not considered to be physiological. Among anthocyanidin 3Gs, delphinidin 3G and petunidin 3G may be the substrates of A3G5GT in *N. menziesii* petals due to the anthocyanin composition of *N. menziesii* petals (Tatsuzawa et al. 2014; **Chapter 2**; **Fig. 6A**). The relative activity of delphidin 3G was 53.8% compared with that of petunidin 3G (100%) (**Table 4**). NmA3G5GT efficiently catalyzed the 5-*O*-glucosylation of both delphinidin 3G and petunidin 3G, indicating that the *N. menziesii* anthocyanin biosynthetic pathway involved in glucosylation may form a metabolic grid as reported for many plants, such as *P. frutescens* (Yamazaki et al. 1999) and *T. hybrida* (Nakamura et al. 2015).

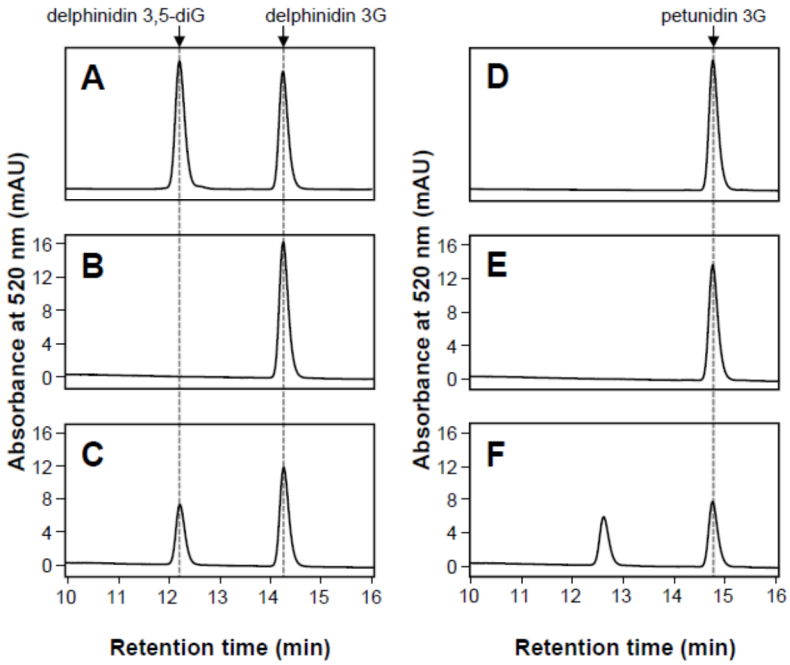

Fig. 15 Enzymatic activity of the purified recombinant NmA3G5GT expressed in *E. coli*. HPLC chromatogram of (A) delphinidin 3-*O*-glucoside and delphinidin 3,5-*O*-diglucoside, (B) delphinidin 3-*O*-glucoside incubated without NmA3G5GT, (C) delphinidin 3-*O*-glucoside incubated with NmA3G5GT, (D) petunidin 3-*O*-glucoside, (E) petunidin 3-*O*-glucoside incubated without NmA3G5GT, and (F) petunidin 3-*O*-glucoside incubated with NmA3G5GT.

Table 4 Relative activity of the recombinant NmA3G5GT toward anthocyanins

Substrate	Product	Relative activity (%)
Pelargonidin 3G	Pelargonidin 3,5-diG	91.4 ± 17.5
Cyanidin 3G	Cyanidin 3,5-diG	57.5 ± 4.1
Delphinidin 3G	Delphinidin 3,5-diG	53.8 ± 1.9
Peonidin 3G	Peonidin 3,5-diG	70.4 ± 4.5
Petunidin 3G	Petunidin 3,5-diG	100
Malvidin 3G	Malvidin 3,5-diG	47.4 ± 1.8
Pelargonidin 3,5-diG	ND	ND
Cyanidin 3,5-diG	ND	ND
Delphinidin 3,5-diG	ND	ND
Peonidin 3,5-diG	ND	ND
Malvidin 3,5-diG	ND	ND

Averages and SD of three reactions are shown. Averages and SD of thee reactions are shown. The relative activity of NmA3G5GT was calculated based on 100% activity toward petunidin 3G. The product derived from petunidin 3G was tentatively determined as petunidin 3,5-diG, because the enzyme catalyzed 5-*O*-glucosylation of pelargonidin 3G, cyanidin 3G, delphinidin 3G, peonidin 3G and malvidin 3G. ND, not detected.

3. 3. 4. Functional analysis of recombinant AMT *in vitro*

Since *N. menziesii* dominantly accumulates petunidin-based anthocyanins, rather than malvidin-based anthocyanins, the substrate specificity of *N. menziesii* AMT was elucidated. Among the two AMT homologs (NmAMT3 and NmAMT6), only NmAMT6 was subjected to further study because they differ in terms of only 5 out of 232 amino acid residues (**Fig. 16**), and preliminary enzymatic characterization of the recombinant NmAMT3 and NmAMT6 indicated that their substrate preferences are similar (data not shown).

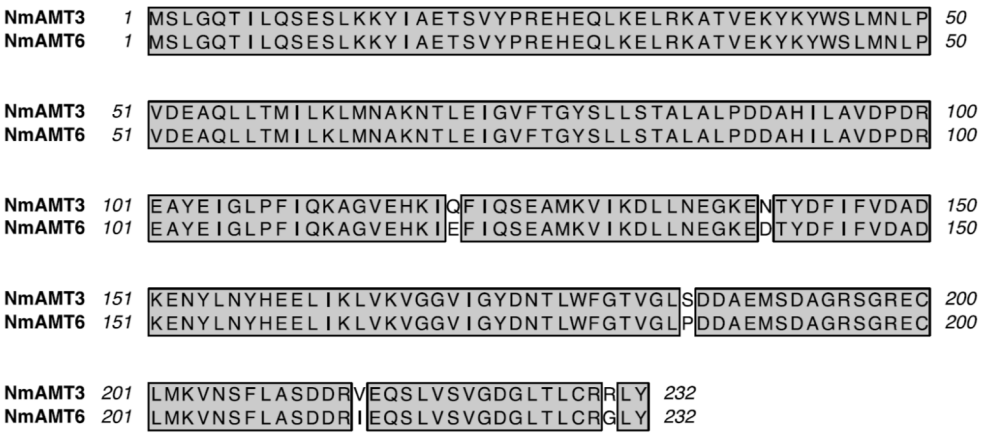

Fig. 16 Alignment of NmAMT3 and NmAMT6. Identical amino acid residues are highlighted in gray.

Table 5 Comparison of substrate preference of NmAMT6 and *P. hybrida MT2* AMT

Substrate	Relative activities (%)	
	NmAMT6	***P. hybrida MT2* AMT**
Delphinidin 3G	100 (Pet 97.8%, Mal 2.2%)	100 (Pet 90.3%, Mal 9.7%)
Delphinidin 3,5-diG	85.7 ± 3.6 (Pet 86.0%, Mal 13.0%)	46.9 ± 11.8 (Pet 98.8%, Mal 1.2%)
Petunidin 3G	8.75 ± 2.2	25.0 ± 12.0

Relative activities are shown relative to delphinidin 3G, which was set at 100%. Data represent averages and SD of three independent assays. Percentages of petunidin (Pet) and malvidin (Mal) glucoside of total products in the reaction mixture are shown in parentheses.

Comparative analyses of substrate and product specificity of NmAMT6 and *P. hybrida MT2* AMT were conducted (**Table 5**). *P. hybrida MT2* AMT preferably produces petunidin over malvidin (Provenzano et al. 2014). The methylation efficiency of recombinant NmAMT6 was much higher for the substrates delphinidin 3G and delphinidin 3,5-diG than for petunidin 3G. In contrast, *P. hybrida MT2* AMT preferably catalyzed methylation of delphinidin 3G than of delphinidin 3,5-diG and petunidin 3G. Reactions of the recombinant NmAMT6 with delphinidin 3G and delphinidin 3,5-diG produced petunidin 3G and petunidin 3,5-diG, respectively, and only small amounts of malvidin 3G (2.2% of total products) and malvidin 3,5-diG (13.0% of total products), respectively. *P. hybrida MT2* AMT yielded more malvidin 3G (9.7%) from delphinidin 3G than NmAMT6 and less malvidin 3,5-diG (1.2%) from delphinidin 3,5-diG.

Interestingly, the ratio of malvidin glucosides produced varied depending on substrates. The low production of malvidin glucosides by NmAMT6 and *P. hybrida MT2* AMT is in contrast to that by *V. vinifera* (Hugueney et al. 2009), *P. hybrida* MF1 and MF2 (Provenzano et al. 2014) and *T. hybrida* (Nakamura et al. 2015) AMTs, which were demonstrated to efficiently catalyze 3′ and 5′-*O*-methylations of delphinidin glucosides to yield malvidin glucosides. *C. persicum* AMT was also shown to catalyze malvidin production (Akita et al. 2011). The low production of malvidin glucosides by NmAMT6 (**Table 5**) is possibly due to its low reactivity to petunidin glucosides. This specificity explains the anthocyanidin composition of *N. menziesii* petals containing petunidin, but not malvidin.

Since NmAMT6 efficiently catalyzed the methylation of both delphinidin 3G (85.7%) and delphinidin 3,5-diG (100%) (**Table 5**), the *N. menziesii* anthocyanin biosynthetic pathway may form a metabolic grid, as reported for many other plants, such as *P. frutescens* (Yamazaki et al. 1997) and *G. triflora* (Fukuchi-Mizutani et al. 2003).

Depleting Mg^{2+} from the reaction mixture decreased the activity of NmAMT6 to < 2% (data not shown), indicating that NmAMT6 activity depends on Mg^{2+}, as is true for AMTs of other plants, including *V. vinifera* (Hugueney et al. 2009). The K_m and k_{cat} values for delphinidin 3G of NmAMT6 were 26.8 ± 4.67 μM and 13,100 ± 312 s^{-1}, respectively. The K_m value of NmAMT6 is consistent with that of *T. hybrida* (Nakamura et al. 2015), *V. vinifera* (Hugueney et al. 2009), *S. lycopersicum* (Roldan et al. 2014) and *P. suffruticosa* (Du et al. 2015) for anthocyanins ranging from 1.1 to 123 μM.

This chapter demonstrated that *N. menziesii* anthocyanin modification genes, such as *NmA3GT*, *NmA3G5GT* and *NmAMT,* were identified and their recombinant enzymes were characterized biochemically. The recombinant NmA3GT exhibited a wide 3GT activity toward not only anthocyanidins but also flavonols. The substrate specificity of NmAMT6 was consistent with the anthocyanin composition of *N. menziesii* petals accumulating mainly petunidin-based anthocyanins rather than malvidin-based anthocyanins. Additionally, *in vitro* activity of NmA3G5GT and NmAMT6 indicated that the biosynthetic pathway from delphinidin 3G to petunidin 3,5-diG forms a metabolic grid in *N. menziesii* petals (**Fig. 17**). The best substrates of NmA3G5GT and NmAMT6 are also delphinidin 3G and petunidin 3G, respectively, suggesting that delphinidin 3G is mainly methylated at the 3′-*O* position by NmAMT6 and then glucosylated at 5-*O* position by A3G5GT. To understand the biosynthesis of petunidin 3*p*CG5MG, gene isolation and functional characterization of ATs catalyzing 3*p*-coumaroylation and 5-malonylation are required.

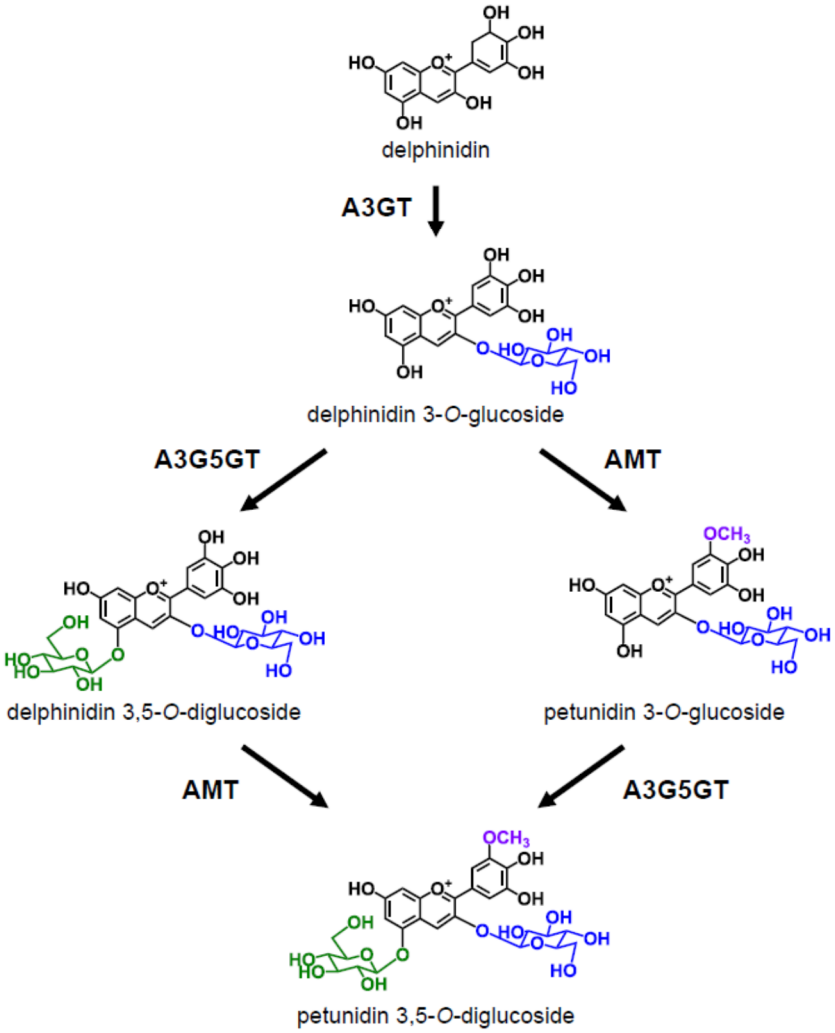

Fig. 17 Biosynthetic pathway of petunidin 3,5-*O*-diglucoside synthesis in *N. menziesii* petals. A3GT, anthocyanisin 3-*O*-glucosyltransferase; A3G5GT, anthocyanisin 3-*O*-glucoside 5-*O*-glucosyltransferase; AMT, *S*-adenosylmethionine-dependent anthocyanin *O*-methyltransferase.

NmA3G5GT gene related to the anthocyanin 5GT cluster was isolated and exhibited 5-*O*-glucosylation activity *in vitro*. Since no contig belonging to the anthocyanin 5GT cluster was obtained from the *N. menziesii* transcriptome, Nm3G5GT may catalyze 5-*O*-glucosylation of anthocyanidin 3G in *N. menziesii*. However, unsuccessful identification of GT belonging to the anthocyanin 5GT cluster is not excluded. To confirm the physiological function of NmA3G5GT, further studies are necessary, such as knockout of *NmA3G5GT* gene in *N. menziesii*, and ectopic expression of *NmA3G5GT* gene in *A. thaliana A5GT* mutant (At4g14090, Salk_108458, Columbia background) and wild-type *N. tabacum* plants accumulating mainly cyanidin 3-*O*-rutinoside in their petals.

The following chapter focuses on key flavone glucosyltransferase genes, which are essential for blue metalloanthocyanin formation.

Chapter 4 Identification and characterization of a novel *N. menziesii* flavone glucosyltransferases that catalyzes flavone 7,4′-*O*-diglucoside, a key component of the blue metalloanthocyanin

4. 1. Introduction

The pure blue color of the *N. menziesii* flower is derived from metalloanthocyanin, nemophilin, which consists of six petunidin-based anthocyanin molecules and six molecules of apigenin 7,4′-diG or its derivatives with two metal ions (Fe^{3+} and Mg^{2+}) in the center of the complex (Yoshida et al. 2009; Yoshida et al. 2015; **Figs. 3A–C**). The two apigenin glucosyl moieties at the 7- and 4′-*O* positions have been shown to be crucial for metalloanthocyanin formation (Kondo et al. 2001; Yoshida et al. 2009).

One plant species may contain more than 100 different GT family 1 members (Yonekura-Sakakibara and Hanada 2011). Flavonoids are very often modified with several glycosyl moieties, and plants adopt various tactics to achieve specific flavonoid modifications. Anthocyanidin 3,5-diG and its derivatives are widely distributed in plant species and synthesized stepwise by A3GT and A3G5GT in *P. frutescens* (Yamazaki et al. 1999), *P. hybrida* (Yamazaki et al. 2002) and *G. triflora* (Nakatsuka et al. 2008), while 5- and 3-*O*-glucosylation of anthocyanidin 3,5-diG in *R. hybrida* and 3′- and 5′-*O*-glucosylation of delphinidin 3,3′,5′-*O*-triglucoside in *C. ternatea* are catalyzed by single enzymes, anthocyanidin 5,3GT and anthocyanin 3′,5′GT, respectively (Ogata et al. 2005; Noda et al. 2017). *A. thaliana* contains many kinds of flavonol glycosides, which have been shown to synthesize stepwise glycosylation by UFGT (Yonekura-Sakakibara et al. 2008; Saito et al. 2013; Yonekura-Sakakibara et al. 2014).

UFGTs whose activity is glycosylation of flavonoids are classified into several

clusters on the basis of their amino acid sequence identities (Fukuchi-Mizutani et al. 2003; Nakatsuka et al. 2008; Yonekura-Sakakibara et al. 2014; Yin et al. 2017). UFGTs catalyzing glycosylation at the same position in flavonoids from different species usually belong to the same clusters, as described below. As mentioned previously (**Chapter 1**), UFGTs can be classified into the following clusters: flavonol/anthocyanidin 3GTs, anthocyanin 5GTs, flavonoid 3′/7GTs and GGTs (Fukuchi-Mizutani et al. 2003; Nakatsuka et al. 2008; Yonekura-Sakakibara et al. 2014; Yin et al. 2017). Interestingly, *C. ternatea* anthocyanin 3′,5′GT belongs to the flavonol/anthocyanidin 3GT cluster (Noda et al. 2017), and the anthocyanin 5GT-like sequence of *Pyrus communis* and *Camellia sinensis* have been suggested to be flavonol 7-*O*-glucosyltransferase (Fischer et al. 2007; Dai et al. 2017). *R. hybrida* anthocyanidin 5,3 GT (Ogata et al. 2005) and *A. majus* chalcone 4′-*O*-glucosyltransferase (Ono et al. 2006) do not belong, but are related to the flavonoid 3′/7GT cluster.

Many UFGTs have been shown to exhibit flavone 4′ or 7-*O*-glucosyltransferase activities *in vitro*. *Dorotheanthus bellidiformis* betanidin 5-*O*-glucosyltransferase (Vogt et al. 1999) showed flavonoid 4′ and 7-*O*-glucosyltransferase activities. *G. max* isoflavone 7-*O*-glucosyltransferases (IF7GT) (GmUGT1 and GmUGT7) (Noguchi et al. 2007; Funaki et al. 2015) exhibited flavone 4′-*O*-glucosyltransferase (F4′GT) activity. *Scutellaria baicalensis* flavonoid 7-*O*-glucosyltransferase (Hirotani et al. 2000), *Beta vulgaris* flavonoid GTs (UGT73A4 and UGT71F1) (Isayenkova et al. 2006), and *D. bellidiformis* betanidin 6-*O*-glucosyltransferase (Vogt et al. 1997), exhibited 7-*O*-glucosylation activity toward apigenin or luteolin *in vitro*. In spite of these studies, our knowledge of flavone glucosylation *in vivo* remains very limited.

In the present study, a set of biosynthetic flavonoid genes including *FNSII* was

isolated from *N. menziesii* (**Chapters 2, 3**) to understand the molecular biology of nemophilin biosynthesis. However, the biosynthesis of apigenin 7,4′-diG has not yet been characterized. In this chapter, it was revealed that F4′GT and flavone 4′-*O*-glucoside 7 *O*-glucosyltransferase (F4′G7GT) sequentially catalyze biosynthesis of flavone 7,4′-diG. The genes encoding these GTs were isolated and characterized *in vitro* and *in vivo*. These genes are expected to be useful molecular tools that alter flower color to a bluer hue by metalloanthocyanin accumulation.

4. 2. Materials and Methods

4. 2. 1. Plant materials

The plant materials are described in **Chapter 2. 2. 1.**.

4. 2. 2. Chemicals

Apigenin, apigenin 7-*O*-glucoside (apigenin 7G), luteolin, luteolin 4′-*O*-glucoside (luteolin 4′G), luteolin 7-*O*-glucoside (luteolin 7G), kaempferol, kaempferol 3-*O*-glucoside (kaempferol 3G), kaempferol 7-*O*-glucoside (kaempferol 7G), quercetin and quercetin 3-*O*-glucoside (quercetin 3G) were purchased from Extrasynthese. Quercetin 4′-*O*-glucoside (quercetin 4′G) was purchased from Tokiwa Phytochemical. Genistein and daidzein were obtained from the Cayman Chemical Company (Ann Arbor, MI, USA). Apigenin 7,4′-diG was provided by Dr. Yoshida (Nagoya University). UDP-glucose and UDP-galactose were purchased from Nacalai Tesque. All of them were of analytical grade.

The apigenin 4′-*O*-glucoside (apigenin 4′G) used for biochemical assays in this study was isolated from an enzymatic reaction mixture with apigenin and recombinant

F4′GT isolated from *N. menziesii*. Its identity was confirmed by comparing it with the chemically synthesized authentic apigenin 4′G whose structure had been verified by NMR measurement (**Fig. 18**).

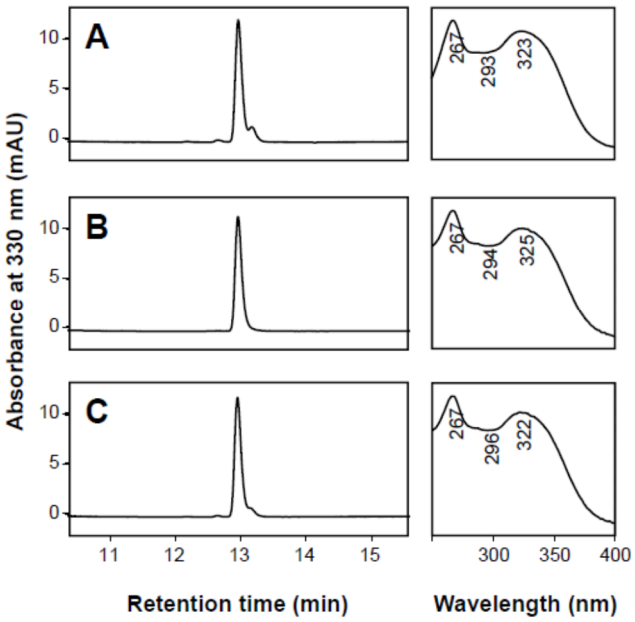

Fig. 18 Comparison of the enzymatically synthesized apigenin 4′-*O*-glucoside with the authentic apigenin 4′-*O*-glucoside. HPLC chromatogram of (A) 15μM authentic apigenin 4′-*O*-glucoside, (B) 15μM enzymatically synthesized apigenin 4′-*O*-glucoside, and (C) co-chromatography of (A) and (B). A UV spectrum of a peak of (A), (B) and (C) are shown in the chromatogram.

4. 2. 3. Chemical synthesis of apigenin

7-*O*-benzylapigenin obtained by the benzylation of apigenin was reacted with 2,3,4,6-tetra-*O*-benzyl-β-D-glucoside under Mitsunobu conditions (Kim et al. 2009) to provide benzyl-protected apigenin 4′-*O*-β-D-glucoside. By removing the benzyl group of the Mitsunobu product, apigenin 4′-*O*-β-D-glucoside was generated as a pale yellow

powder.

Pale yellow powder analytical data: ^{1}H NMR (methanol-d_4, 800 MHz); δ 3.44 (^{1}H, *dd*, $J_{H,H}$=9.2, 9.2 Hz, Glc-3), 3.49 (^{1}H, *m*, Glc-2), 3.50 (^{1}H, *m*, Glc-4), 3.51 (^{1}H, *ddd*, $J_{H,H}$=2.8, 5.8, 8.4 Hz, Glc-5), 3.71 (^{1}H, *dd*, $J_{H,H}$=5.7, 12.2 Hz, Glc-6), 3.92 (^{1}H, *dd*, $J_{H,H}$=2.2, 12.1 Hz, Glc-6), 5.04 (^{1}H, *d*, 7.44 Hz, H-1”), 6.22 (^{1}H, *d*, $J_{H,H}$=1.8 Hz, H-6), 6.47 (^{1}H, *d*, $J_{H,H}$=1.9 Hz, H-8), 6.66 (^{1}H, *s*, H-3), 7.25 (^{2}H, *d*, $J_{H,H}$=8.9 Hz, H-3′), 7.95 (^{2}H, *d*, $J_{H,H}$=8.9 Hz, H-2′); ^{13}C NMR (methanol-d_4, 200 MHz) δ 62.48 (Glc-6), 71.30 (Glc-3), 74.81 (Glc-4), 77.95(Glc-2), 78.34 (Glc-5), 95.09 (C-8), 100.21(C-6), 101.74(Glc-1), 104.89(C-3), 105.43 (C-10), 118.07 (C-3′), 126.19 (C-1′), 129.19 (C-2′), 159.47 (C-9), 162.09 (C-4′), 163.29 (C-5), 165.59 (C-2), 166.15 (C-7), 183.89 (C-4); HRMS (ESI) Calcd. for $C_{21}H_{21}O_{10}$ $[M+H]^{+}$ 433.1129. Found 433.1118.

NMR spectra were acquired using a Bruker AVANCE III HD 800 spectrometer equipped with a 5-mm TCI cryogenic probe and Z-axis gradient (Bruker Biospin). All spectra were measured at 25 °C, using 5 mm NMR tubes. Standard Bruker pulse sequences were employed. The data analyses were carried out with Bruker TopSpin 3.2 software (Bruker Biospin). Chemical shift was reported in parts per million (ppm) relative to the peaks from methanol-d_4 (CD_3OD, δ_H 3.31ppm, δ_C 49.00ppm). The data for ^{1}H NMR are reported as follows: chemical shift, integration, multiplicity (s = singlet, d = doublet, t = triplet, m = multiplet) and coupling constants in Hertz.

High-resolution mass spectra were obtained using an ion-trap time-of-flight mass spectrometer (Shimadzu LCMS-IT-TOF). A YMC-Triart C18 column (50×2.1 mm, 3.0 μm; YMC) was used for separation at 40ºC with a linear gradient using solvents F (H_2O:formic acid, 99.9:0.1, v/v) and G (methanol:formic acid, 99.9:0.1, v/v), from 10% to 90% solvent G for 4 min, followed by isocratic elution using 90% solvent G for 3

min at a flow rate of 0.3 ml min^{-1}. In this experiment, I collaborated with Bioorganic Research Institute, Suntory Foundation for Life Sciences.

4. 2. 4. Preparation of crude proteins from *N. menziesii* petals

The relevant methods are described in **Chapter 3. 2. 3.**.

4. 2. 5. Detection of *N. menziesii* F4′GT and F4′G7GT activities

Glucosyltransferase activities were measured in a 100 μl reaction mixture consisting of 5 μg crude protein extract, 1 mM UDP-glucose or UDP-galactose as a sugar donor, 20 μM apigenin, apigenin 4′G or apigenin 7G as an acceptor, and 0.1 M Tris–HCl buffer (pH 7.5). After pre-incubation for 10 min at 30 °C, the reaction was initiated by the addition of the crude protein extract. After incubation at 30 °C for 0, 1, 2, 5, 10, 20, 30, 40, 60, 90 or 120 min, the reaction was terminated by the addition of 100 μl of 90% acetonitrile (v/v) containing 0.1% TFA. HPLC analysis was performed as described above (**Chapter 3. 2. 6.**).

4. 2. 6. Isolation of *N. menziesii* glucosyltransferase genes

A BLAST homology search was performed with the amino acid sequences of *G. triflora* anthocyanin 3′-*O*-glucosyltransferase against a petal transcriptome database consisting of 61,491 contigs derived from the normalized cDNA sequence library of *N. menziesii* petals (**Chapter 2. 2. 4.**) using BLASTX 2.2.17 (tblastn, expectation value set to 10) to obtain homologous contigs. The sequences obtained were aligned with known GTs from various plant species using MacVector Assembler version 14.5.2 to identify contigs encoding *N. menziesii* GTs. Those *N. menziesii* GT amino acid sequences were used for

phylogenetic analysis. A Neighbour-Joining tree was constructed using 1,000 bootstrap replicates with CLUSTALW version 2.1 (http://clustalw.ddbj.nig.ac.jp/). A phylogenetic tree was constructed using Dendroscope version 3.5.9 (http://dendroscope.org/).

The contigs expressed more strongly in petals at stages 1 and 2 but rarely expressed in leaves, were also analyzed with respect to petal and leaf RPKM values. The full-length cDNAs were amplified by RT-PCR using total petal RNA and a pair of primers (**Table 1**) designed based on the 5′ and 3′ parts of the genes with Super ScriptII Reverse Transcriptase (Invitrogen) and KOD-plus polymerase (TOYOBO). The PCR conditions were: 2 min at 94 °C followed by 30 cycles of 15 s at 94 °C, 30 s at 55 °C, 30 s at 68 °C for 1 min, followed by cooling to 4 °C. The amplified DNA fragment (**Table 1**) was subcloned into pCR-TOPO vectors and sequenced. A GeneRacer kit (Invitrogen) was used to obtain full-length cDNA sequences when the contigs contained only partial sequences.

4. 2. 7. Characterization of NmF4′GT and NmF4′G7GT *in vitro*

A total of 24 *GT* cDNAs were isolated from *N. menziesii*, including *NmGT8* and *NmGT22*, and subcloned into a pET15b vector (Novagen) and expressed in *E. coli* BL2 cells using the Overnight Express Auto Induction System 1 (Novagen) at 25 °C overnight.

The activities of the recombinant proteins were measured in 100 μl of a reaction mixture consisting of the recombinant crude protein extract (14 μg) and 1 mM UDP-glucose, 10–25 μM flavone, and 0.1 M Tris–HCl buffer (pH 7.5). The reaction mixture was incubated at 30 °C for 30 min, and the reaction was terminated by adding 100 μl of 90% acetonitrile containing 0.1% TFA. As a control, BL21 cells were

transformed with the empty vector, pET15b, and the crude protein extract was assayed under the same conditions. HPLC analysis was performed as described above (**Chapter 3. 2. 6.**).

The substrate preference of NmGT8 was measured using 2.5 μM flavonoid and 300 ng of purified recombinant protein in a 100 μl reaction mixture. The recombinant protein was purified to homogeneity by HisTag affinity chromatography with the Profinia protein purification system (Bio-Rad). Reactions were performed at 30 ℃ for 3 min. The substrate preference of NmGT22 was determined using 7.5 μM flavonoid and 50 ng of purified protein. Reactions were carried out at 30 ℃ for 15 min. The activity of NmGT22 in the presence of an equal amount of NmGT8 was measured in a 100 μl reaction mixture containing 20 μM apigenin and 300 ng of purified recombinant NmGT8 and NmGT22. Heat treatment to inactivate the purified recombinant enzymes was carried out at 100 ℃ for 7 min.

Activity toward betanidin was assessed in a 100 μl reaction mixture consisting of recombinant purified protein, 1 mM UDP-glucose, 10 mM Na-ascorbate and 140 mM KPB (pH 7.5). The reaction mixture was incubated at 30 ℃ for 15 min, then the reaction was terminated by adding 20 μl of 10% phosphoric acid. HPLC analysis was performed as described above (**Chapter 3. 2. 4.**).

4. 2. 8. Characterization of *NmGT3* and *NmGT4 in vivo* using *P. hybrida*

A vector was constructed on a pBIN-PLUS binary vector (van Engelen et al. 1995) to express *NmGT3* or *NmGT4* in *P. hybrida* cv. Surfinia bouquet Red. Because *P. hybrida* does not synthesize flavones, *T. hybrida FNSII* was inserted in the binary vector. The genes were regulated by an enhanced *Cauliflower mosaic virus* 35S (CaMV 35S)

promoter (Mitsuhara et al. 1996) and *HSP18.2* terminator (Nagaya et al. 2010). *P. hybrida* transformation was performed as previously described (Fukuchi-Mizutani et al. 2003) using *Agrobacterium tumefaciens* Agl0 (Lazo et al. 1991) harboring a binary vector. More than 20 transgenic lines were obtained, and all of them were subjected to further analysis after confirming the transcript of the transgenes by RT-PCR.

The collected petals of the transgenic petunia plants were lyophilized and their flavonoids were extracted using eight times (v/w) of 50% acetonitrile (v/v) containing 0.1% TFA. After being centrifuged at 12,400×g for 5 min, the supernatant was subjected to HPLC analysis for flavone analysis as previously described (**Chapter 2. 2. 3.**). Flavone aglycone analysis was performed as previously described (**Chapter 2. 2. 3.**).

4. 2. 9. Determination of NmF4′GT and NmF4′G7GT kinetic parameters

The kinetic parameters of NmF4′GT with apigenin were determined using a purified NmF4′GT enzyme (300 ng) added to the reaction mixture containing 1.25–20 μM apigenin, 1 mM UDP-glucose and 0.1 M Tris–HCl buffer (pH 7.5) in a 100 μl reaction mixture. The reaction mixture was incubated at 30 °C for 3 min, and flavones were quantified by HPLC analysis as described above (**Chapter 3. 2. 6.**).

The kinetic parameters of NmF4′G7GT with apigenin and apigenin 4′G were determined by adding 1 μg and 50 ng of the purified enzyme, respectively, to 100 μl of the reaction mixture containing 1.25–12.5 μM of one of the substrates and 1 mM UDP-glucose in 0.1 M Tris–HCl buffer (pH 7.5). The reaction mixture was incubated at 30 °C for 15 min, and flavones were quantified as mentioned above. V_{max} and K_m values were determined using a Lineweaver–Burk plot.

4. 2. 10. Characterization of *NmF4'GT* and *NmF4'G7GT in vivo* using tobacco culture cells

N. tabacum Bright Yellow 2 (tobacco BY-2) (RIKEN Gene Bank RPC 1) (Nagata et al. 1992) cells and their corresponding transgenic cells were maintained in modified Linsmaier–Skoog medium (Nagata et al. 1981) with a 3% inoculum and vigorous rotation in the dark at 27 °C and then subcultured every week. The binary vectors to express *NmGT8* and/or *NmGT22* in tobacco BY-2 cells were constructed on a pBIN-PLUS binary vector (van Engelen et al. 1995). The genes were regulated by an enhanced CaMV35S promoter (Mitsuhara et al. 1996) and *HSP18.2* terminator (Nagaya et al. 2010). Tobacco BY-2 cell transformation was performed as described previously (Shindo et al. 2006) using *A. tumefaciens* Agl0 (Lazo et al. 1991) harboring a binary vector. More than 20 transgenic cell lines were obtained for each construct, and all of them were subjected to further analysis after confirming the presence of the transgenes by RT-PCR.

Wild-type and transgenic cell cultures were diluted (3 ml of culture into 97 ml of new medium) and grown at 27 °C for 3 days. Apigenin dissolved in 50% acetonitrile was added to 4 ml of culture to a final concentration of 162 μM. The cultures were maintained at 27 °C for an additional two nights. The cells were harvested at 1,600×g at 15 °C for 15 min. The collected cells were ground in liquid nitrogen using a pestle before being thawed in 2 ml of methanol containing 1% HCl and stored overnight at room temperature. After being centrifuged at 12,400×g for 5 min, the supernatant was subjected to HPLC analysis. HPLC was performed using a Shim-pack FC-ODS column (15 cm×4.6 mm; Shimadzu) at 40 °C with a linear gradient using solvents A (H_2O:TFA, 99.9:0.1, v/v) and H (H_2O:methanol:TFA, 9.9:90:0.1, v/v), from 20% to 100% solvent H

for 90 min, followed by isocratic elution using 100% solvent B for 5 min at a flow rate of 0.6 ml min^{-1}. Flavonoids were detected at a range of absorbances between 250 and 600 nm using a photodiode array detector (SPD-M20A, Shimadzu). Peak identification was based on retention time, spectra and co-chromatography with the authentic compounds.

4. 3. Results and discussion

4. 3. 1. Analysis of apigenin 7,4′-*O*-diglucoside synthesis in the crude petal protein extracts

The order of glucosylations during the biosynthesis of apigenin 7,4′-diG, an essential component of nemophilin, was elucidated using the crude proteins extracted from *N. menziesii* petals. The results of a time-course experiment investigating apigenin glucosylation are shown in **Fig. 19A**. Apigenin was depleted within 60 min as a result of UDP-glucose-dependent glucosylation. The amount of apigenin 4′G increased for 40 min, but then decreased with concomitant increases in apigenin 7,4′-diG. Most apigenin (83.9%) was converted to apigenin 7,4′-diG, and the rest to apigenin 7G in 120 min. These results indicate that the *N. menziesii* crude protein extract catalyzes a synthesis of apigenin 4′G from apigenin and then of apigenin 7,4′-diG from apigenin 4′G (**Fig. 20**). The detection of a small amount of apigenin 7G (15.6%) indicates that the extract also exhibited weak 7-*O*-glucosylation activity toward apigenin (dotted line in **Fig. 20**), and that 4′-*O*-glucosylation activity does not catalyze apigenin 7G. When UDP-galactose was used as a sugar donor, no products were detected (data not shown). When apigenin 4′G was used as a substrate, it was converted into apigenin 7,4′-diG within 60 min (**Fig. 19B**), while there was no significant conversion of apigenin 7G to apigenin 7,4′-diG

even after 120 min (**Fig. 19C**). These results confirm that apigenin is glucosylated first at the 4′-*O* position and then at the 7-*O* position.

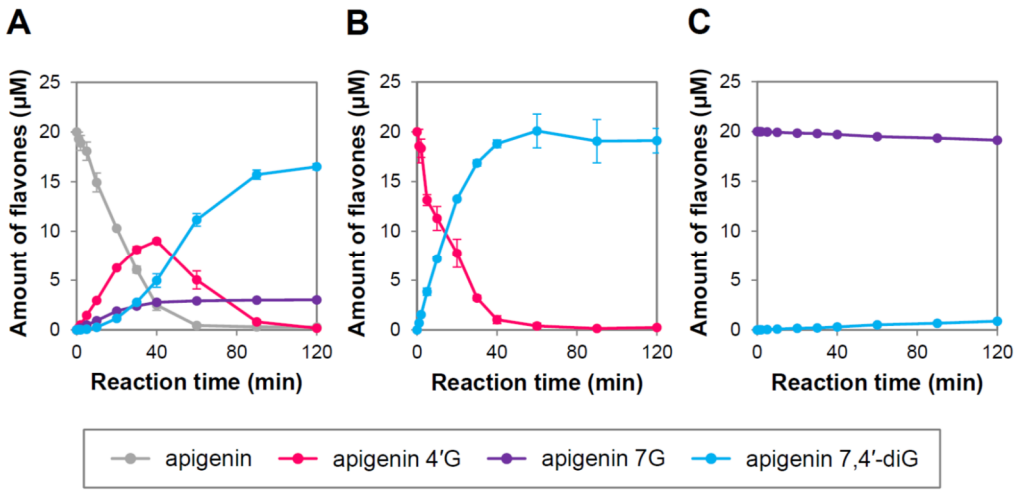

Fig. 19 Biosynthetic activity leading to apigenin 7,4′-*O*-diglucoside synthesis in *N. menziesii* petals. F4′GT and F4′G7GT activities were detected in the crude *N. menziesii* petal protein extract. The averages and SD of three independent measurements are shown. (A) Timeline of apigenin 7,4′-*O*-diglucoside, apigenin 4′-*O*-glucoside, and apigenin 7-*O*-glucoside synthesis and accumulation from apigenin. (B) Timeline of apigenin 7,4′-*O*-diglucoside synthesis and accumulation from apigenin 4′-*O*-glucoside. (C) Timeline of apigenin 7,4′-*O*-diglucoside synthesis and accumulation from apigenin 7-*O*-glucoside.

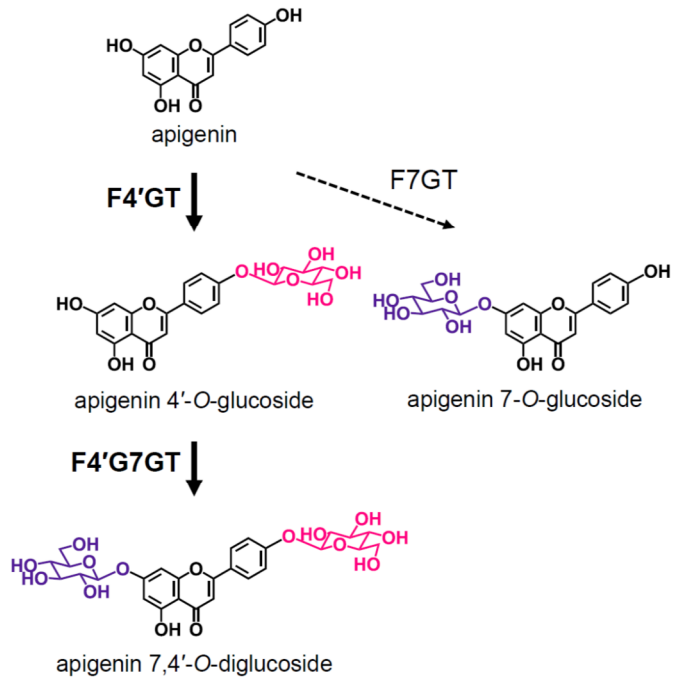

Fig. 20 Biosynthetic pathway of apigenin 7,4′-*O*-diglucoside and apigenin 7-*O*-glucoside synthesis in *N. menziesii* petals. The dotted line indicates a minor pathway leading to apigenin 7-*O*-glucoside. F4′GT, flavone 4′-*O*-glucosyltransferase; F4′G7GT, flavone 4′-*O*-glucoside 7-*O*-glucosyltransferase; F7GT, flavone 7-*O*-glucosyltransferase.

4. 3. 2. Isolation of *N. menziesii GT* cDNAs using transcriptome data

A BLAST homology search with *G. triflora* anthocyanin 3′GT resulted in 150 contigs from the *N. menziesii* transcriptome, including *c103* and *c1526*, which were designated as *NmA3GT* and *NmA3G5GT* in **Chapter 3**, respectively. Of these, 38 contigs expressed strongly in stage 1 and 2 petals but rarely in leaves were selected as candidates for *F4′GT* and *F4′G7GT*, given that these genes are expected to be expressed in a co-ordinated manner with *FNSII*, transcripts, which are abundant in the stage 1 and 2

petals but not in leaves (**Chapter 2**). The two contigs showing the highest RPKM in exons at stage 1 were *c4985* (RPKM value = 710.5) and *c1526* (278.3) (**Fig. 21**). *c1526* had the highest RPKM value (343.8) among GT homologs at stage 2. The expression profiles of *c4985* and *c1526* are consistent with those of *CHS*, *CHI* and *FNSII* in *N. menziesii*, all of which are expressed strongly in petals at stage 1 and 2 and weakly in leaves (**Chapter 2**). Full-length clones of *c4985* and *c1526* were obtained and referred to as *NmGT8* and *NmGT22*, identified as *NmA3G5GT* in **Chapter 3**, respectively. Among the 10 most highly expressed contigs in stage 1 petals (**Fig. 21**), further sequence analyses revealed that *c28874*, *c7634*, *c39734*, *c31592* and *c57111* corresponded to *NmGT8* and that *c12619* and *c13699* corresponded to *NmGT22*, which suggests that *NmGT8* and *NmGT22* are expressed much more strongly than the other *GT* genes at early petal stages. *c889* corresponds to *NmGT6*.

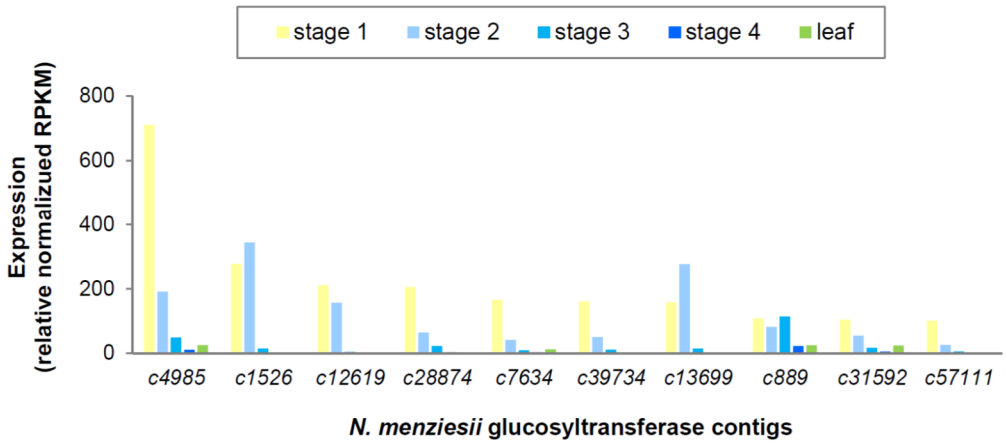

Fig. 21 Transcriptional profiles of *N. menziesii* glucosyltransferase contigs. Expression levels (RPKM values) at 4 developmental stages of the 10 most highly expressed contigs in stage 1 petals are shown.

In addition to *NmGT8* and *NmGT22*, 15 *GT* cDNAs from the 38 contigs were isolated. The additional 7 *GT* cDNAs belonging to or related to the flavonoid 3′/7GT cluster were isolated in the expectation that *F4′GT* and *F4′G7GT* would belong to or be related to the flavonoid 3′/7GT cluster. A total of 24 *GT* cDNAs were obtained (**Table 6**). Phylogenetic analyses revealed that NmGT0, NmGT3 and NmGT4 belong to the flavonoid 3′/7GT cluster; NmGT8, NmGT9 and NmGT10 are related to the flavonoid 3′/7GT cluster; NmGT24, identified as NmA3GT in **Chapter 3** (*c564* and *c103* correspond to *NmGT24*) belong to the flavonol/anthocyanidin 3GT cluster; NmGT22, identified as NmA3G5GT in **Chapter 3**, is related to the anthocyanin 5GT cluster; and NmGT11, NmGT26, NmGT27 and NmGT28 belong to the GGT cluster. NmGT1, NmGT2, NmGT5, NmGT6, NmGT7, NmGT13, NmGT14, NmGT16, NmGT17, NmGT18, NmGT21 and NmGT29 do not belong to any clusters (**Fig. 22**).

Table 6 List of glucosyltransferase genes isolated in the present study

Clone name	Contig number	Forward primer/ Reverse primer	Accession number	UGT number
NmGT0	*c3093*	GGAATTCCATATGACGGCTCAATTTCATGT/ CG GGATCCTTAATTGTGTTCTTCTTCCGCT	LC368259	UGT73BD1
NmGT1	*c21325*	GGAATTCCATATGGGAAGCTTGATAAAT/ CGGGATCCCTATCTAGTAATATGGGCA	LC368260	UGT93P1
NmGT2	*c7523*	CCGCTCGAGATGGCTAATATCAAAGATCA/ CGGGATCCCTATCTGGTAATGTGTGCAAT	LC368261	UGT93P2
NmGT3	*c14484*	GGAATTCCATATGCCATCAATCCTGAGCAATA/ CGGGATCC TTAGTTAATTTTTACCTTTAAACCA	LC368262	UGT89P1
NmGT4	*c19672*	GGAATTC CATATG GCAGCTCAGCTTCATGTT/ CGGGATCCTCATATCTTGTTTGATTGTGA	LC368263	UGT73BD2
NmGT5	*c10672*	GGAATTC CATATG ACTAACCCTTGTAAT/ CGGGATCCTTATCTAGTTATGTGAGA	LC368264	UGT93Q1
NmGT6	*c84*	GGAATTCCATATG TTCAAAGTAGCCAAGCTT/	LC368265	UGT85A60

		CGGGATCCTTAACAATTAACGGTAACA		
NmGT7	*c402*	CCGCTCGAG ATGGAGTCAGCTTTAGGTGA/ CGGGATCCTTATACAACTAAACTGCC	LC368266	UGT95C1
NmGT8	*c4985*	GGAATTCCATATGGAGAAAAAAACTATT/ CGGGATCCCTATTTCCAACCATCCAGTA	LC328827	UGT88P1
NmGT9	*c17153*	AGCATATG GGACTGGAAGGTAGTA/ ATGGATCCCTAGTATAAAACAGAAATTTGC	LC368267	UGT71AF1
NmGT10	*c16952*	CTCGAGATGGAGAAGAAAACTACTAC/ GGATCCTTATTGTTTCCAAATATTTAGTAGTTTGG	LC368268	UGT88P2
NmGT11	*c13349*	ATGGATAGTAAGAAGCATACTGG/ TTATCCAGATCCTTTGTTACAAAG	LC368269	UGT94AH1
NmGT13	*c49797*	ATGGCTAATMTCAAAAATCAT/ CTATCGGGTAATGTGTGCAATG	LC368270	UGT93P3
NmGT14	*c1645*	ATGAGTTCCTCCATATATCCAGAG/ CTAATTTGACACCGAAGAGATAAG	LC368271	UGT85A61
NmGT16	*c1772*	ATGATGGTGGGTGGTCACATAGTA/ CTACGACTTCCTGTTCGATAGAA	LC368272	UGT85AB1
NmGT17	*c3551*	ATGGCTGATACAACAATGGCACC/ TTATGGTGTGACTGTCGCTTTA	LC368273	UGT709J5
NmGT18	*c2333*	ATGCAGGAAGTGAAAGGDTC/ TCACTTGTTGAGAGACAATGAG	LC368274	UGT76U1
NmGT21	*c31710*	ATGAGTAATCCACATGTTCTAATC/ TCATACAATTGAAGATAGTCCC	LC368275	UGT83Q1
NmGT22	*c1526*	ATGGAATGCAAAAATCCAGATTC/ CTAGGTAATAAATCTGAAATTATTG	LC328828	UGT84A34
NmGT24	*c564*	CATATGTCAAAACAACACCATGTAGC/ GGATCCTCATAACAACATAGATAAGAGTG	LC368276	UGT78A20
NmGT26	*c1995*	ATGGGCGAAAACAATAAACTCCAC/ CTAGGTTGTCTTTTGGCT	LC368277	UGT91R9
NmGT27	*c5914*	ATGGATTCACAGAGTAGTTCGAAAC/ CTAGAGCTTGTCCAACTGTTGTAC	LC368278	UGT79H1
NmGT28	*c257*	ATGGAGAAAAACAATCTTCATGTTG/ CTAAGGAGCAGCCATAGCCTTC	LC368279	UGT79A11
NmGT29	*c5982*	ATGGTTAAATCTGATTCAAATAAGCC/ TTAATTATTGCTACTACTTTTAG	LC368280	UGT86A17

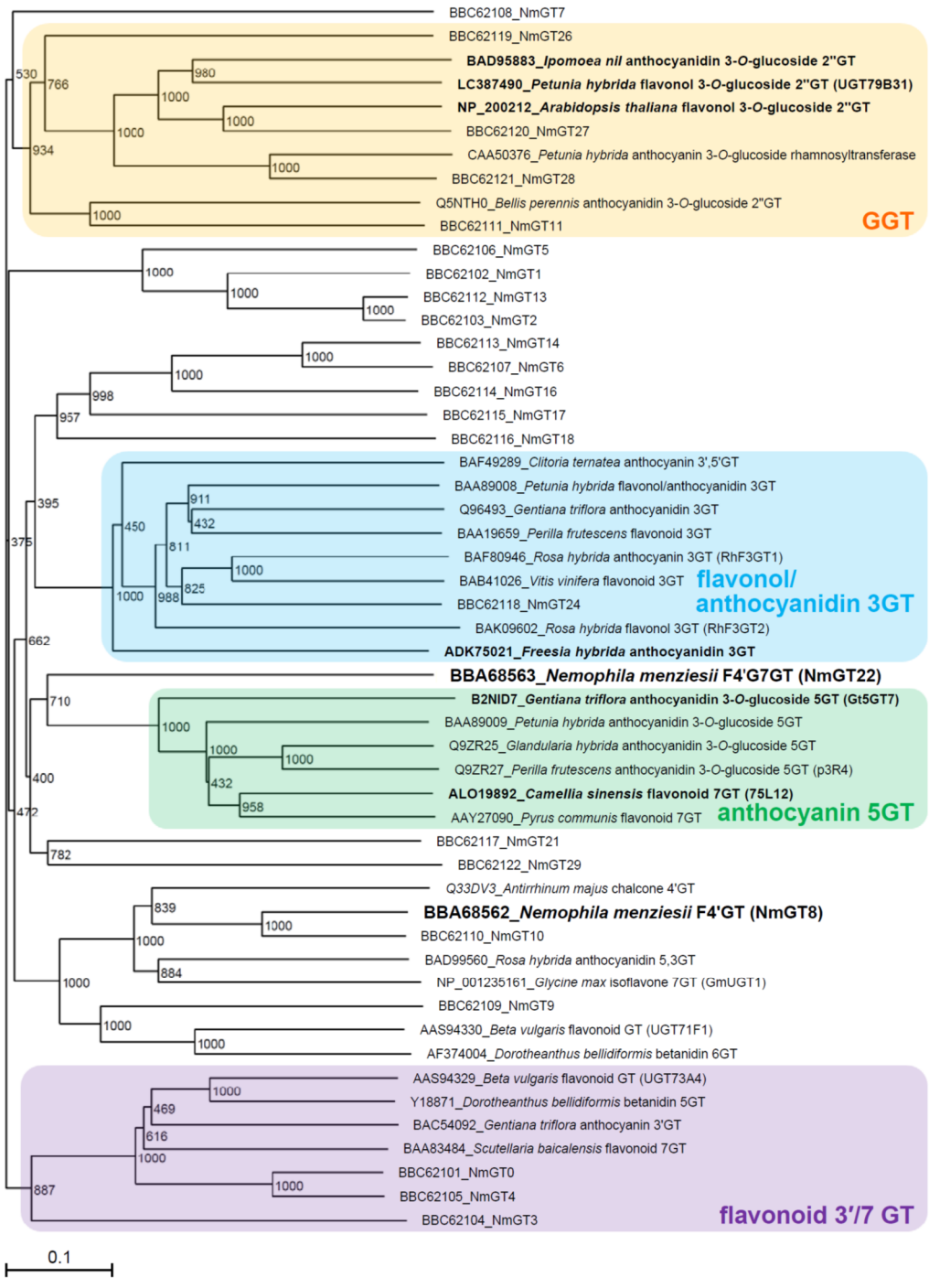
BBC62108_NmGT7
BBC62119_NmGT26
BAD95883_Ipomoea nil anthocyanidin 3-O-glucoside 2"GT
LC387490_Petunia hybrida flavonol 3-O-glucoside 2"GT (UGT79B31)
NP_200212_Arabidopsis thaliana flavonol 3-O-glucoside 2"GT
BBC62120_NmGT27
CAA50376_Petunia hybrida anthocyanin 3-O-glucoside rhamnosyltransferase
BBC62121_NmGT28
Q5NTH0_Bellis perennis anthocyanidin 3-O-glucoside 2"GT
BBC62111_NmGT11
GGT
BBC62106_NmGT5
BBC62102_NmGT1
BBC62112_NmGT13
BBC62103_NmGT2
BBC62113_NmGT14
BBC62107_NmGT6
BBC62114_NmGT16
BBC62115_NmGT17
BBC62116_NmGT18
BAF49289_Clitoria ternatea anthocyanin 3',5'GT
BAA89008_Petunia hybrida flavonol/anthocyanidin 3GT
Q96493_Gentiana triflora anthocyanidin 3GT
BAA19659_Perilla frutescens flavonoid 3GT
BAF80946_Rosa hybrida anthocyanin 3GT (RhF3GT1)
BAB41026_Vitis vinifera flavonoid 3GT
BBC62118_NmGT24
flavonol/
anthocyanidin 3GT
BAK09602_Rosa hybrida flavonol 3GT (RhF3GT2)
ADK75021_Freesia hybrida anthocyanidin 3GT
BBA68563_Nemophila menziesii F4'G7GT (NmGT22)
B2NID7_Gentiana triflora anthocyanidin 3-O-glucoside 5GT (Gt5GT7)
BAA89009_Petunia hybrida anthocyanidin 3-O-glucoside 5GT
Q9ZR25_Glandularia hybrida anthocyanidin 3-O-glucoside 5GT
Q9ZR27_Perilla frutescens anthocyanidin 3-O-glucoside 5GT (p3R4)
ALO19892_Camellia sinensis flavonoid 7GT (75L12)
AAY27090_Pyrus communis flavonoid 7GT
anthocyanin 5GT
BBC62117_NmGT21
BBC62122_NmGT29
Q33DV3_Antirrhinum majus chalcone 4'GT
BBA68562_Nemophila menziesii F4'GT (NmGT8)
BBC62110_NmGT10
BAD99560_Rosa hybrida anthocyanidin 5,3GT
NP_001235161_Glycine max isoflavone 7GT (GmUGT1)
BBC62109_NmGT9
AAS94330_Beta vulgaris flavonoid GT (UGT71F1)
AF374004_Dorotheanthus bellidiformis betanidin 6GT
AAS94329_Beta vulgaris flavonoid GT (UGT73A4)
Y18871_Dorotheanthus bellidiformis betanidin 5GT
BAC54092_Gentiana triflora anthocyanin 3'GT
BAA83484_Scutellaria baicalensis flavonoid 7GT
BBC62101_NmGT0
BBC62105_NmGT4
BBC62104_NmGT3
flavonoid 3'/7 GT
0.1

Fig. 22 A phylogenetic tree of UFGTs. The amino acid sequences of 24 GTs obtained from *N. menziesii*, including NmF4′GT (NmGT8) and NmF4′G7GT (NmGT22), and 29 known UFGTs from various other plant species were aligned. Accession numbers for those GTs in the database and species names are shown. GTs whose functions have been studied *in vivo* are shown with bold letters. Scale bar = 0.1 amino acid substitutions per site.

4. 3. 3. Characterization of NmGT8 and NmGT22 *in vitro*

The 24 GT cDNAs obtained were expressed in *E. coli* and subjected to a glucosylation assay for apigenin, luteolin and their glucosides. NmGT8 expressed in *E. coli* displayed F4′GT activity (**Fig. 23C**). Although NmGT0 catalyzed 7-*O*-glucosylation of flavones *in vitro* (**Fig. 24C**), the RPKM value was very low (14.47), so this activity may not occur *in vivo*. NmGT3 and NmGT4 exhibited flavone 4′,7GT activities *in vitro* (**Figs. 24F, G**) but these activities were not detected when they were expressed in transgenic *P. hybrida* (**Fig. 25**). NmGT22 catalyzed 7-*O*-glucosylation of flavones (apigenin and luteolin) and flavone 4′Gs (apigenin 4′G and luteolin 4′G) (**Fig. 23F**), while it exhibited A3G5GT activity *in vitro* in **Chapter 3**. The other 19 GTs (NmGT1, NmGT2, NmGT5, NmGT6, NmGT7, NmGT9, NmGT10, NmGT11, NmGT13, NmGT14, NmGT16, NmGT17, NmGT18, NmGT21, NmGT24, NmGT26, NmGT27, NmGT28 and NmGT29) exhibited no flavone GT activity. They may catalyze the glucosylation of plant secondary compounds except for flavones in *N. menziesii* petals. Based on these results, NmGT8 and NmGT22 were determined to correspond to F4′GT and F4′G7GT, respectively, and were subjected to further study.

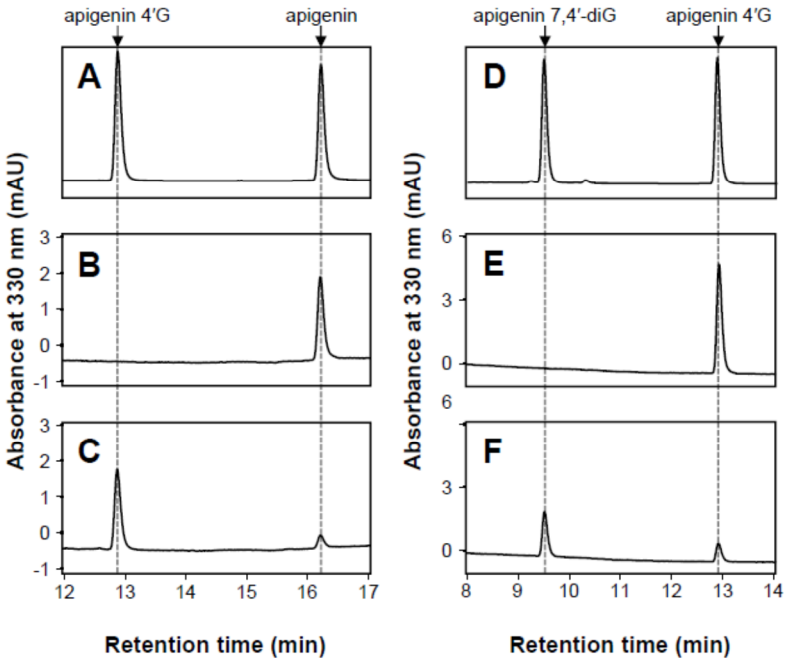

Fig. 23 Enzymatic activity of the purified recombinant NmGT8 or NmGT22 expressed in *E. coli.* HPLC chromatogram of (A) apigenin and apigenin 4′-*O*-glucoside, (B) apigenin incubated in the reaction mixture without NmGT8, (C) apigenin incubated with NmGT8, (D) apigenin 4′-*O*-glucoside and apigenin 7,4′-*O*-diglucoside, (E) apigenin 4′-*O*-glucoside incubated in the reaction mixture without NmGT22, and (F) apigenin 4′-*O*-glucoside incubated with NmGT22.

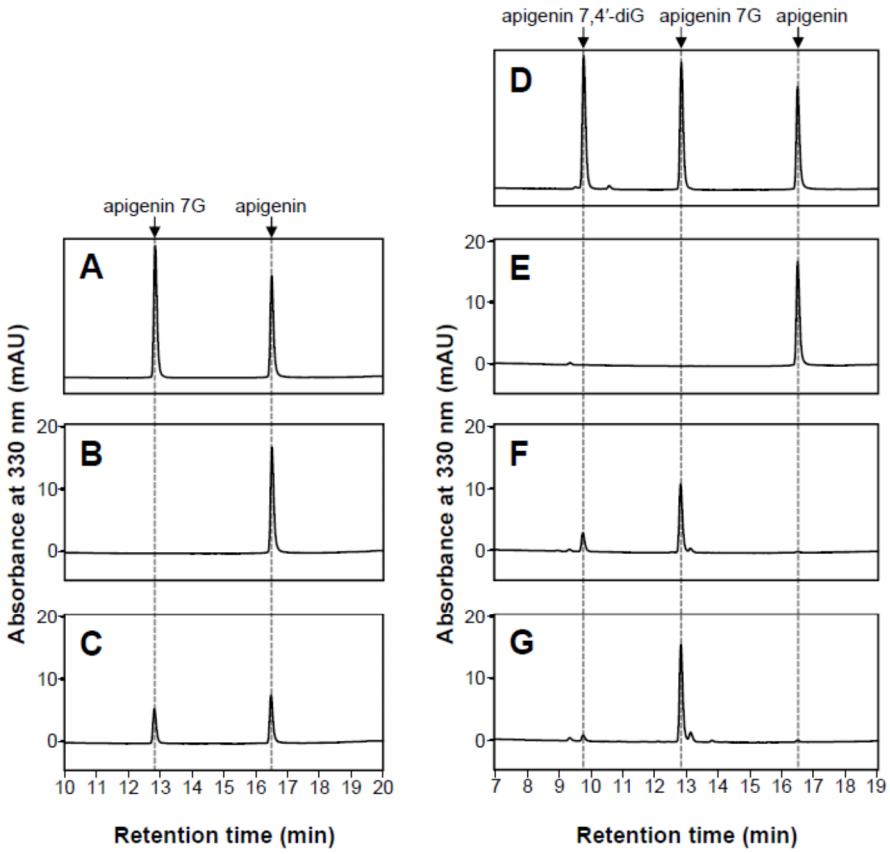

Fig. 24 Enzymatic activity of protein crude extracts of *E. coli* expressing *NmGT0*, *NmGT3* or *NmGT4*. HPLC chromatogram of (A) apigenin and apigenin 7-*O*-glucoside, (B) apigenin incubated with the extract of *E. coli* host, (C) apigenin incubated with *E. coli* expressing *NmGT0*, (D) apigenin, apigenin 7-*O*-diglucoside and apigenin 7,4′-*O*-diglucoside, (E) apigenin incubated with the extract of *E. coli* host, (F) apigenin incubated with the extract of *E. coli* expressing *NmGT3*, and (G) apigenin incubated with the extract of *E. coli* expressing *NmGT4*.

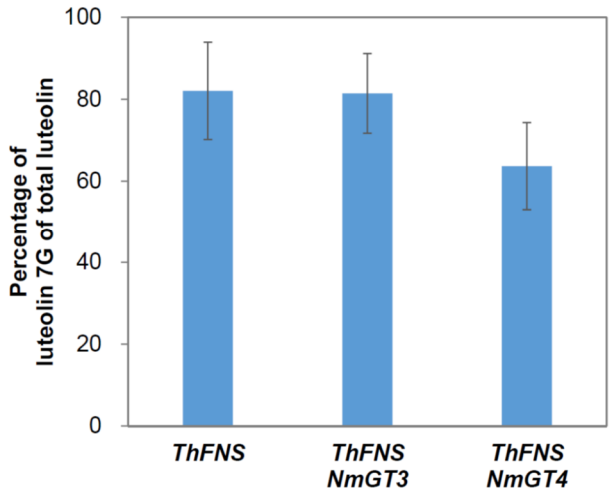

Fig. 25 Amount of luteolin 7-*O*-glucoside in petunia plants expressing *FNSII* and *NmGT3* or *NmGT4*. Percentage of luteolin 7-*O*-glucoside of total luteolin was measured in transgenic petunia plants expressing *ThFNS*, *ThFNS* and *NmGT3*, and *ThFNS* and *NmGT4*. The averages and SD of at least four independent transgenic petunias are shown.

The purified recombinant NmGT8 efficiently catalyzed 4′-*O*-glucosylation of apigenin (**Fig. 23C**). It also catalyzed 4′-*O*-glucosylation of luteolin, albeit less efficiently, though it did not catalyze glucosylation of apigenin 4′G, luteolin 4′G, apigenin 7G or luteolin 7G (**Table 7**). Additionally, it weakly catalyzed 4′-*O*-glucosylation of kaempferol and strongly catalyzed 4′-*O*-glucosylation of quercetin, but it did not catalyze glucosylation of isoflavones (genistein and daidzein) or betanidin (**Table 7**). Betanidin is a red floral pigment and belongs to betalains, a different class of compounds from flavonoids. Although *N. menziesii* petals contain kaempferol 3-*O*-(6-*O*-rhamnosyl)-glucoside-7-*O*-glucoside and its derivatives, but not flavonol

4′-*O*-glucosides (Tatsuzawa et al. 2014; **Chapter 2**), the flavonol 4′-*O*-glucosyltransferase activity of NmGT8 was detected *in vitro*. Further study on this *in vitro* activity toward flavonols was necessary.

The recombinant NmGT22 catalyzed 7-*O*-glucosylation of apigenin 4′G to yield apigenin 7,4′-diG (**Table 8**; **Fig. 23F**). NmGT22 efficiently catalyzed 7-*O*-glucosylation of apigenin 4′G followed by luteolin 4′G. Interestingly, it also catalyzed 7-*O*-glucosylation of apigenin and, to some extent, luteolin (**Table 8**). It did not catalyze glucosylation of isoflavones (genistein and daidzein) or betanidin.

Apigenin 7,4′-diG was efficiently synthesized from apigenin *in vitro* when equal amounts of NmGT8 and NmGT22 were added to the reaction mixture (**Fig. 26E**), while the addition of NmGT8 or NmGT22 alone resulted in synthesis of apigenin 4′G and apigenin 7G, respectively (**Figs. 26C, D**). These results indicate that NmGT8 and NmGT22 co-ordinate to produce apigenin 7,4′-diG from apigenin.

Table 7 Relative activity of the recombinant NmGT8 toward flavones, flavonols, isoflavones and betanidin

Substrate	Product	Relative activity (%)
Apigenin	Apigenin 4'G	100
Apigenin 4'G	ND	ND
Apigenin 7G	ND	ND
Luteolin	Luteolin 4'G	52.6 ± 3.7
Luteolin 4'G	ND	ND
Luteolin 7G	ND	ND
Kaempferol	Kaempferol 4'G	14.5 ± 1.2
Kaempferol 3G	ND	ND
Kaempferol 7G	ND	ND
Quercetin	Quercetin 4'G	62.4 ± 4.0
Quercetin 3G	ND	ND
Genistein	ND	ND
Daidzein	ND	ND
Betanidin	ND	ND

Averages and SD of three reactions are shown. The relative activity of NmGT8 was calculated based on 100% activity toward apigenin. The product derived from kaempferol was tentatively determined as kaempferol 4'G, because the product was different from kaempferol 3G and kaempferol 7G and the enzyme catalyzed 4'-*O*-glucosylation of quercetin. The condition of a reaction with betanidin as a substrate is different from that with flavones, flavonols and isoflavones as substrates. See text for details. ND, not detected.

Table 8 Relative activity of the recombinant NmGT22 toward flavones, flavonols, isoflavones and betanidin

Substrate	Product	Relative activity (%)
Apigenin	Apigenin 7G	27.8 ± 3.6
Apigenin 4'G	Apigenin 7,4'-diG	100
Apigenin 7G	ND	ND
Luteolin	Luteolin 7G	25.1 ± 1.4
Luteolin 4'G	Luteolin 7,4'-diG	42.4 ± 12.3
Luteolin 7G	ND	ND
Kaempferol	ND	ND
Kaempferol 3G	ND	ND
Kaempferol 7G	ND	ND
Quercetin	ND	ND
Quercetin 3G	ND	ND
Genistein	ND	ND
Daidzein	ND	ND
Betanidin	ND	ND

Averages and SD of three reactions are shown. The relative activity of NmGT22 was calculated based on 100% activity toward apigenin 4'G. The condition of a reaction with betanidin as a substrate is different from that with flavones, flavonols and isoflavones as substrates. See text for details. ND, not detected.

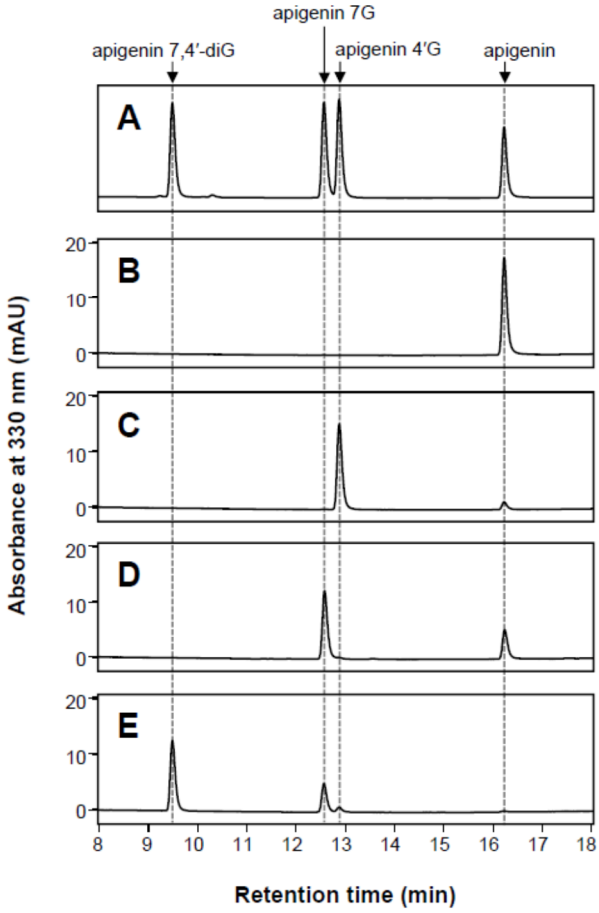

Fig. 26 Accumulation of apigenin 7,4′-*O*-diglucoside due to recombinant NmGT8 and NmGT22. Recombinant NmGT8 and NmGT22 were added to the reaction mixture. HPLC chromatogram of apigenin, apigenin 4′-*O*-glucoside, apigenin 7-*O*-glucoside and apigenin 7,4′-*O*-diglucoside (A), the reaction mixture after reaction of heat-treated NmGT8 and heat-treated NmGT22 with apigenin (B), NmGT8 and heat-treated NmGT22 (C), heat-treated NmGT8 and NmGT22 (D), and NmGT8 and NmGT22 (E).

The kinetic parameters of NmGT8 and NmGT22 are shown in **Table 9**. The K_m value of NmGT8 toward apigenin was less than one-third of that of NmGT22, which indicates that NmGT8 has a higher affinity for apigenin than NmGT22. The K_m values of NmGT8 and NmGT22 toward apigenin (2.3 ± 0.7 μM and 7.5 ± 1.2 μM, respectively) were in the range of K_m values (2.4–137 μM) previously reported, including that of *B. vulgaris* flavonoid 7-*O*-glucosyltranferase (UGT71F1) toward quercetin (Isayenkova et al. 2006), *G. max* IF7GT (GmUGT1) toward genistein (Noguchi et al. 2007), *P. frutescens* A3G5GT toward cyanidin 3G (Yamazaki et al. 1999) and *S. baicalensis* flavonoid 7-*O*-glucosyltranferase toward baicalein (Hirotani et al. 2000). NmGT22 showed comparable affinity for apigenin and apigenin 4′G, but also a k_{cat}/K_m value about three-fold higher toward apigenin 4′G (0.12 ± 0.01 s^{-1} μM^{-1}) than toward apigenin (0.03 ± 0.00 s^{-1} μM^{-1}). These results indicate that the combination of the high affinity of NmGT8 for apigenin and the high velocity of 7-*O*-glucosylation of apigenin 4′G catalyzed by NmGT22 results in efficient accumulation of apigenin 7,4′-diG.

Table 9 Kinetic parameters of NmGT8 and NmGT22

Enzyme	Substrate	k_{cat} (s^{-1})	K_m (μM)	k_{cat}/K_m (s^{-1} μM^{-1})
NmGT8	Apigenin	0.22 ± 0.03	2.28 ± 0.71	0.10 ± 0.02
NmGT22	Apigenin	0.24 ± 0.03	7.54 ± 1.25	0.03 ± 0.00
NmGT22	Apigenin 4'G	0.73 ± 0.13	6.66 ± 0.71	0.11 ± 0.01

The recombinant NmGT8 and NmGT22 were expressed in *E. coli* and purified with HisTag.

4. 3. 4. Characterization of *NmGT8* and *NmGT22 in vivo*

Tobacco BY-2 cells can be used to easily and quickly (in a few days) confirm flavone GT activities *in vivo* due to their ability to import flavone dissolved in medium into cells. Tobacco BY-2 cells expressing *NmGT8* (cell line NmGT8-05), *NmGT22* (NmGT22-16) and both *NmGT8* and *NmGT22* (NmGT8/NmGT22-24) were fed with apigenin to reveal their function *in vivo*. The results of HPLC analysis are shown in **Fig. 27**. Wild-type BY-2 cells fed with apigenin synthesized apigenin 7G (**Fig. 27C**), as shown by endogenous flavonoid 7GT activity (Taguchi et al. 2003). Apigenin 4′G was detected in NmGT8-5 cells (**Fig. 27D**), indicating that NmGT8 functions as a F4′GT *in vivo*. A small amount of apigenin 7,4′-diG was synthesized due to a combination of apigenin 4′GT activity derived from NmGT8 and endogenous 7GT activity. The HPLC chromatogram of NmGT22-16 (**Fig. 27E**) was similar to that of the host cells (**Fig. 27C**). This is unsurprising, since introduced NmGT22-derived F7GT activity is not distinguishable from endogenous flavonoid 7GT activity. Apigenin 7,4′-diG was clear in NmGT8/NmGT22-24 (**Fig. 27F**), suggesting that *NmGT8* and *NmGT22* catalyze sequential glucosylations of apigenin to yield apigenin 7,4′-diG *in vivo.*

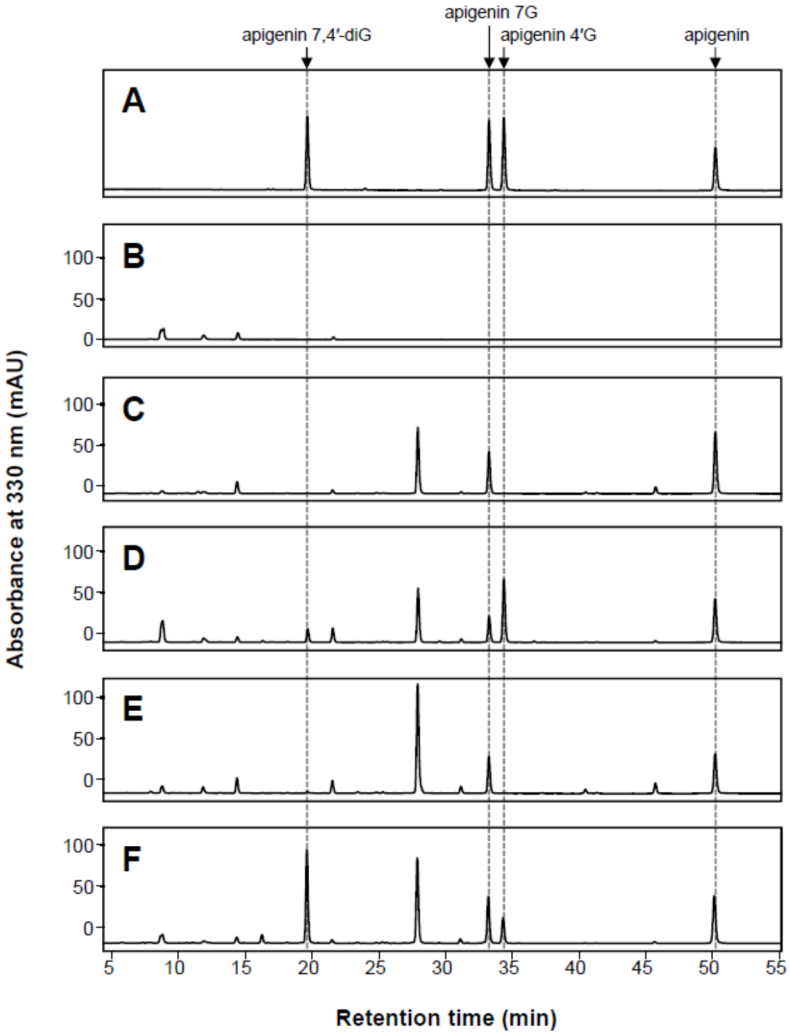

Fig. 27 Apigenin derivative profiles of *NmGT8* and *NmGT22* expressed in tobacco BY-2 cells. Wild-type tobacco BY-2 cells and their transgenic cells were fed with apigenin and cultured over two nights; these cell extractions were subjected to HPLC analysis. (A) apigenin, apigenin 4′-*O*-glucoside, apigenin 7-*O*-glucoside and apigenin 7,4′-*O*-diglucoside, (B) tobacco BY-2 host cells without apigenin, (C) tobacco BY-2 host cells, (D) transgenic tobacco BY-2 cells expressing *NmGT8*, (E) transgenic tobacco BY-2 cells expressing *NmGT22*, and (F) transgenic tobacco BY-2 cells expressing *NmGT8* and *NmGT22*.

The study described in this chapter showed that *N. menziesii* apigenin 7,4′-diG is biosynthesized in a sequential manner by F4′GT and F4′G7GT. F4′G7GT also catalyzes the glucosylation of flavones to some extent. The genes encoding these enzymes, *NmGT8* and *NmGT22*, respectively, have been successfully identified and sequenced. These two GTs were biochemically characterized, and their *in vivo* function in apigenin 7,4′-diG biosynthesis was elucidated.

Chapter 5 General Discussion and Concluding Remarks

The present study showed that I identified 21 genes encoding 15 kinds of flavonoid biosynthetic proteins (CHS, CHI, F3H, FNSII, F3′5′H, DFR, ANS, GST, R2R3-MYB, bHLH, EFP, A3GT, flavonol 3-*O*-glucosyltransferase (Flavonol 3GT), A3G5GT, AMT, F4′GT and F4′G7GT) belonging to the flavonoid biosynthetic pathway in *N. menziesii* petals. I have characterized the biosynthetic pathway leading to the compositions of nemophilin, one of pure blue metalloanthocyanins by isolating the structural genes in the pathway and conducting a biochemical study.

A number of *AMT* genes involved in the biosynthesis of malvidin-based anthocyanins have been identified (Hugueney et al. 2009; Lucker et al. 2010; Akita et al. 2011; Provenzano et al. 2014; Nakamura et al. 2015; Du et al. 2015). However, *AMT* gene involved in dominant accumulation of petunidin-based anthocyanin has not yet been isolated. NmAMT isolated from *N. menziesii* is an intriguing methyltransferase that almost exclusively yielded petunidin-based anthocyanins, rather than malvidin-based anthocyanins (**Chapter 3**). The *AMT* gene can be a useful molecular tool for shifting the flavonoid biosynthetic pathway to petunidin-based anthocyanin biosynthesis to produce nemophilin.

Previously, flavone glucosylation had mainly been studied on the basis of *in vitro* measurements (Vogt et al. 1997; Vogt et al. 1999; Hirotani et al. 2000; Isayenkova et al. 2006; Noguchi et al. 2007; Funaki et al. 2015); *in vivo* studies of flavone glucosylation were scarce. This is the first report on the isolation of *F4′GT* and *F4′G7GT* exhibiting their activities *in vivo*, and this study has shed new light on flavone biosynthesis (**Chapter 4**). Co-expressions of these GTs can lead to the efficient synthesizing of

apigenin 7,4′-diG in other plants, which is essential for blue metalloanthocyanin formation.

The petal transcriptome data of *N. menziesii* could show that *CHS*, *CHI*, *F3H* and *FNSII* are expressed in the early step, and *F3′5′H* and *ANS* are in the late step involved in the flavonoid biosynthetic pathway of *N. menziesii* petals. This result suggests that the flavonoid biosynthetic genes isolated in this study were generally expressed in a well-coordinated manner, as has been reported in many other plants.

Interestingly, in *N. menziesii* petals *A3GT*, *A3G5GT* and *AMT* are expressed strongly at stages 1 and 2 (**Fig. 13**), although anthocyanin-modified genes typically function at later stages of flavonoid biosynthetic pathway than *ANS*, significantly in petals. In the case of NmA3GT, the recombinant enzyme expressed in *E. coli* exhibited not only A3GT activity but also Flavonol 3GT activity (**Chapter 3**). The enzyme may function as Flavonol 3GT at an early stage and then as AG3GT at the late stage in *N. menziesii* petals. Such a GT exhibiting 3-*O*-glucosylation toward both anthocyanidins and flavonols was isolated from *P. hybrida* (Yamazaki et al. 2002), whose expression patterns were slightly earlier than those of CHS and DFR (Brugliera et al. 1999). NmGT22 was shown to exhibit A3G5GT activity by expression in *E. coli* (**Chapter 3**) and F4′G7GT activity by expression in tobacco BY-2 cells (**Chapter 4**), indicating that a single enzyme may play two roles, A3G5GT and F4′G7GT, in the flavonoid biosynthetic pathway. Further analyses are necessary to show that NmF4′G7GT is also physiological A3G5GT and that NmA3GT/NmFlavonol 3GT functions in *N. menziesii*.

Among the 24 kinds of family 1 GT cDNAs isolated in **Chapter 4**, only three GTs (F4′GT, F4′G7GT/A3G5GT and A3GT/Flavonol 3GT) were functionally studied, so much remains to be investigated to understand the full picture of family 1 GTs in *N.*

menziesii. The GT catalyzing 7-*O*-glucosylation of flavonol has not yet been isolated.

In the case of *Rosaceae* plants, *P. communis* flavonol 7-*O*-glucosyltransferase belongs to the anthocyanin 5GT cluster (Fischer et al. 2007) and 5-*O*-glucosylation of anthocyanins is catalyzed by *R. hybrida* anthocyanidin 5,3GT (Ogata et al. 2005) related to the flavonoid 3′/7GT cluster. The fact that *N. menziesii* F4′G7GT is related to the anthocyanin 5GT cluster suggests that the alteration of UFGT specificity is flexible, and the acquisition of new functions has occurred in the pre-existing *anthocyanin 5GT* gene several times throughout plant evolution.

A transcriptome analysis is useful to identify genes involved in flavonoid biosynthesis. Most flavonoid-related genes were successfully isolated and partial sequences of *FLS* and *ATs* were found, but these were not subjected to further examination in the present study. However, it should be noted that the elucidation of the function of a gene by amino acid sequence homology is not always accurate, so functional analysis is essential. For example, though it is possible to predict the function of a UFGT by phylogenetic analysis, *N. menziesii* F4′G7GT related to the anthocyanin 5GT cluster was shown to be flavonoid 7-*O*-glucosyltransferase.

Among genes which are essential for synthesizing the components of nemophilin (petunidin 3*p*CG5MG and apigenin 7G4′MG), three genes remain unidentified in this study. These genes encode ATs catalyzing aromatic acylation and malonylation in the biosynthetic pathway of petunidin 3*p*CG5MG (**Fig. 4C**), and malonylation in that of apigenin 7G4′MG (**Fig. 4D**), respectively. Two acylations in petunidin 3*p*CG5MG biosynthesis are catalyzed by anthocyanidin 3-*O*-glucoside-6″-*O*-*p*-coumaroyltransferase (A3AT) from *P. frutescens* (Yonekura-Sakakibara et al. 2000) and anthocyanin

5-*O*-glucoside-6″-*O*-malonyltransferase (A5MaT) from *Salvia splendens* and *A. thaliana* (Suzuki et al. 2001; D'Auria et al. 2007), respectively, in place of the ATs encoded by two of three unidentified genes from *N. menziesii*. On the other hand, there is no report on the isolation of genes which substitute for the other unidentified gene encoding the AT catalyzing the malonylation in apigenin 7G4′MG biosynthesis. In addition to nemophilin, four other blue metalloanthocyanins have been determined from *C. communis* (Tamura et al. 1986), *S. patens* (Takeda et al. 1994), *C. cyanus* (Kondo et al. 1998) and *S. uliginosa* (Mori et al. 2008), all of whose flower color are blue. These metalloanthocyanins have the differences in their components (Yoshida et al. 2009). One of them is the number of malonyl groups of the component. The necessity for the malonylation in apigenin 7G4′MG biosynthesis to accumulate blue metalloanthocyanin was examined by the reconstruction experiment. It showed that not only apigenin 7G4′MG but also apigenin 7,4′-diG can form blue and stable metalloanthocyanin by mixing with petunidin 3*p*CG5MG, Fe^{3+} and Mg^{2+} *in vitro* (**Fig. 28**), suggesting that the malonylation of apigenin 7,4′-diG is not essential for forming blue and stable metalloanthocyanin at least *in vitro*. These results indicate that a set of isolated genes from *N. menziesii* in this study, *P. frutescens A3AT* and *S. splendens/A. thaliana A5MaT* would lead to blue and stable metalloanthocyanin formation and blue flower coloration.

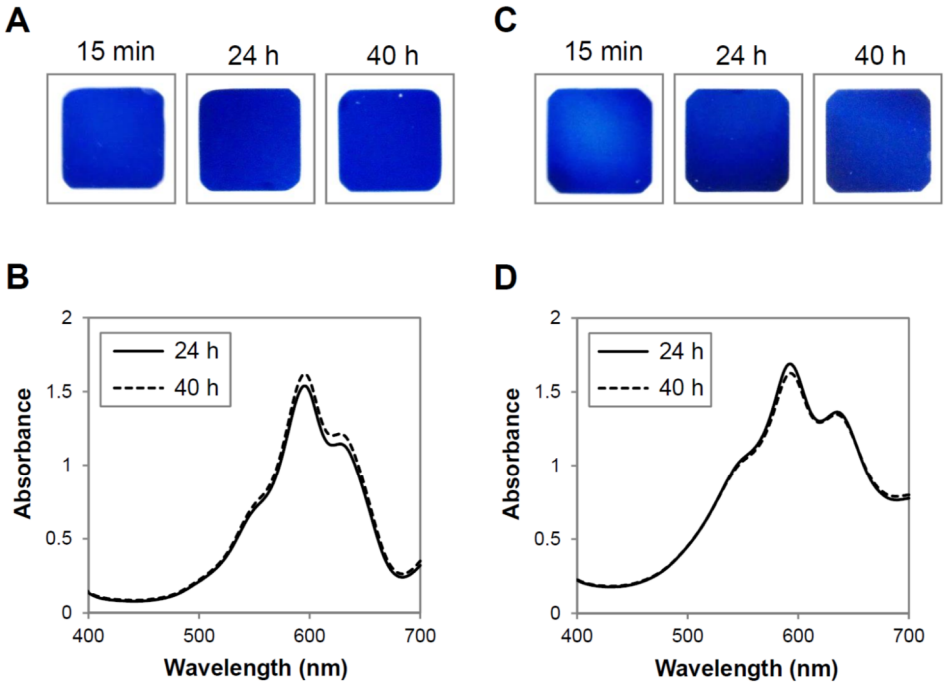

Fig. 28 Coloration and color stabilities of metalloanthocyanin reconstructed *in vitro*. (A) Photos of a solution taken 15 min (left), 24 h (middle) and 40 h (right) after mixing 2.5 mM petunidin 3*p*CG5MG, 0.4 mM Fe^{3+} and 25 mM Mg^{2+} with 4 mM apigenin 7G4′MG in 130 mM citrate-phosphate buffer solution (pH 5.0). (B) Absorption spectrum of the solution of (A) diluted by half. (C) Photos of a solution taken 15 min (left), 24 h (middle) and 40 h (right) after mixing 2.5 mM petunidin 3*p*CG5MG, 0.4 mM Fe^{3+} and 25 mM Mg^{2+} with 4 mM apigenin 7,4′-diG in 130 mM citrate-phosphate buffer solution (pH 5.0). (D) Absorption spectrum of the solution of (C).

To completely understand the whole process of the metalloanthocyanin biosynthesis in *N. menziesii*, some issues on specificity for flavonoid transport to the vacuolar or metabolon formation for flavonoid biosynthetic enzymes in *N. menziesii* petals must be solved. However, although those issues still remain unsolved in this study, the ectopic accumulation of apigenin 7,4′-diG, an essential component of metalloanthocyanin, in other plant cells was succeeded by co-expression of *NmF4'GT* and *NmF7,4'GT* isolated in this study (**Chapter 4**).

Now that the molecular tools to engineer the components of blue metalloanthocyanins (petunidin 3*p*CG5MG and apigenin 7,4′-diG) have been obtained, we have moved one step closer to the accumulation of metalloanthocyanins in heterogonous plants and engineering pure blue flowers in other species. The dream of developing a ‘blue rose’ will come true.

References

Aida, R. (2008) *Torenia fournieri* (torenia) as a model plant for transgenic studies. *Plant Biotechnology*. 25: 541–545.

Akashi, T., Fukuchi-Mizutani, M., Aoki, T., Ueyama, Yonekura-Sakakibara, K., Tanaka, Y. et al. (1999) Molecular cloning and biochemical characterization of a novel cytochrome P450, flavone synthase II, that catalyzes direct conversion of flavanones to flavones. *Plant and Cell Physiology*. 40: 1182–1186.

Akita, Y., Kitamura, S., Hase, Y., Narumi, I., Ishizaka, H., Kondo, E. et al. (2011) Isolation and characterization of the fragrant cyclamen *O*-methyltransferase involved in flower coloration. *Planta*. 234: 1127–1136.

Andersen, O.M. and Jordheim, M. (2006) The anthocyanins. *In* Flavonoids Chemistry, Biochemistry and Applications. Edited by Andersen, O.M. and Markham, K.R. pp. 471–551. CRC Press, Boca Raton, FL.

APG. (2016) An update of the Angiosperm Phylogeny Group classification for the orders and families of flowering plants: APG II. *Botanical Journal of the Linnean Society*. 141: 399–436.

Ballester, A.-R., Molthoff, J., de Vos, R., Hekkert, B. t. L., Orzaez, D., Fernandez-Moreno, J.-P. et al. (2010) Biochemical and molecular analysis of pink tomatoes: deregulated expression of the gene encoding transcription factor SlMYB12 leads to pink tomato fruit color. *Plant Physiology*. 152: 71–84.

Ban, Z., Qin, H., Mitchell, A. J., Liu, B., Zhang, F., Weng, J.-K. et al. (2018) Noncatalytic chalcone isomerase-fold proteins in *Humulus lupulus* are auxiliary components in prenylated flavonoid biosynthesis. *Proceedings of the National*

Academy of Sciences of the United States of America. 115: 5223–5232.

Baudry, A., Heim, M. A., Dubreucq, B., Caboche, M., Weisshaar, B. and Lepiniec, L. (2004) TT2, TT8, and TTG1 synergistically specify the expression of *BANYULS* and proanthocyanidin biosynthesis in *Arabidopsis thaliana*. *The Plant Journal*. 39: 366–380.

Biolley, J. P. and Jay, M. (1993) Anthocyanins in modern roses: chemical and colorimetric features in relation to the colour range. *Journal of Experimental Botany*. 44: 1725–1734.

Bloor, S.J. (1997) Blue flower colour derived from flavonol-anthocyanin co-pigmentation in *Ceanothus papillosus*. *Phytochemistry*. 45: 1399–1405.

Brazier-Hicks, M., Evans, K. M., Gershater, M. C., Puschmann, H., Steel, P. G. and Edwards, R. (2009) The *C*-glycosylation of flavonoids in cereals. *The Journal of Biological Chemistry*. 284: 17926–17934.

Brockington, S. F., Yang, Y., Gandia-Herrero, F., Covshoff, S., Hibberd, J. M., Sage, R. F. et al. (2015) Lineage-specific gene radiations underlie the evolution of novel betalain pigmentation in Caryophyllales. *New Phytologist*. 207: 1170–1180.

Brugliera, F., Barri-Rewell, G., Holton, T.A. and Mason, J.G. (1999) Isolation and characterization of a flavonoid 3′-hydroxylase cDNA clone corresponding to the *Ht1* locus of *Petunia hybrida*. *The Plant Journal*.19: 441–451.

Brugliera, F., Tao, G. Q., Tems, U., Kalc, G., Mouradova, E., Price, K. et al. (2013) Violet/blue chrysanthemums-metabolic engineering of the anthocyanin biosynthetic pathway results in novel petal colors. *Plant and Cell Physiology*. 54: 1696–1710.

Burbulis, I. E. and Winkel-Shirley, B. (1999) Interactions among enzymes of the *Arabidopsis* flavonoid biosynthetic pathway. *Proceedings of the National Academy*

of Sciences of the United States of America. 96: 12929–12934.

Butelli, E., Titta. L., Giorgio, M., Mock, HP., Matros, A., Peterek, S. et al. (2008) Enrichment of tomato fruit with health-promoting anthocyanins by expression of select transcription factors. *Natature Biotechnology*. 26: 1301–1308.

Czemmel, S., Stracke, R., Weisshaar, B., Cordon, N., Harris, N. N., Walker, A. R. et al. (2009) The grapevine R2R3-MYB transcription factor VvMYBF1 regulates flavonol synthesis in developing grape berries. *Plant Physiology*. 151: 1513–1530.

Dai, X., Zhuang, J., Wu, Y., Wang, P., Zhao, G., Liu, Y. et al. (2017) Identification of a flavonoid glucosyltransferase involved in 7-OH site glycosylation in Tea plants (*Camellia sinensis*). *Scientific Reports*. 7: 5926.

D'Auria, J. C., Reichelt, M., Luck, K., Svatoš, A. and Gershenzon, J. (2007) Identification and characterization of the BAHD acyltransferase malonyl CoA: anthocyanidin 5-*O*-glucoside-6″-*O*-malonyltransferase (At5MAT) in *Arabidopsis thaliana*. *FEBS Letters*. 581: 872–878.

Davies, K. M. (2000) Plant color and fragrance. *In* Metabolic engineering of plant secondary metabolism. Edited by Verpoorte, R. and Alfermann, A. W. pp. 127–163. Kluwer Academic Publishers, Netherlands.

De Vetten, N., Quattrocchio, F., Mol, J. and Koes, R. (1997) The *an11* locus controlling flower pigmentation in petunia encodes a novel WD-repeat protein conserved in yeast, plants, and animals. *Genes and Development*. 11: 1422–1434.

Du, H., Wu, J., Ji, K. X., Zeng, Q. Y., Bhuiya, M. W., Su, S. et al. (2015) Methylation mediated by an anthocyanin, *O*-methyltransferase, is involved in purple flower coloration in *Paeonia*. *Journal of Experimental Botany*. 66: 6563–6577.

Fischer, T.C., Gosch, C., Pfeiffer, J., Halbwirth, H., Halle, C., Stich, K. et al. (2007)

Flavonoid genes of pear (*Pyrus communis*). *Trees*. 21: 521–529.

Forkmann, G. and Heller, W. (1999) Biosynthesis of flavonoids. *In* Complehensive Natural Products Chemistry. Volume 1. Polyketides and Other Secondary Metabolites Including Fatty Acids and Their Derivatives. Edited by Sankawa, U. pp. 713–748. Elsevier, Oxford.

Francisco, R. M., Regalado, A., Ageorges, A., Burla, B. J., Bassin, B., Eisenach, C. et al. (2013) ABCC1, an ATP binding cassette protein from grape berry, transports anthocyanidin 3-*O*-glucosides. *The Plant Cell*. 25: 1840–1854.

Fujino, N., Tenma, N., Waki, T., Ito, K., Komatsuzaki, Y., Sugiyama, K. et al. (2018) Physical interactions among flavonoid enzymes in snapdragon and torenia reveal the diversity in the flavonoid metabolon organization of different plant species. *The Plant Journal*. 94: 372–392.

Fukuchi-mizutani, M., Okuhara, H., Fukui, Y., Nakao, M., Katsumoto, Y., Yonekura-sakakibara, K. et al. (2003) Biochemical and molecular characterization of a novel UDP-glucose: anthocyanin 3'-*O*-glucosyltransferase, a key enzyme for blue anthocyanin biosynthesis, from gentian. *Society*. 132: 1652–1663.

Funaki, A., Waki, T., Noguchi, A., Kawai, Y., Yamashita, S., Takahashi, S. and Nakayama, T. (2015) Identification of a highly specific isoflavone 7-*O*-glucosyltransferase in the soybean (*Glycine max* (L.) Merr.). *Plant and Cell Physiology*. 56: 1512–1520.

Gachon, C. M. M., Langlois-Meurinne, M. and Saindrenan, P. (2005) Plant secondary metabolism glycosyltransferases: the emerging functional analysis. *Trends in Plant Science*. 10: 542–549.

Gong, Z. Z., Yamazaki, M., Sugiyama, M., Tanaka, Y. and Saito, K. (1997) Cloning

and molecular analysis of structural genes involved in anthocyanin biosynthesis and expressed in a forma-specific manner in *Perilla frutescens*. *Plant Molecular Biology*. 35: 915–927.

Goto, T. (1987) Structure, stability and color variation of natural anthocyanins. *Progress in the Chemistry of Organic Natural Products*. 52: 113–158.

Goto, T., Kondo, T., Kawai, T. and Tamura, H. (1984) Structure of cinerarin, a tetra-acylated anthocyanin isolated from the blue garden cineraria, *Senecio cruentus*. *Tetrahedron Letters*. 25: 6021–6024.

Goto, T., Kondo, T., Tamura, H., Imagawa, H., Iino, A. and Takeda, K. (1982) Structure of gentiodelphin, an acylated anthocyanin isolated from *Gentiana makinoi*, that is stable in dilute aqueous solution. *Tetrahedron Letters*. 23: 3695–3698.

Grotewold, E. (2006) The genetics and biochemistry of floral pigments. *Annual Review of Plant Biology*. 57: 761–780.

Harborne, J. B. and Williams, C. A. (2000) Advances in flavonoid research since 1992. *Phytochemistry*. 55: 481–504.

He, X., Li, Y., Lawson, D. and Xie, DY. (2017) Metabolic engineering of anthocyanins in dark tobacco varieties. *Physiologia Plantarum*. 159: 2–12.

Heller, W. and Forkmann, G. (1994) Biosynthesis of flavonoid. *In* The Flavonoids. Edited by Harborne, J.B. pp. 499–535. Chapman & Hall, Washington, DC.

Hirotani, M., Kuroda, R., Suzuki, H. and Yoshikawa, T. (2000) Cloning and expression of UDP-glucose: flavonoid 7-*O*-glucosyltransferase from hairy root cultures of *Scutellaria baicalensis*. *Planta*. 210: 1006–1013.

Holton, T. A., Brugliera, F. and Tanaka, Y. (1993) Cloning and expression of flavonol synthase from *Petunia hybrida*. *The Plant Journal*. 4: 1003–1010.

Hsu, Y. H., Tagami, T., Matsunaga, K., Okuyama, M., Suzuki, T., Noda, N. et al. (2017) Functional characterization of UDP-rhamnose-dependent rhamnosyltransferase involved in anthocyanin modification, a key enzyme determining blue coloration in *Lobelia erinus*. *The Plant Journal*. 89: 325–337.

Hugueney, P., Provenzano, S., Verries, C., Ferrandino, A., Meudec, E., Batelli, G. et al. (2009) A novel cation-dependent *O*-methyltransferase involved in anthocyanin methylation in grapevine. *Plant Physiology*. 150: 2057–2070.

Ichino, T., Fuji, K., Ueda, H., Takahashi, H., Koumoto, Y., Takagi, J. et al. (2014) GFS9/TT9 contributes to intracellular membrane trafficking and flavonoid accumulation in *Arabidopsis thaliana*. *The Plant Journal*. 80: 410–423.

Imayama, T., Yoshihara, N., Fukuchi-Mizutani, M., Tanaka, Y., Ino, I. and Yabuya, T. (2004) Isolation and characterization of a cDNA clone of UDP-glucose: anthocyanin 5-*O*-glucosyltransferase in *Iris hollandica*. *Plant Science*. 167: 1243–1248.

Isayenkova, J., Wray, V., Nimtz, M., Strack, D. and Vogt, T. (2006) Cloning and functional characterisation of two regioselective flavonoid glucosyltransferases from *Beta vulgaris*. *Phytochemistry*. 67: 1598–1612.

Jiang, W., Yin, Q., Wu, R., Zheng, G., Liu, J., Dixon, R. A. and Pang, Y. (2015) Role of a chalcone isomerase-like protein in flavonoid biosynthesis in *Arabidopsis thaliana*. *Journal of Experimental Botany*. 66: 7165–7179.

Johnson, E.T., Yi, H., Shin, B., Oh, B.-J., Cheong, H. and Choi, G. (1999) *Cymbidium hybrida* dihydroflavonol 4-reductase does not efficiently reduce dihydrokaempferol to produce orange pelargonidin-type anthocyanins. *The Plant Journal.* 19: 81–85.

Jones, P. and Vogt, T. (2001) Glycosyltransferases in secondary plant metabolism: tranquilizers and stimulant controllers. *Planta*. 213: 164–174.

Ju, Z., Sun, W., Meng, X., Liang, L., Li, Y., Zhou, T. et al. (2018) Isolation and functional characterization of two 5-*O*-glucosyltransferases related to anthocyanin biosynthesis from *Freesia hybrida*. *Plant Cell. Tissue and Organ Culture (PCTOC)*. 135: 99–110.

Katsumoto, Y., Fukuchi-Mizutani, M., Fukui, Y., Brugliera, F., Holton, T. A., Karan, M. et al. (2007) Engineering of the rose flavonoid biosynthetic pathway successfully generated blue-hued flowers accumulating delphinidin. *Plant and Cell Physiology*. 48: 1589–1600.

Kazuma, K., Noda, N. and Suzuki, M. (2003) Flavonoid composition related to petal color in different lines of *Clitoria ternatea*. *Phytochemistry*. 64: 1133–1139.

Kim, S. H., Naveen Kumar, C., Kim, H. J., Kim, D. H., Cho, J., Jin, C. and Lee, Y. S. (2009) Glucose-containing flavones-their synthesis and antioxidant and neuroprotective activities. *Bioorganic and Medicinal Chemistry Letters*. 19: 6009–6013.

Koes, R., Verweij, W. and Quattrocchio, F. (2005) Flavonoids: a colorful model for the regulation and evolution of biochemical pathways. *Trends in Plant Science*. 10: 236–242.

Kogawa, K., Kato, N., Kazuma, K., Noda, N. and Suzuki, M. (2007) Purification and characterization of UDP-glucose: anthocyanin 3′,5′-*O*-glucosyltransferase from *Clitoria ternatea*. *Planta*. 226: 1501–1509.

Kondo, T., Oyama, K. I. and Yoshida, K. (2001) Chiral molecular recognition on formation of a metalloanthocyanin: a supramolecular metal complex pigment from blue flowers of *Salvia patens*. *Angewandte Chemie - International Edition*. 40: 894–897.

Kondo, T., Suzuki, K., Yoshida, K., Oki, K., Ueda, M., Isobe, M. and Goto, T. (1991) Structure of cynanodelphin, a tetra-*p*-hydroxybenzoated anthocyanin from blue flower of *Delphinium hybridum*. *Tetrahedron Letters*. 32: 6375–6378.

Kondo, T., Ueda, M., Isobe, M. and Goto, T. (1998) A new molecular mechanism of blue color development with protocyanin, a supramolecular pigment from cornflower, *Centaurea cyanus*. *Tetrahedron Letters*. 39: 8307–8310.

Lazo, G., Stein, P. and Ludwig, R. (1991) A DNA transformation-competent *Arabidopsis* genomic library in *Agrobacterium*. *Biotechnology*. 9: 963–967.

Li, C., Qiu, J., Ding, L., Huang, M., Huang, S., Yang G. et al. (2017) Anthocyanin biosynthesis regulation of DhMYB2 and DhbHLH1 in *Dendrobium* hybrids petals. *Plant Physiology and Biochemistry*.112: 335–345.

Li, H. and Durbin, R. (2009) Fast and accurate short read alignment with Burrows-Wheeler transform. *Bioinformatics*. 25: 1754–1760.

Li, H., Handsaker, B., Wysoker, A., Fennell, T., Ruan, J., Homer, N. et al. (2009) The Sequence Alignment/Map format and SAMtools. *Bioinformatics*. 25: 2078–2079.

Lucker, J., Martens, S. and Lund, S. T. (2010) Characterization of a *Vitis vinifera* cv. Cabernet Sauvignon 3′,5′-*O*-methyltransferase showing strong preference for anthocyanins and glycosylated flavonols. *Phytochemistry*. 71: 1474–1484.

Martens, S., Forkmann, G., Britsch, L., Wellmann, F., Matern, U. and Lukačin, R. (2003) Divergent evolution of flavonoid 2-oxoglutarate-dependent dioxygenases in parsley. *FEBS Letters*. 544: 93–98.

Martin, C., Prescott, A., Mackay, S., Bartlett, J. and Vrijlandt, E. (1991) Control of anthocyanin biosynthesis in flowers of *Antirrhinum majus*. *The Plant Journal*. 1: 37–49.

Martens, S. and Forkmann, G. (1999) Cloning and expression of flavone synthase II from *Gerbera* hybrids. *The Plant Journal*. 20: 611–618.

Matsuba, Y., Sasaki, N., Tera, M., Okamura, M., Abe, Y., Okamoto, E. et al. (2010) A novel glucosylation reaction on anthocyanins catalyzed by acyl-glucose-dependent glucosyltransferase in the petals of carnation and delphinium. *The Plant Cell*. 22: 3374–3389.

Meyer, P., Heidmann, I., Forkmann, G. and Saedler, H. (1987) A new petunia flower colour generated by transformation of a mutant with a maize gene. *Nature*. 330: 677–678.

Mehrtens, F. (2005) The Arabidopsis transcription factor MYB12 is a flavonol-specific regulator of phenylpropanoid biosynthesis. *Plant Physiology*. 138: 1083–1096.

Mii, M. (2012) Aoi Kochoran / daria no kaihatsu (Development of blue *Phalenopsis* and blue *Dahlia*). *Noukou to Engei (Agriculture and Horticulture)*. 67: 42–46.

Mitsuhara, I., Ugaki, M., Hirochika, H., Ohshima, M., Murakami, T., Goto, Y. et al. (1996) Efficient promoter cassettes or enhanced expression of foreign genes in dicotyledonous and monocotyledonous plants. *Plant and Cell Physiology*. 37: 49–59.

Miyahara, T., Sakiyama, R., Ozeki, Y. and Sasaki, N. (2013) Acyl-glucose-dependent glucosyltransferase catalyzes the final step of anthocyanin formation in *Arabidopsis*. *Journal of Plant Physiology*. 170: 619–624.

Miyahara, T., Takahashi, M., Ozeki, Y. and Sasaki, N. (2012) Isolation of an acyl-glucose-dependent anthocyanin 7-*O*-glucosyltransferase from the monocot *Agapanthus africanus*. *Journal of Plant Physiology*. 169: 1321–1326.

Miyahara, T., Tani, T., Takahashi, M., Nishizaki, Y., Ozeki, Y. and Sasaki, N. (2014)

Isolation of anthocyanin 7-*O*-glucosyltransferase from canterbury bells (*Campanula medium*). *Plant Biotechnology*. 31: 555–559.

Mori, M., Kondo, T. and Yoshida, K. (2008) Cyanosalvianin, a supramolecular blue metalloanthocyanin, from petals of *Salvia uliginosa*. *Phytochemistry*. 69: 3151–3158.

Mori, M., Kondo, T. and Yoshida, K. (2009) Anthocyanin components and mechanism for color development in blue *Veronica* flowers. *Bioscience, Biotechnology, and Biochemistry*. 73: 2329–2331.

Morita, Y. and Hoshino, A. (2018) Recent advances in flower color variation and patterning of Japanese morning glory and petunia. *Breeding Science*. 138: 128–138.

Morita, Y., Takagi, K., Fukuchi-Mizutani, M., Ishiguro, K., Tanaka, Y., Nitasaka, E. et al. (2014) A chalcone isomerase-like protein enhances flavonoid production and flower pigmentation. *The Plant Journal*. 78: 294–304.

Morita, Y., Tanase, K., Ohmiya, A., Hisamatsu, T. and Nakayama, M. (2015) Isolation and characterization of enhancer of flavonoid production genes from floricultural crops. *Scientific reports of the Faculty of Agriculture, Meijo University*. 51: 35–41.

Nagata, T., Nemoto, Y. and Hasezawa, S. (1992) Tobacco BY-2 cell line as the “HeLa” cell in the cell biology of higher plants. *International Review of Cytology*. 132: 1–30.

Nagata, T., Okada, K., Takebe, I. and Matsui, C. (1981) Delivery of tobacco mosaic virus RNA into plant protoplasts mediated by reverse-phase evaporation vesicles (liposomes). *Molecular Genetics and Genomics.* 184: 161–165.

Nagatomo, Y., Usui, S., Ito, T., Kato, A., Shimosaka, M. and Taguchi, G. (2014) Purification, molecular cloning and functional characterization of flavonoid

C-glucosyltransferases from *Fagopyrum esculentum* M. (buckwheat) cotyledon. *The Plant Journal*. 80: 437–449.

Nagaya, S., Kawamura, K., Shinmyo, A. and Kato, K. (2010) The *HSP* terminator of *Arabidopsis thaliana* increases gene expression in plant cells. *Plant and Cell Physiology*. 51: 328–332.

Nakamura, N., Katsumoto, Y., Brugliera, F., Demelis, L., Nakajima, D., Suzuki, H. and Tanaka, Y. (2015) Flower color modification in *Rosa hybrida* by expressing the *S*-adenosylmethionine: anthocyanin 3′,5′-*O*-methyltransferase gene from *Torenia hybrida*. *Plant Biotechnology*. 32: 109–117.

Nakatsuka, T., Haruta, K. S., Pitaksutheepong, C., Abe, Y., Kakizaki, Y., Yamamoto, K. et al. (2008) Identification and characterization of R2R3-MYB and bHLH transcription factors regulating anthocyanin biosynthesis in gentian flowers. *Plant and Cell Physiology*. 49: 1818–1829.

Nakatsuka, T., Sato, K., Takahashi, H., Yamamura, S. and Nishihara, M. (2008) Cloning and characterization of the UDP-glucose: anthocyanin 5-*O*-glucosyltransferase gene from blue-flowered gentian. *Journal of Experimental Botany*. 59: 1241–1252.

Nakatsuka, T., Saito, M., Yamada, E., Fujita, K., Kakizaki, Yuko. and Nishihara, M. (2012) Isolation and characterization of GtMYBP3 and GtMYBP4, orthologues of R2R3-MYB transcription factors that regulate early flavonoid biosynthesis, in gentian flowers. *Journal of Experimental Botany*. 63: 6505–6517.

Nakayama, T., Suzuki, H. and Nishino, T. (2003) Anthocyanin acyltransferases: specificities, mechanism, phylogenetics, and applications. *Journal of Molecular Catalysis B: Enzymatic*. 23: 117–132.

Nishizaki, Y., Sasaki, N., Yasunaga, M., Miyahara, T., Okamoto, E., Okamoto, M. et al. (2014) Identification of the glucosyltransferase gene that supplies the *p*-hydroxybenzoyl-glucose for 7-polyacylation of anthocyanin in delphinium. *Journal of Experimental Botany*. 65: 2495–2506.

Nishizaki, Y., Yasunaga, M., Okamoto, E., Okamoto, M., Hirose, Y., Yamaguchi, M. et al. (2013) *p*-Hydroxybenzoyl-glucose is a zwitter donor for the biosynthesis of 7-polyacylated anthocyanin in delphinium. *The Plant Cell*. 25: 4150–4165.

Noda, N., Kazuma, K., Sasaki, T., Kogawa, K. and Suzuki, M. (2006) Molecular cloning of 1-*O*-acylglucose dependent anthocyanin aromatic acyltransferase in ternatin biosynthesis of butterfly pea (*Clitoria ternatea*). *Plant and Cell Physiology*. 47(S109).

Noda, N., Yoshioka, S., Kishimoto, S., Nakayama, M., Douzono, M., Tanaka, Y. and Aida, R. (2017) Generation of blue chrysanthemums by anthocyanin B-ring hydroxylation and glucosylation and its coloration mechanism. *Science Advances*. 3: 1–11.

Noguchi, A., Saito, A., Homma, Y., Nakao, M., Sasaki, N., Nishino, T. et al. (2007) A UDP-glucose: isoflavone 7-*O*-glucosyltransferase from the roots of soybean (*Glycine max*) seedlings. *The Journal of Biological Chemistry*. 282: 23581–23590.

Ohmiya, A., Hirashima, M., Yagi, M., Tanase, K. and Yamamizo, C. (2014) Identification of genes associated with chlorophyll accumulation in flower petals. *PLoS ONE*. 9: 1–16.

Ohmiya, A., Sasaki, K., Nashima, K., Oda-Yamamizo, C., Hirashima, M. and Sumitomo, K. (2017) Transcriptome analysis in petals and leaves of chrysanthemums with different chlorophyll levels. *BMC Plant Biology*. 17: 1–15.

Ogata, J., Kanno, Y., Itoh, Y., Tsugawa, H. and Suzuki M. (2005) Plant biochemistry: anthocyanin biosynthesis in roses. *Nature* 435: 757–758.

Ono, E., Fukuchi-Mizutani, M., Nakamura, N., Fukui, Y., Yonekura-sakakibara, K., Yamaguchi, M. et al. (2006) Yellow flowers generated by expression of the aurone biosynthetic pathway. *Proceedings of the National Academy of Sciences of the United States of America*. 103: 11075–11080.

Pedras, M. S. C., Zaharia, I. L., Gai, Y., Zhou, Y. and Ward, D. E. (2001) *In planta* sequential hydroxylation and glycosylation of a fungal phytotoxin: avoiding cell death and overcoming the fungal invader. *Proceedings of the National Academy of Sciences of the United States of America*. 98: 747–752.

Provenzano, S., Spelt, C., Hosokawa, S., Nakamura, N., Brugliera, F., Demelis, L. et al. (2014) Genetic control and evolution of anthocyanin methylation. *Plant Physiology*. 165: 962–977.

Qi, Y., Lou, Q., Quan, Y., Liu, Y. and Wang, Y. (2013) Flower-specific expression of the phalaenopsis flavonoid 3′, 5′-hydoxylase modifies flower color pigmentation *in Petunia* and *Lilium*. *Plant Cell, Tissue and Organ Culture*. 115: 263–273.

Quattrocchio, F. (1993) Regulatory genes controlling anthocyanin pigmentation are functionally conserved among plant species and have distinct sets of target genes. *The Plant Cell Online*. 5: 1497–1512.

Rausher, M. D. (2006) The evolution of flavonoids and their genes. *The Science of Flavonoids*. 175–211.

Roldan, M. V. G., Outchkourov, N., Van Houwelingen, A., Lammers, M., De La Fuente, I. R., Ziklo, N. et al. (2014) An *O*-methyltransferase modifies accumulation of methylated anthocyanins in seedlings of tomato. *The Plant Journal*. 80: 695–708.

Ryan, K. G., Swinny, E. E., Winefield, C. and Markham, K. R. (2001) Flavonoids and UV photoprotection in *Arabidopsis* mutants. *Zeitschrift Fur Naturforschung - Section C Journal of Biosciences*. 56: 745–754.

Saito, K., Kobayashi, M., Gong, Z., Tanaka, Y. and Yamazaki, M. (1999) Direct evidence for anthocyanidin synthase as a 2-oxoglutarate-dependent oxygenase: molecular cloning and functional expression of cDNA from a red forma of *Perilla frutescens*. *The Plant Journal*. 17: 181–189.

Saito, K., Yonekura-Sakakibara, K., Nakabayashi, R., Higashi, Y., Yamazaki, M., Tohge, T. and Fernie, A. R. (2013) The flavonoid biosynthetic pathway in *Arabidopsis*: structural and genetic diversity. *Plant Physiology and Biochemistry*. 72: 21–34.

Sasaki, N. and Nakayama, T. (2015) Achievements and perspectives in biochemistry concerning anthocyanin modification for blue flower coloration. *Plant and Cell Physiology*. 56: 28–40.

Sasaki, N., Nishizaki, Y., Yamada, E., Tatsuzawa, F., Nakatsuka, T., Takahashi, H. and Nishihara, M. (2015) Identification of the glucosyltransferase that mediates direct flavone *C*-glucosylation in *Gentiana triflora*. *FEBS Letters*. 589: 182–187.

Seitz, C., Ameres, S., Schlangen, K., Forkmann, G. and Halbwirth, H. (2015) Multiple evolution of flavonoid 3′,5′-hydroxylase. *Planta*. 242: 561–573.

Shindo, T., Takahashi, T., Nihira, T., Yamada, Y., Kato, K. and Shinmyo, A. (2006) *Streptomyces*-derived induction system for gene expression in cultured plant cells. *Journal of Bioscience and Bioengineering*. 102: 552–559.

Shiono, M., Matsugaki, N. and Takeda, K. (2005) Structure of the blue cornflower pigment. *Nature*. 436: 791.

Shiono, M., Matsugaki, N. and Takeda, K. (2008) Structure of commelinin, a blue complex pigment from the blue flowers of *Commelina communis*. *Proceedings of the Japan Academy. Series B, Physical and Biological Sciences*. 84: 452–456.

Shoji, K., Miki, N., Nakajima, N., Momonoi, K., Kato, C. and Yoshida, K. (2007) Perianth bottom-specific blue color development in tulip cv. Murasakizuisho requires ferric ions. *Plant and Cell Physiology*. 48: 243–251.

Smith, T. F., Gaitatzes, C., Saxena, K. and Neer, E. J. (1999) The WD repeat: a common architecture for diverse functions. *Trends in Biochemical Sciences*. 24: 181–185.

Sparvoli, F., Martin, C., Scienza, A., Gavazzi, G. and Tonelli, C. (1994) Cloning and molecular analysis of structural genes involved in flavonoid and stilbene biosynthesis in grape (*Vitis vinifera* L.). *Plant Molecular Biology*. 24: 743–755.

Spelt, C., Quattrocchio, F., Mol, J. N. M. and Koes, R. (2000) *anthocyanin1* of petunia encodes a basic helix-loop-helix protein that directly activates transcription of structural anthocyanin genes. *The Plant Cell*. 12: 1619–1631.

Stracke, R., Ishihara, H., Huep, G., Barsch, A., Mehrtens, F., Niehaus, K. and Weisshaar, B. (2007) Differential regulation of closely related R2R3-MYB transcription factors controls flavonol accumulation in different parts of the *Arabidopsis thaliana* seedling. *The Plant Journal*. 50: 660–677.

Sui, X., Gao, X., Ao, M., Wang, Q., Yang, D., Wang, M. et al. (2011) cDNA cloning and characterization of UDP-glucose: anthocyanidin 3-*O*-glucosyltransferase in F*reesia hybrida*. *Plant Cell Reports*. 30: 1209–1218.

Sun, W., Liang, L., Meng, X., Li, Y., Gao, F., Liu, X. et al. (2016) Biochemical and molecular characterization of a flavonoid 3-*O*-glycosyltransferase responsible for

anthocyanins and flavonols biosynthesis in *Freesia hybrida*. *Frontiers in Plant Science*. 7: 1–14.

Suzuki, H., Nakayama, T., Yonekura-Sakakibara, K., Fukui, Y., Nakamura, N., Nakao, M. et al. (2001) Malonyl-CoA: anthocyanin 5-*O*-glucoside-6‴-*O*-malonyltransferase from scarlet sage (*Salvia splendens*) flowers. *The Journal of Biological Chemistry*. 276: 49013–49019.

Taguchi, G., Ubukata, T., Hayashida, N., Yamamoto, H. and Okazaki, M. (2003) Cloning and characterization of a glucosyltransferase that reacts on 7-hydroxyl group of flavonol and 3-hydroxyl group of coumarin from tobacco cells. *Archives of Biochemistry and Biophysics.* 420: 95–102.

Takeda, K., Yanagisawa, M., Kifune, T., Kinoshita, T. and Timberlake, C. (1994) A blue pigment complex in flowers of *Salvia patens*. *Phytochemistry*. 35: 1167–1169.

Tamura, H., Kondo, T. and Goto, T. (1986) The composition of commelinin, a highly associated metalloanthocyanin present in the blue flower petals of *Commelina communis*. *Tetrahedron Letters*. 27: 1801–1804.

Tanaka, Y. and Brugliera, F. (2006) Flower color. *In* Flowering and Its Manipulation. Edited by Ainswor, C. pp 201–239. Blackwell, London.

Tanaka, Y. and Brugliera, F. (2013) Flower colour and cytochromes P450. *Philosophical Transactions of the Royal Society of London. Series B, Biological Sciences*. 368: 20120432.

Tanaka, Y., Brugliera, F., Kalc, G., Senior, M., Dyson, B., Nakamura, N. et al. (2010) Flower color modification by engineering of the flavonoid biosynthetic pathway: practical perspectives. *Bioscience, Biotechnology, and Biochemistry*. 74: 1760–1769.

Tanaka, Y., Fukuchi-Mizutani, M. and Mason, J. (2003) Cloned genes. *In* Encyclopedia of Rose Science. Edited by Robert, A. pp 341–347. Elsevier, Amsterdam.

Tanaka, Y., Sasaki, N. and Ohmiya, A. (2008) Biosynthesis of plant pigments: anthocyanins, betalains and carotenoids. *The Plant Journal*. 54: 733–749.

Tanaka, Y., Tsuda, S. and Kutsumi, T. (1998) Metabolic engineering to modify flower color. *Plant and Cell Physiology*. 39: 1119–1126.

Tanaka, Y., Yonekura, K., Fukuchi-Mizutani, M., Fukui, Y., Fujiwara, H., Ashikari, T. and Kusumi, T. (1996) Molecular and biochemical characterization of three anthocyanin synthetic enzymes from *Gentiana triflora*. *Plant and Cell Physiology*. 37: 711–716.

Tatsuzawa, F., Toki, K., Ohtani, Y., Kato, K., Saito, N., Honda, T. and Mii, M. (2014) Floral pigments from the blue flowers of *Nemophila menziesii* ‘Insignis Blue’ and the purple flower of its variants. *Journal of the Japanese Society for Horticultural Science*. 83: 259–266.

Ueyama, Y., Suzuki, K., Fukuchi-Mizutani, M., Fukui, Y., Miyazaki, K., Ohkawa, H. et al. (2002) Molecular and biochemical characterization of torenia flavonoid 3'-hydroxylase and flavone synthase II and modification of flower color by modulating the expression of these genes. *Plant Science*. 163: 253–263.

Umemoto, N., Abe, Y., Cano, EA., Okumyra, M., Sasaki, N. and Yoshida, S. (2014) Carnation serine carboxypeptidase-like acyltransferase is important for anthocyanin malyltransferase activity and formation of anthocyanic vacuolar inclusions. Paper presented at the XXVIIth international conference on polyphenols (ICP2014), Nagoya, Japan.

van Engelen, FA., Molthoff, JW., Conner, AJ, Nap, J-P, Pereira, A. and Stiekema, WJ.

(1995) pBINPLUS: an improved plant transformation vector based on pBIN19. *Transgenic Research*. 4: 288–290.

van Nocker, S. and Ludwig, P. (2003) The WD-repeat protein superfamily in arabidopsis: conservation and divergence in structure and function. *BMC Genomics*. 4: 1–11.

Vogt, T., Grimm, R. and Strack, D. (1999) Cloning and expression of a cDNA encoding betanidin 5-*O*-glucosyltransferase, a betanidin- and flavonoid-specific enzyme with high homology to inducible glucosyltransferases from the Solanaceae. *The Plant Journal*. 19: 509–519.

Vogt, T., Zimmermann, E., Grimm, R., Meyer, M. and Strack, D. (1997) Are the characteristics of betanidin glucosyltransferases from cell-suspension cultures of *Dorotheanthus bellidiformis* indicative of their phylogenetic relationship with flavonoid glucosyltransferases? *Planta*. 203: 349–361.

Waki, T., Yoo, D. C., Fujino, N., Mameda, R., Denessiouk, K., Yamashita, S. et al. (2016) Identification of protein-protein interactions of isoflavonoid biosynthetic enzymes with 2-hydroxyisoflavanone synthase in soybean (*Glycine max* (L.) Merr.). *Biochemical and Biophysical Research Communications*. 469: 546–551.

Winkel, BSJ. (2004) Metabolic channeling in plants. *Annu Rev Plant Biol*. 55: 85–107.

Wolf, L., Rizzini, L., Stracke, R., Ulm, R. and Rensing, S. A. (2010) The molecular and physiological responses of *Physcomitrella patens* to ultraviolet-B radiation. *Plant Physiology*. 153: 1123–1134.

Wu, Q., Wu, J., Li, S. S., Zhang, H. J., Feng, C. Y., Yin, D. D. et al. (2016) Transcriptome sequencing and metabolite analysis for revealing the blue flower formation in waterlily. *BMC Genomics*. 17: 1–13.

Yabuya, T., Nakamura, M., Iwashina, T., Yamaguchi, M. and Takehara, T. (1997) Anthocyanin-flavone copigmentation in bluish purple flowers of Japanese garden iris (*Iris ensata thunb.*). *Euphytica*. 98: 163–167.

Yamazaki, M., Gong, Z., Fukuchi-Mizutani, M., Fukui, Y., Tanaka, Y., Kusumi, T. et al. (1999) Molecular cloning and biochemical characterization of a novel anthocyanin 5-*O*-glucosyltransferase by mRNA differential display for plant forms regarding anthocyanin. *The Journal of Biological Chemistry*. 274: 7405–7411.

Yamazaki, M., Yamagishi, E., Gong, Z., Fukuchi-Mizutani, M., Fukui, Y., Tanaka, Y. et al. (2002) Two flavonoid glucosyltransferases from *Petunia hybrida*: molecular cloning, biochemical properties and developmentally regulated expression. *Plant Molecular Biology*. 48: 401–411.

Yin, Q., Shen, G., Di, S., Fan, C., Chang, Z. and Pang, Y. (2017) Genome-wide identification and functional characterization of UDP-glucosyltransferase genes involved in flavonoid biosynthesis in *Glycine max***.** *Plant and Cell Physiology*. 58: 1558–1572.

Yonekura-Sakakibara, K. and Hanada, K. (2011) An evolutionary view of functional diversity in family 1 glycosyltransferases. *The Plant Journal*. 66: 182–193.

Yonekura-Sakakibara, K., Nakabayashi, R., Sugawara, S., Tohge, T., Ito, T., Koyanagi, M. et al. (2014) A flavonoid 3-*O*-glucoside: 2"-*O*-glucosyltransferase responsible for terminal modification of pollen-specific flavonols in *Arabidopsis thaliana*. *The Plant Journal*. 79: 769–782.

Yonekura-sakakibara, K., Tanaka, Y., Fukuchi-mizutani, M. and Fujiwara, H. (2000) Molecular and biochemical characterization of a novel hydroxycinnamoyl-CoA: anthocyanin 3-*O*-glucoside-6"-*O*-acyltransferase from *Perilla frutescens*. *Plant and*

Cell Physiology. 41: 495–502.

Yonekura-Sakakibara, K., Tohge, T., Matsuda, F., Nakabayashi, R., Takayama, H., Niida, R. et al. (2008) Comprehensive flavonol profiling and transcriptome coexpression analysis leading to decoding gene-metabolite correlations in *Arabidopsis*. *The Plant Cell Online*. 20: 2160–2176.

Yoshida, k., Kawachi, M., Mori, M., Maeshima, M., Kondo, M. et al. (2005) The involvement of tonoplast proton pumps and $Na^+(K^+)/H^+$ exchangers in the change of petal color during flower opening of morning glory, *Ipomoea tricolor* cv. Heavenly Blue. *Plant and Cell Physiology*. 46: 407–415.

Yoshida, K., Mori, M. and Kondo, T. (2009) Blue flower color development by anthocyanins: from chemical structure to cell physiology. *Natural Product Reports*. 26: 884–915.

Yoshida, K., Tojo, K., Mori, M., Yamashita, K., Kitahara, S., Noda, M. and Uchiyama, S. (2015) Chemical mechanism of petal color development of *Nemophila menziesii* by a metalloanthocyanin, nemophilin. *Tetrahedron*. 71: 9123–9130.

Yoshida, K., Toyama-Kato, Y., Kameda, K. and Kondo, T. (2003) Sepal color variation of *Hydrangea macrophylla* and vacuolar pH measured with a proton-selective microelectrode. *Plant and Cell Physiology*. 44: 262–268.

Yoshihara, N., Imayama, T., Fukuchi-Mizutani, M., Okuhara, H., Tanaka, Y., Ino, I. and Yabuya, T. (2005) cDNA cloning and characterization of UDP-glucose: anthocyanidin 3-*O*-glucosyltransferase in *Iris hollandica*. *Plant Science*. 169: 496–501.

Zhao, J. (2015) Flavonoid transport mechanisms: how to go, and with whom. *Trends in Plant Science*. 20: 576–585.

Zhao, J. and Dixon, R. A. (2009) MATE transporters facilitate vacuolar uptake of epicatechin 3'-*O*-glucoside for proanthocyanidin biosynthesis in *Medicago truncatula* and *Arabidopsis*. *The Plant Cell Online*. 21: 2323–2340.

Acknowledgements

Undertaking this Ph.D. has been a truly life-changing experience for me, and it would not have been possible without the support, guidance and encouragement that I received from a great number of people.

First, I would like to express my greatest appreciation to my supervisor, Dr. Tetsuro Mimura of Kobe University, for giving me this precious opportunity of undertaking a Ph.D. His generous support was of great assistance during my study and in the entire process of writing this thesis. This would not have been achieved without his guidance and encouragement.

Besides my supervisor, I would like to express the deepest appreciation to the rest of my thesis committee: Dr. Masaharu Mizutani, Dr. Hidehiro Fukaki and Dr. Kimitsune Ishizaki, all of Kobe University, for their constructive comments and warm encouragement during my study.

I am sincerely grateful to all my colleagues at Suntory Global Innovation Center Ltd.; especially, Dr. Keisuke Matsui, for his continued support and insightful comments during my study. He was always ready to assist me when I had any difficulties or queries regarding the experiments. Dr. Yukihisa Katsumoto and Dr. Noriko Nakamura offered me valuable advice on my study and considerable assistance in my work. In addition, I would like to offer my special thanks to Ms. Kanako Ishiguro, Ms. Tomoko Nakajima and Ms. Yuki Ohnishi, for their technical assistance.

I deeply appreciate Dr. Manabu Horikawa and Dr. Kohtaro Sugahara of Suntory Foundation for Life Sciences, Dr. Takayuki Mizuno of the National Museum of Nature and Science and Ms. Sun Hee Choi of Hokkaido University, for their valuable cooperation during my experiments.

I would like to express my gratitude to Dr. Yoshihiro Ozeki of Tokyo University of Agriculture and Technology for providing betanidin, and Dr. Ko Kato of Nara Institute of Science and Technology for providing *HSP18.2* terminator and tobacco BY-2 cell.

I am grateful to the members of Mimura's laboratory for their timely assistance and warm encouragement.

A special thanks also to my first supervisor, Dr. Tatsuo Kakimoto of Osaka University, for teaching me what research was and gave me the opportunity to find pleasure in research during my graduate school career. His great guidance in my science life helped me in all the time of research and writing of this thesis.

My greatest appreciation, particularly, goes to my supervisor at Suntory Global Innovation Center Ltd, Dr. Yoshikazu Tanaka, for his elaborative guidance and invaluable discussion that made my research a great achievement. I am truly grateful that he has always taught attentively how to think logically about my research since I entered the company, and how to write papers for submission and this thesis. I am also deeply grateful to him for providing this intriguing theme.

Finally, I extend my indebtedness to my friends and family for supporting me spiritually throughout the writing of this thesis and my life in general. I thank you all again.